Theory and Design of Switching Power Inductors for Electromagnetic Interference Assessment and Suppression in Power Electronics Systems

Shuo Wang, Ph. D

Power Electronics and Electrical Power Research Lab

University of Florida

Aug. 2023

1. Power Inductor Basics

Toroidal Power Inductor

Low Permeability Material w/o Air Gaps:

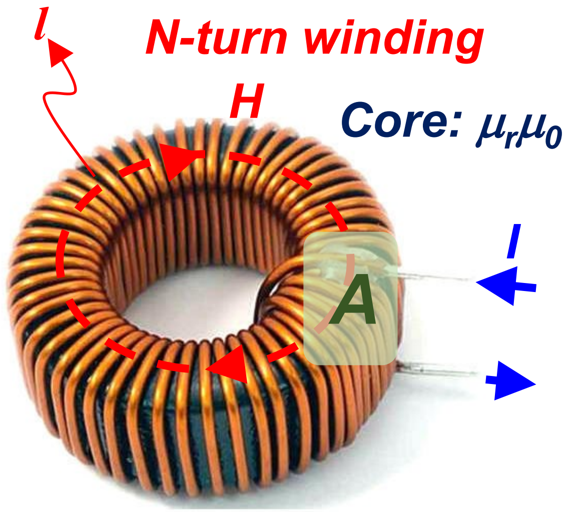

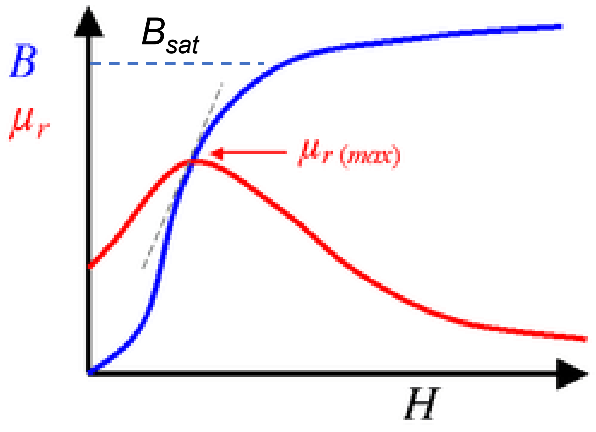

Magnetic Field Intensity H: $H = \dfrac{NI}{l}, B = \mu_r \mu_0 H < B_{sat}$

Inductance: $L = \dfrac{\mu_r \mu_0 A}{l} N^2$

Core Volume: $V = Al$

Magnetic Energy: $E_M = \int_v \frac{1}{2}\mu_r \mu_0 H^2 dv = \frac{1}{2}\mu_r \mu_o \left(\frac{NI}{l}\right)^2 Al = \frac{1}{2} LI^2$

EE Core Power Inductor

High Permeability Material w/ Air Gaps:

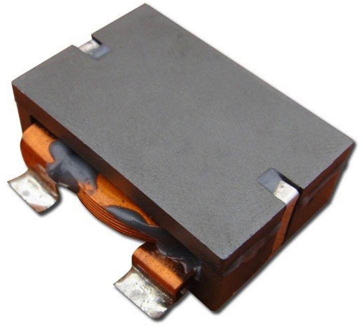

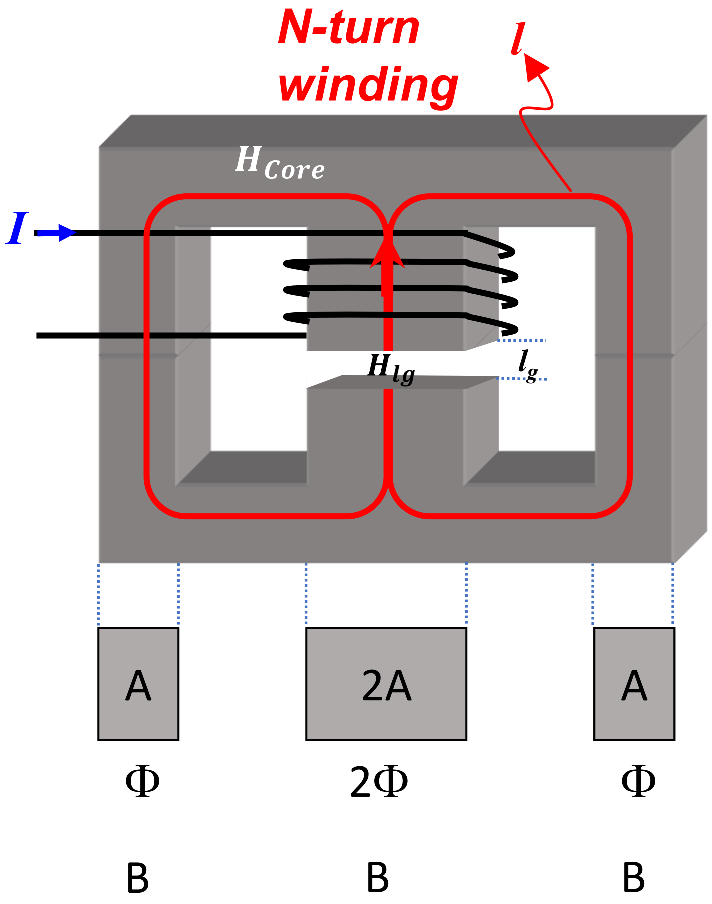

Air gap is used to store energy and prevent saturation

$$B < B_{sat}$$

Magnetic Field Intensity:

$$2\Phi = 2BA = 2\mu_r\mu_0 H_{Core} A = 2\mu_0 H_{\lg} A,$$

$$NI = H_{Core} l + H_{\lg} l_g \approx H_{\lg} l_g$$

$$H_{\lg} = \frac{\mu_r NI}{l + \mu_r l_g} >> H_{Core} = \frac{NI}{l + \mu_r l_g}$$

Magnetic Energy:

$$E_M = \frac{1}{2} LI^2 = \frac{\mu_0}{2} \int_v (\mu_r H_{Core}{}^2 + H_{\lg}{}^2) dv$$

$$\approx \frac{\mu_o}{2} \left(\frac{\mu_r NI}{l + \mu_r l_g} \right)^2 2Al_g$$

Inductance:

$$L \approx \mu_o \left(\frac{N}{l / \mu_r + l_g} \right)^2 2Al_g \approx \frac{2\mu_o A}{l_g} N^2$$

Power Inductor Design

Core saturation constraint:

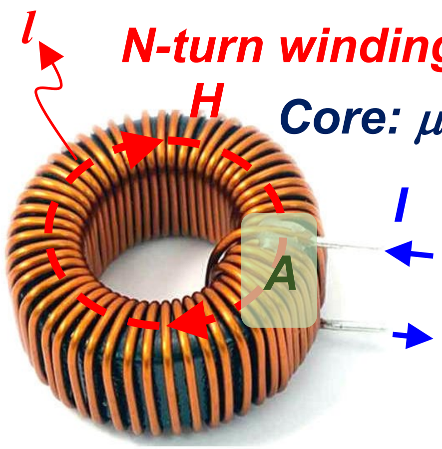

$$\begin{cases} \mu_r\mu_0 \dfrac{NI_{\max}}{l} < B_{sat} \\ L = \dfrac{\mu_r\mu_0 A}{l} N^2 \end{cases}$$

$$\Rightarrow I_{\max}\sqrt{\frac{\mu_r\mu_0 L}{V}} < B_{sat}$$

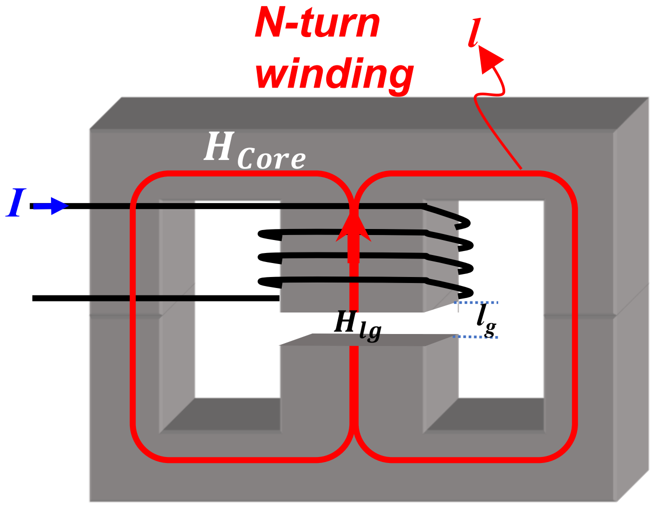

$$\begin{cases} \dfrac{\mu_0 NI_{\max}}{l_g} < B_{sat} \\ L \approx \dfrac{2\mu_o A}{l_g} N^2 \end{cases}$$

$$\Rightarrow I_{\max}\sqrt{\frac{\mu_0 L}{V_g}} < B_{sat}$$

Winding power loss constraint (winding power loss due to eddy currents induced by the magnetic flux of air gap is not included):

$$P_w = I_{DC}^2 R_{DC} + \sum_{n=1}^{\infty} I_n^2 R_n < P_{w\_\max}$$

- If the DC current is dominant

$$P_w = I_{DC}^2 \rho \frac{Nl_T}{A_w} < P_{w\_\max} \Rightarrow A_w > I_{DC}^2 \rho \frac{Nl_T}{P_{w\_\max}}$$

- If AC current is dominant

$$P_w = \sum_{n=1}^{\infty} I_n^2 R_n < P_{w\_\max}$$

(Usually, the fundamental is dominant)

Inductor's 1st order Self-parasitic Model

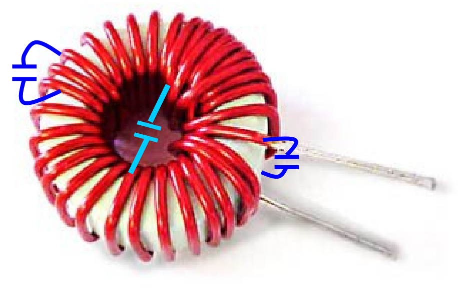

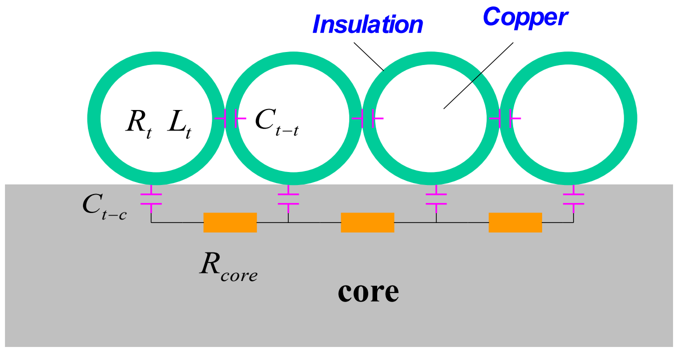

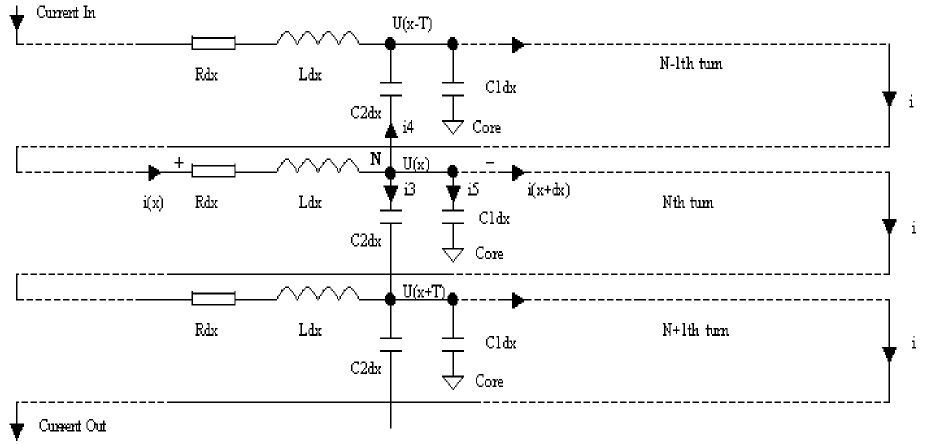

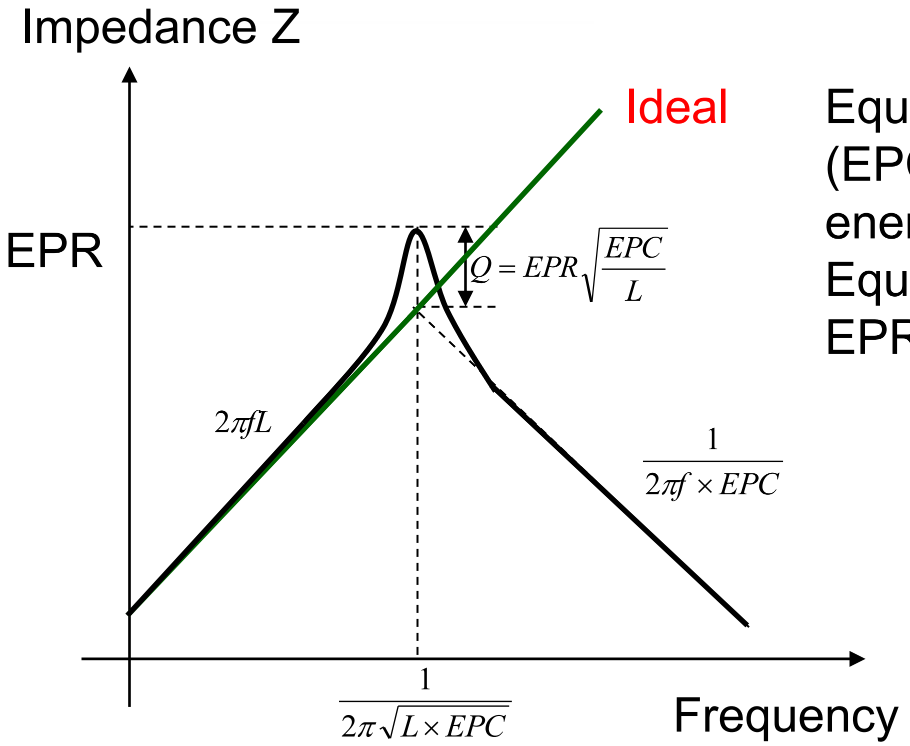

Equivalent parallel capacitance (EPC) represents the electric energy

Equivalent parallel resistance EPR represents the power loss

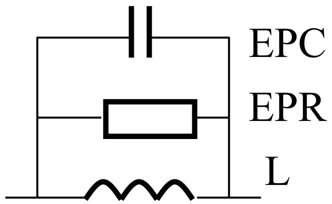

1st order approximation

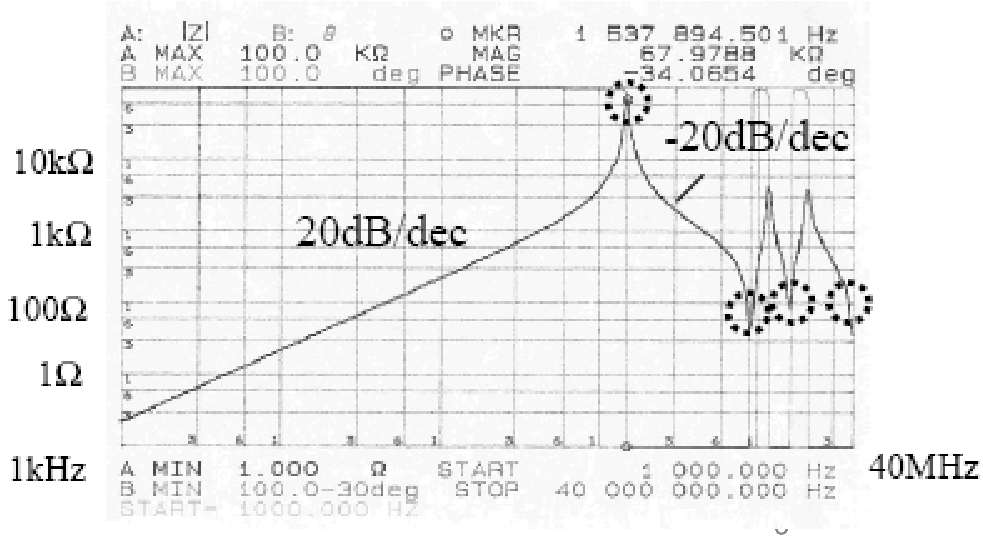

2.1 DM and CM Conductive EMI in Power Electronics Systems

Differential Mode (DM) and Common Mode (CM) Currents

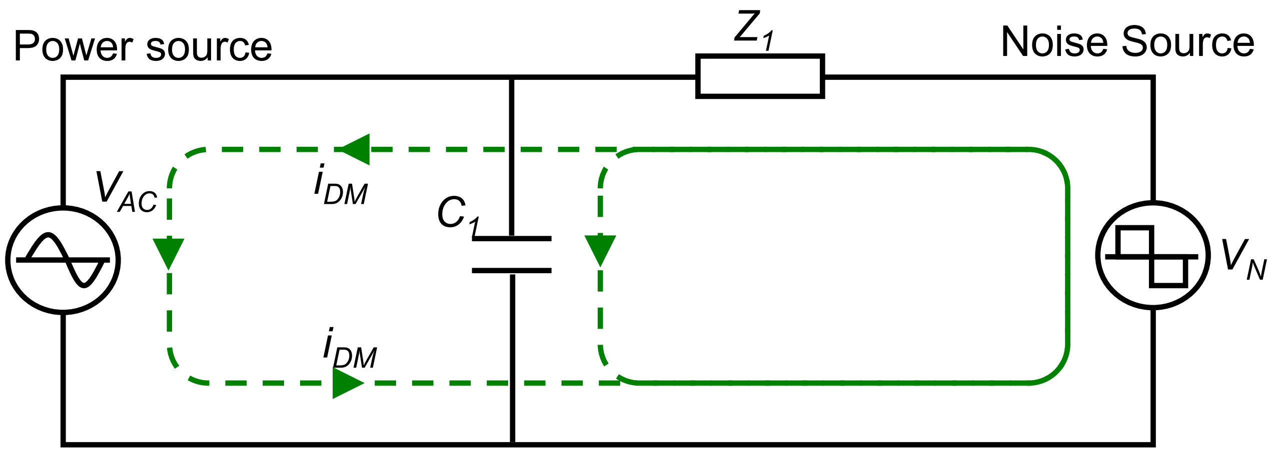

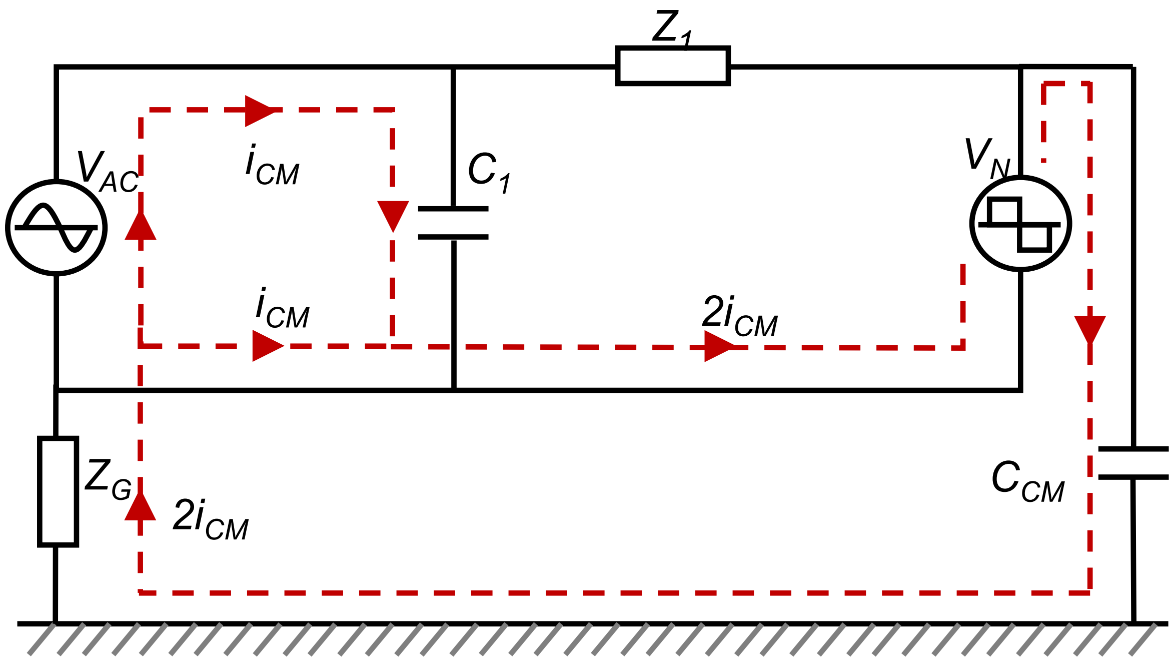

Differential mode (DM) current:

The current flowing between two power delivery paths

Common mode (CM) current:

The current flowing between two power delivery paths and the reference ground

Line Impedance Stabilization Networks (LISNs)

One pair for single phase EMI measurement

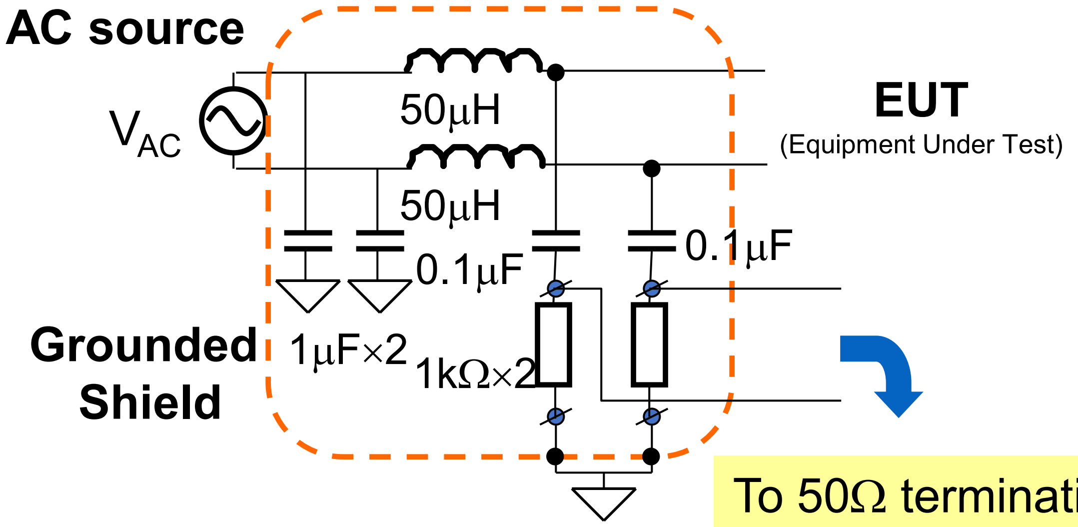

To 50Ω terminations or a spectrum analyzer

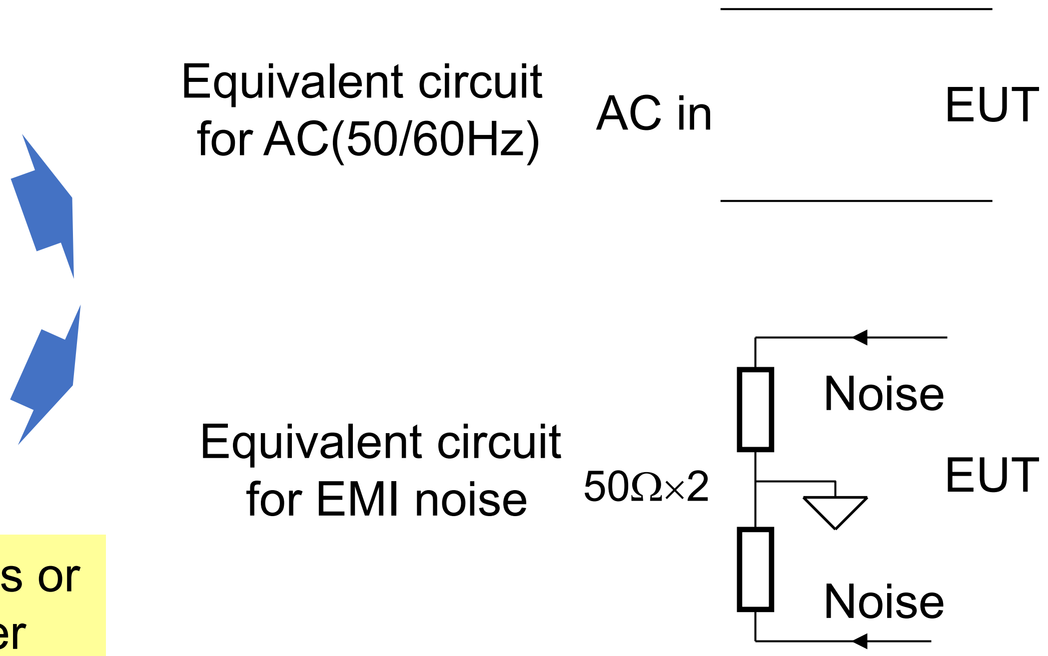

Three LISNs are needed for three phase EMI measurement (may have different parameters)

Understand the DM Conducted EMI Noise (A Buck Converter Example)

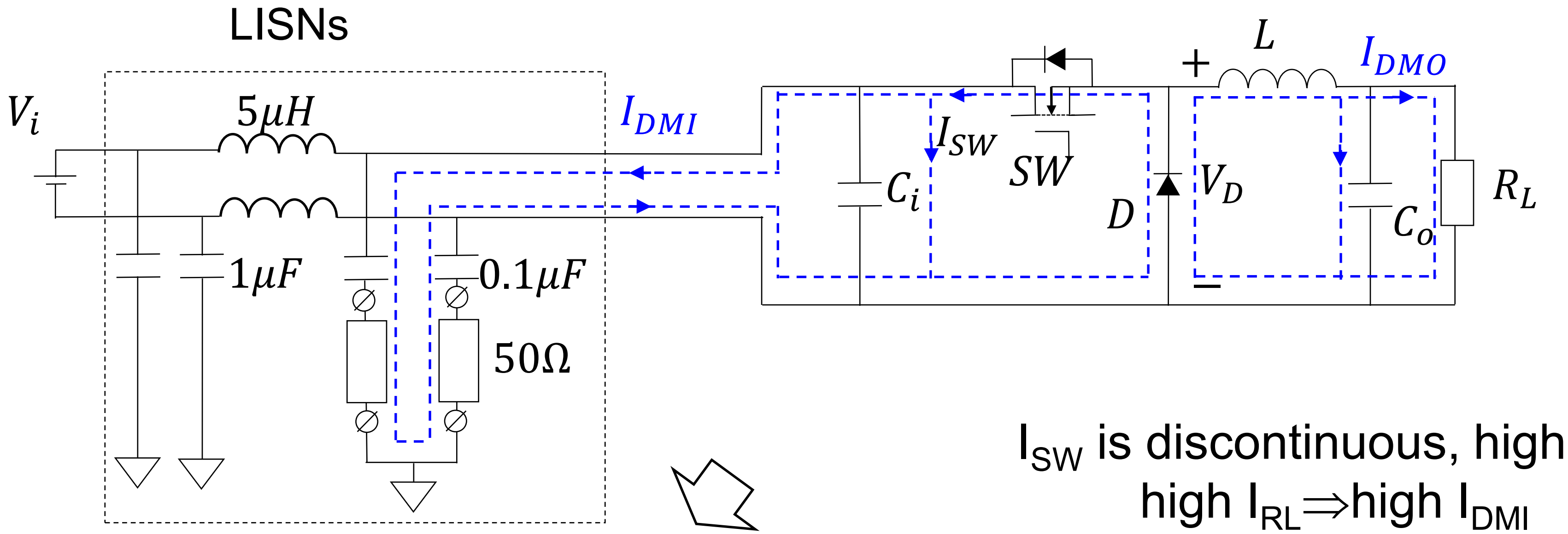

Switching Waveforms

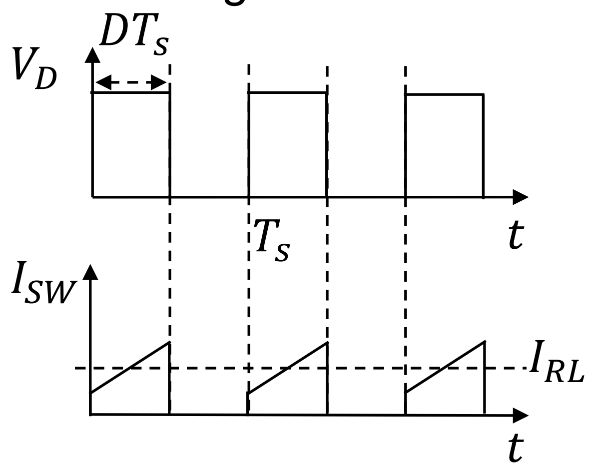

I_{SW} is discontinuous, high I_{DMI}

high $I_{RL} \Rightarrow$ high I_{DMI}

I_L is continuous

DM Noise Model

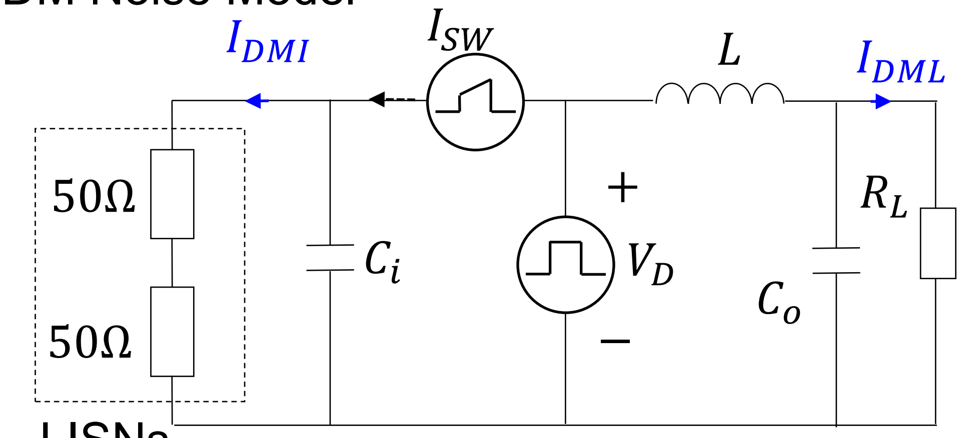

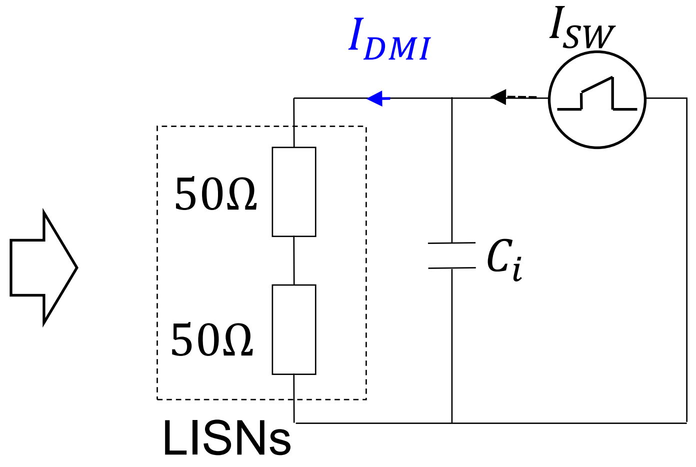

Input DM Noise

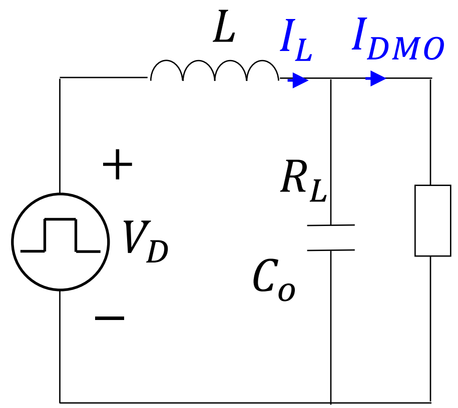

Output DM Noise

Dr. Shuo Wang, University of Florida, shuowang@ieee.org

Understand the CM Conductive EMI Noise

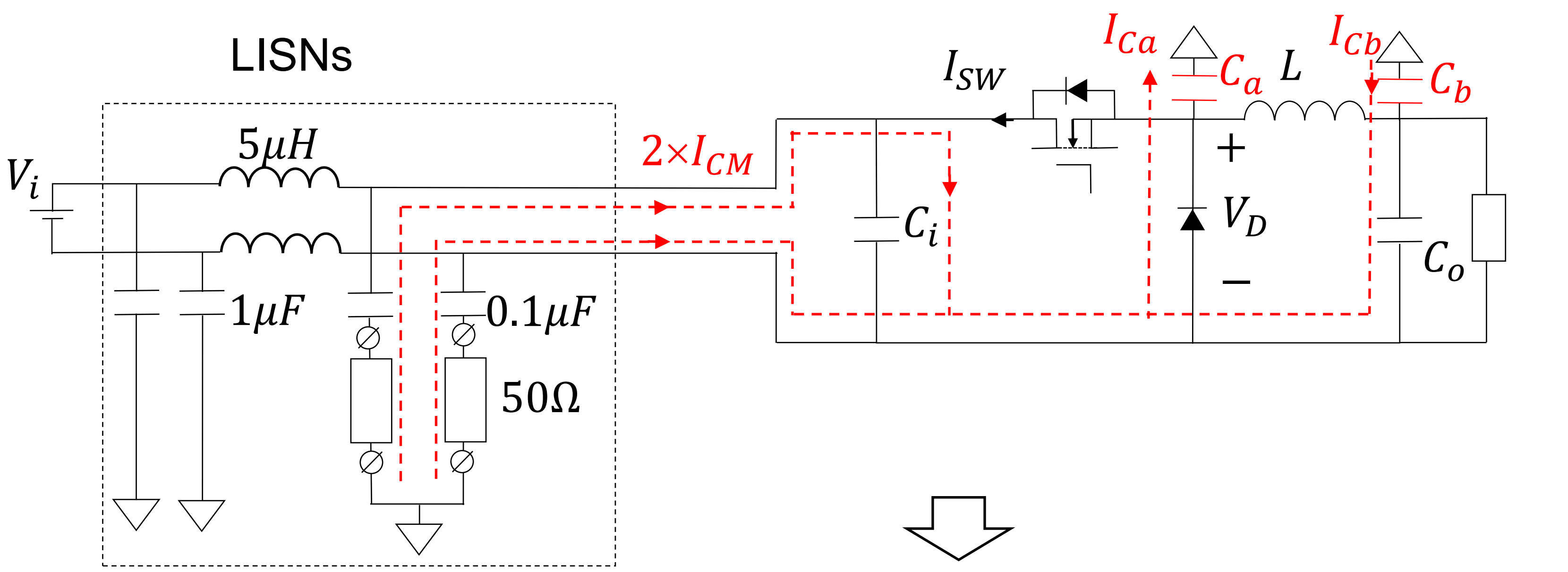

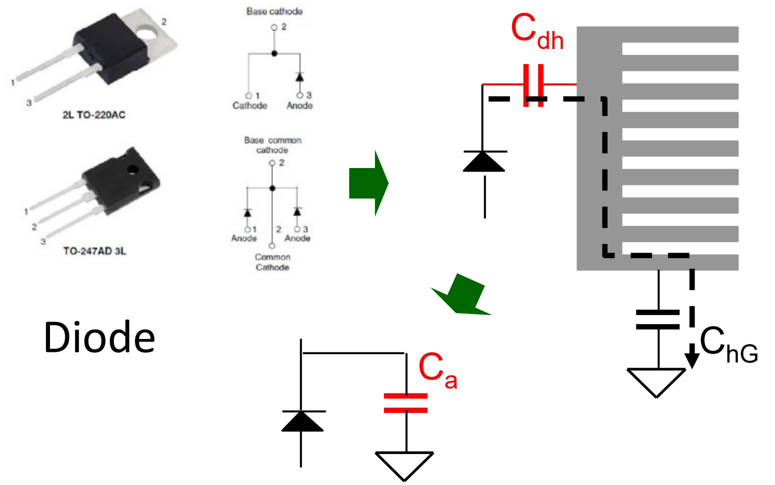

Diode

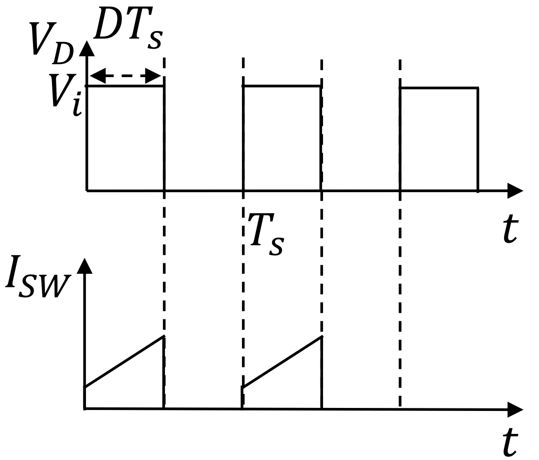

Switching Waveforms

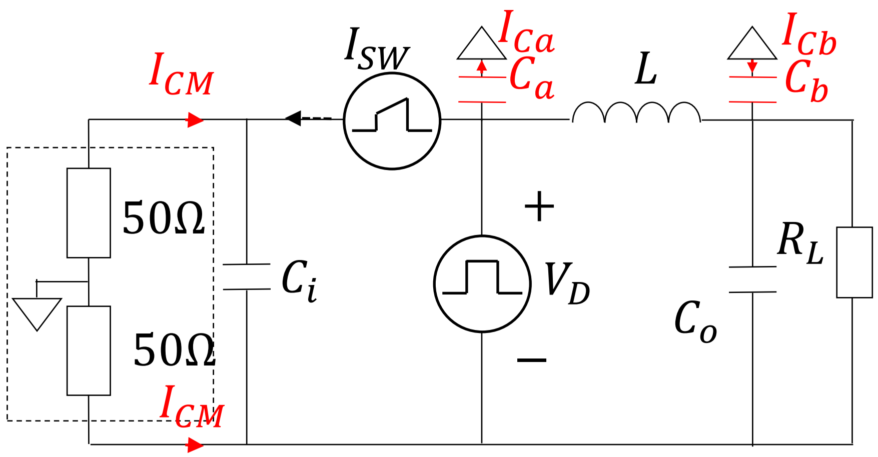

LISNs CM Noise Model

Higher V_i, higher f_s ➡ higher I_{CM}
C_b is in parallel with LISNs!

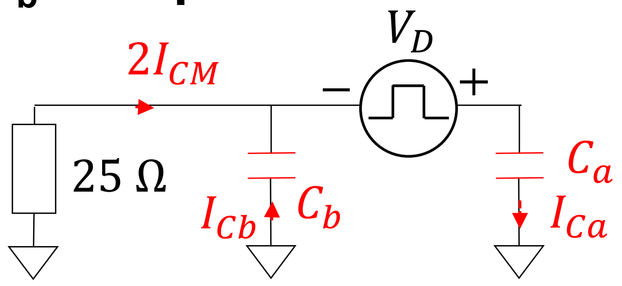

Input and output CM noise

Measurement and Separation of CM and DM Noise

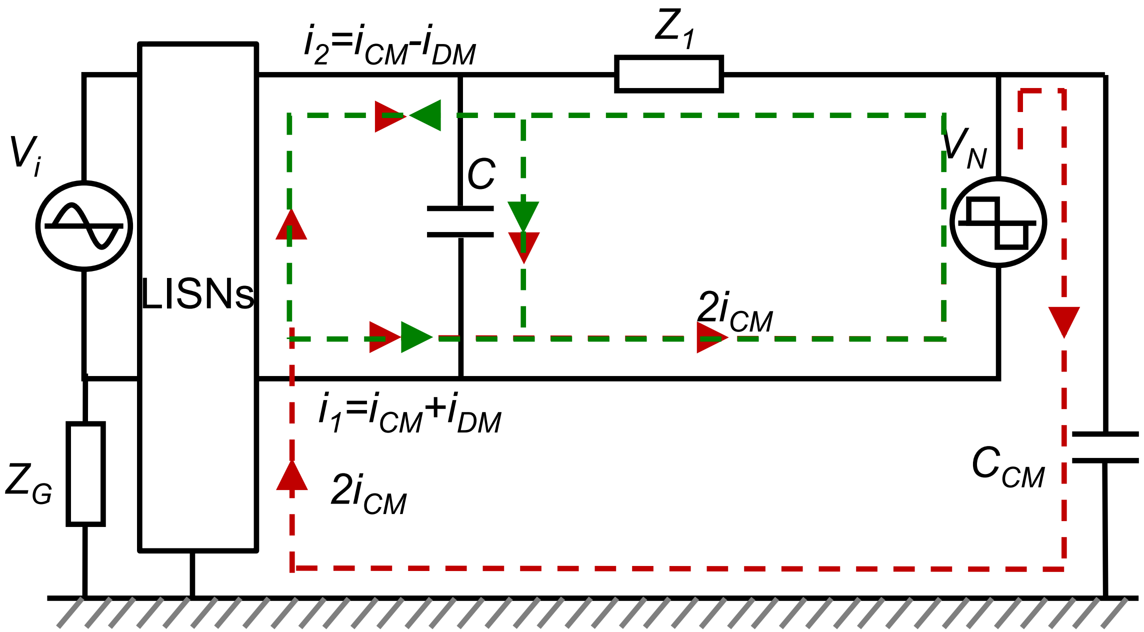

$$i_{CM}=\frac{i_1+i_2}{2},\quad i_{DM}=\frac{i_1-i_2}{2}$$

Method 1: using a current transformer:

CM Current Sensing: $2i_{CM}$

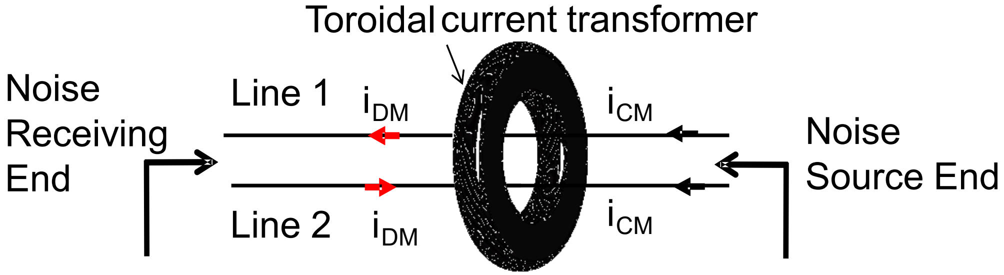

DM Current Sensing: $2i_{DM}$

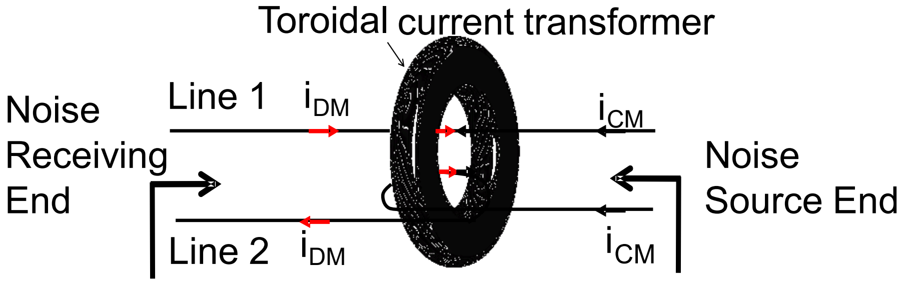

Total Current: $i_{DM}\pm i_{CM}$

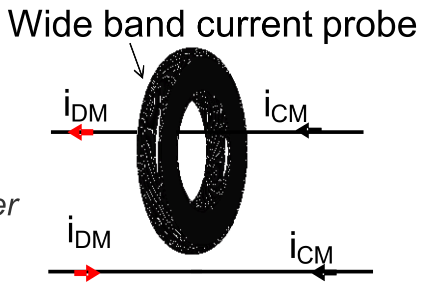

Method 2: using a noise separator

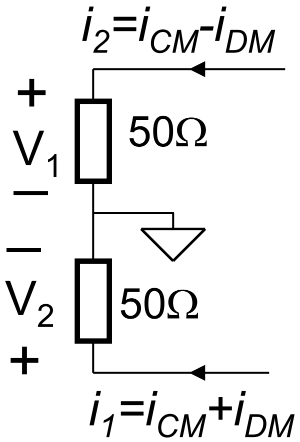

$$V_{CM}=\frac{V_1+V_2}{2}$$

$$V_{DM}=\frac{V_1-V_2}{2}$$

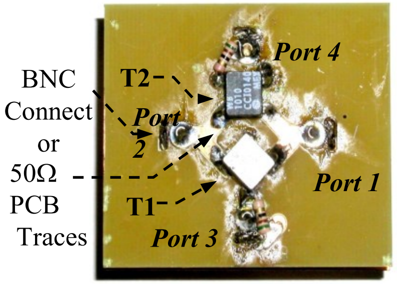

Use a noise separator

Reference: Shuo Wang, F. C. Lee and W. G. Odendaal, "Characterization, evaluation, and design of noise Separator for conducted EMI noise diagnosis," in *IEEE Transactions on Power Electronics*, vol. 20, no. 4, pp. 974-982, July 2005

Conducted EMI Noise Measurement Setups

FCC test setup (10kHz-30MHz)

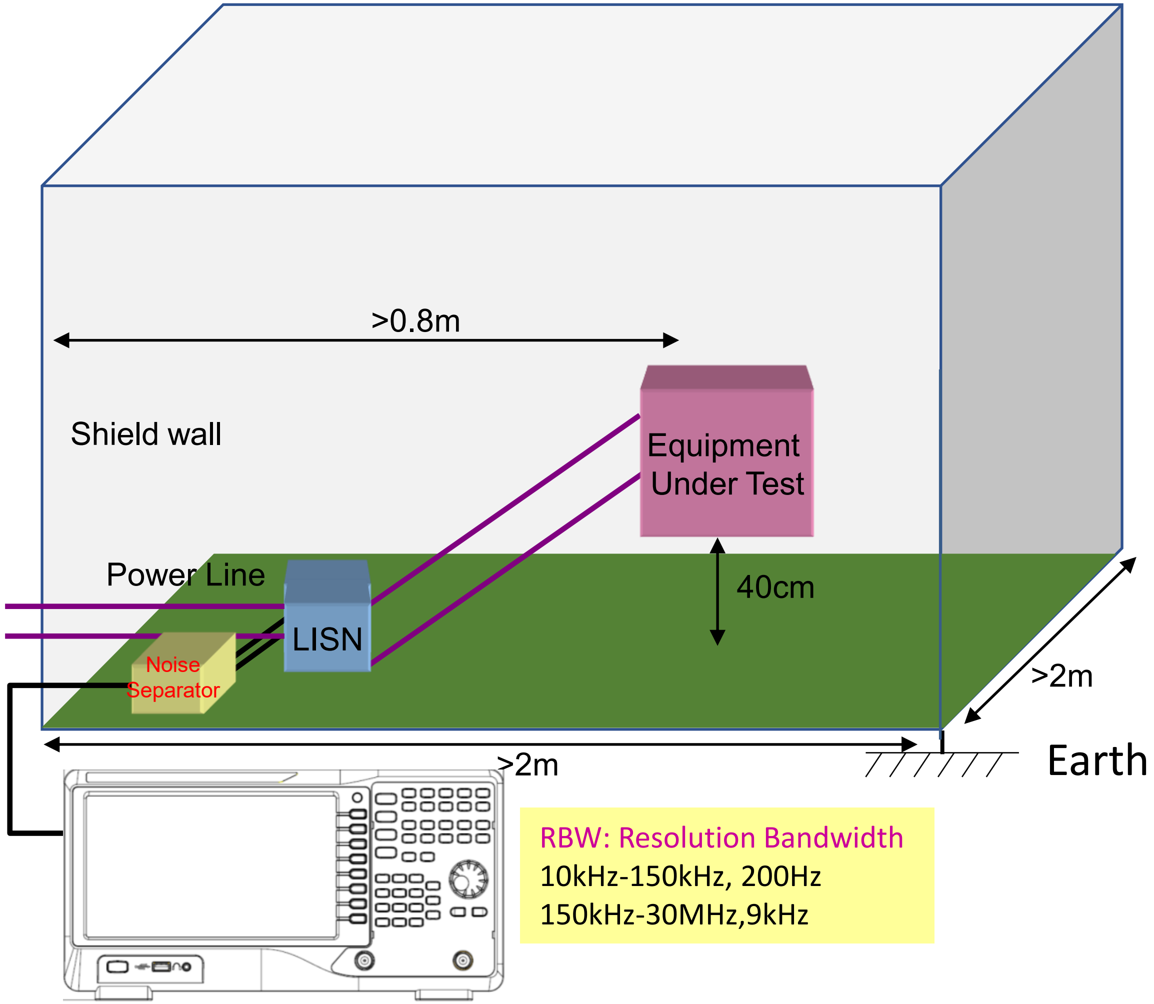

RBW: Resolution Bandwidth
10kHz-150kHz, 200Hz
150kHz-30MHz,9kHz

CISPR 25 setup (150kHz-108MHz)

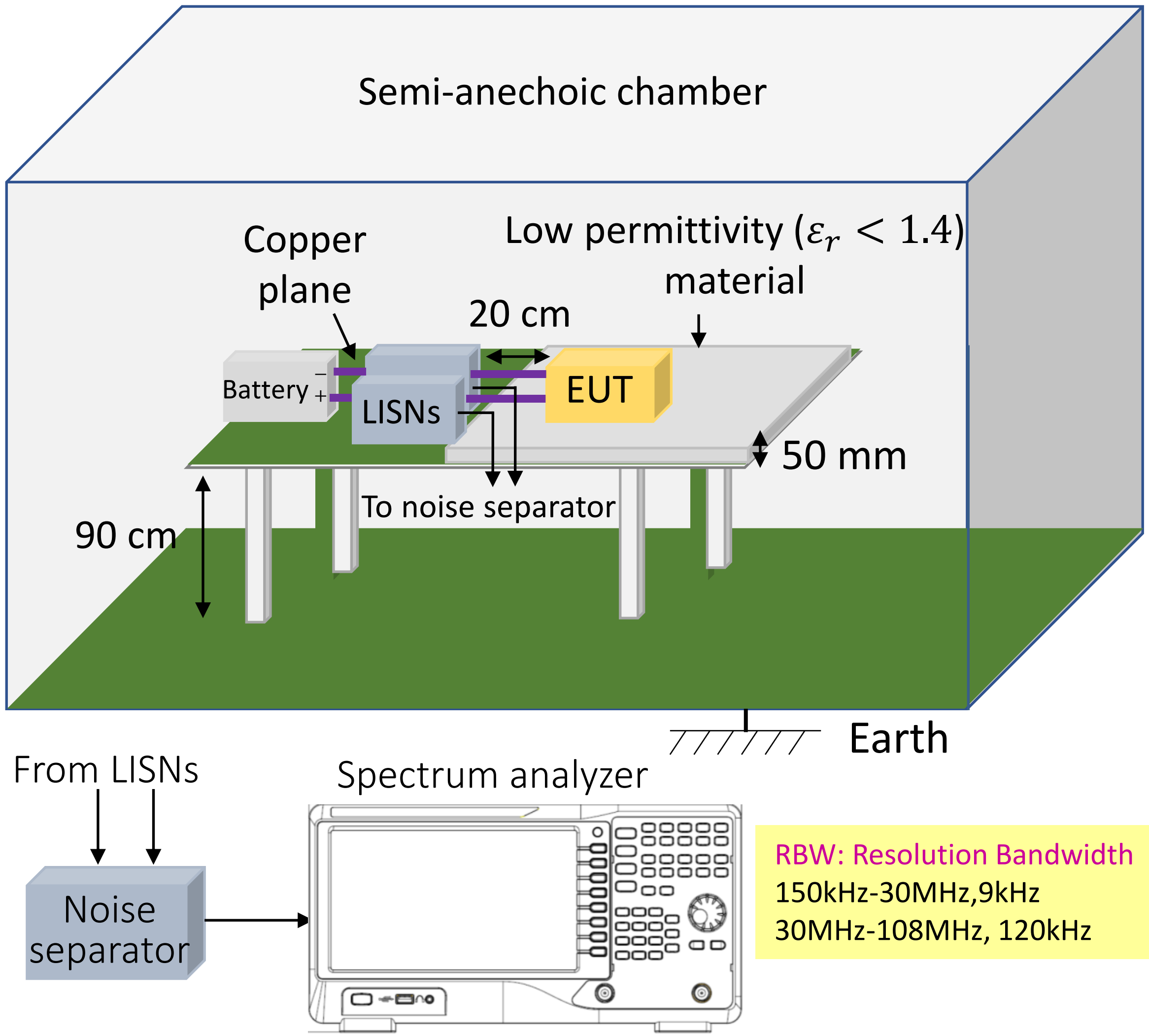

RBW: Resolution Bandwidth
150kHz-30MHz,9kHz
30MHz-108MHz, 120kHz

Mixed Mode (MM) Currents

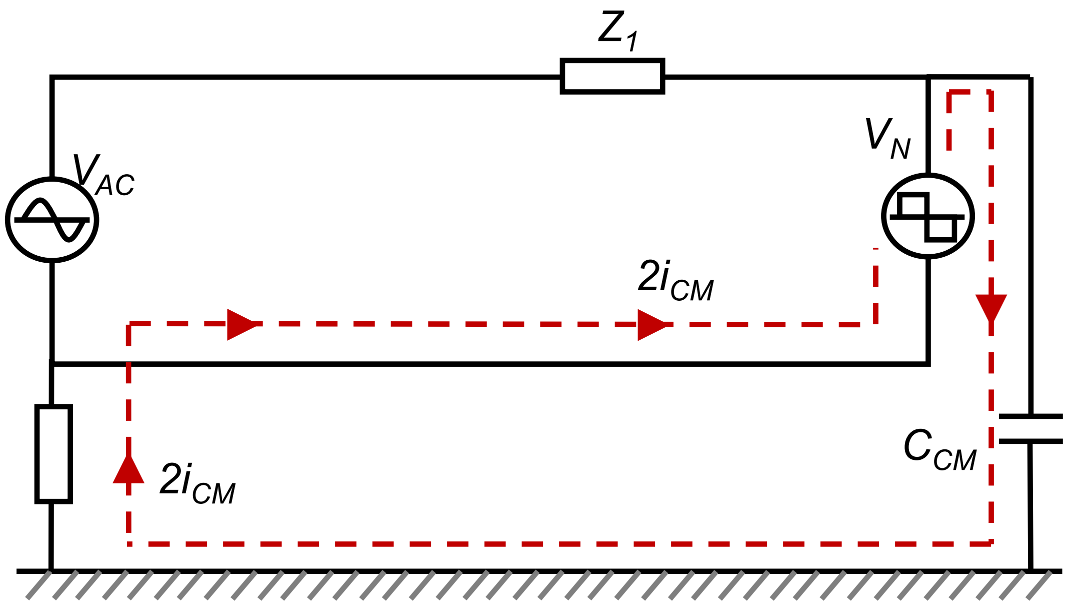

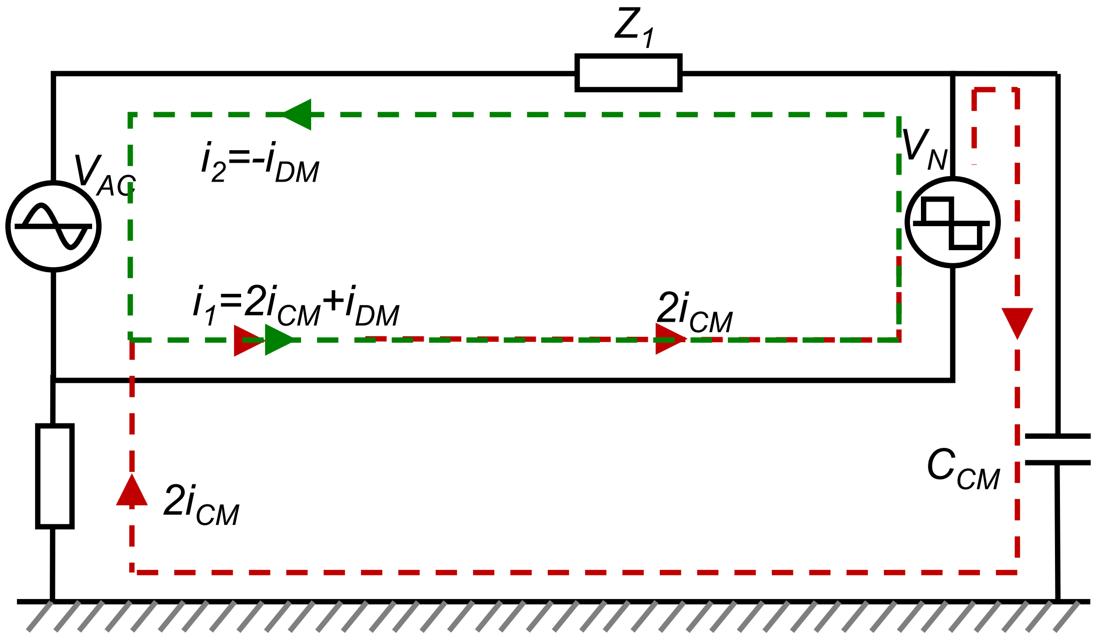

Mixed mode (MM) current:

$2i_{CM}$ flows through one power delivery path only

$$\frac{i_1 + i_2}{2} = i_{CM}$$

$$\frac{i_1 - i_2}{2} = i_{DM} + i_{CM} \neq i_{DM}$$

Mixed mode EMI can be avoided by balancing two lines using DM capacitors.

2.2 Power Inductors and Conductive Emissions

Parasitic Model of Power Inductors

1. **Inductance *L* represents the magnetic energy of the inductor**
2. **Winding capacitance *EPC* represents the electric energy of the inductor**
3. **Resistance *EPR* represents the power loss of the inductor**

<u>Under investigation:</u>
A single layer toroidal inductor

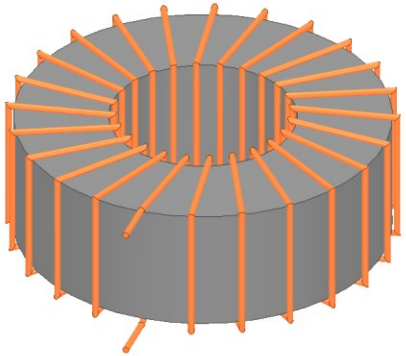

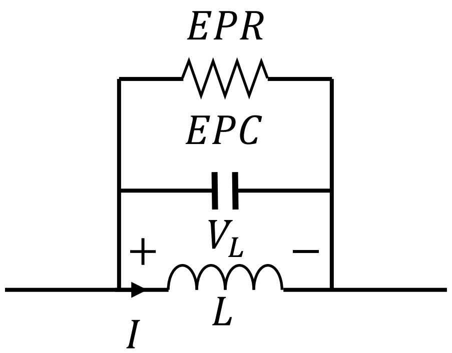

Winding resistance is ignored here

Magnetic energy E_H determines inductance:

$$E_H = \frac{L}{4}|I|^2 \approx \int_{V_{Core}} \frac{\mu'}{4}|H|^2 dv \Rightarrow L = \frac{4E_H}{|I|^2}$$

Electric energy E_E determines capacitance:

$$E_E = \frac{EPC}{4}|V_L|^2 \Rightarrow EPC = \frac{4E_E}{V_L^2}$$

Power loss P determines resistance:

$$P = \frac{|V_L|^2}{2EPR} \Rightarrow EPR = \frac{V_L^2}{2P}$$

(Amplitudes are used for I, V_L and H)

Role of Electric Field in Winding Capacitance EPC

Electric field distribution outside the core

Capacitance due to the voltage difference of winding turns and cores

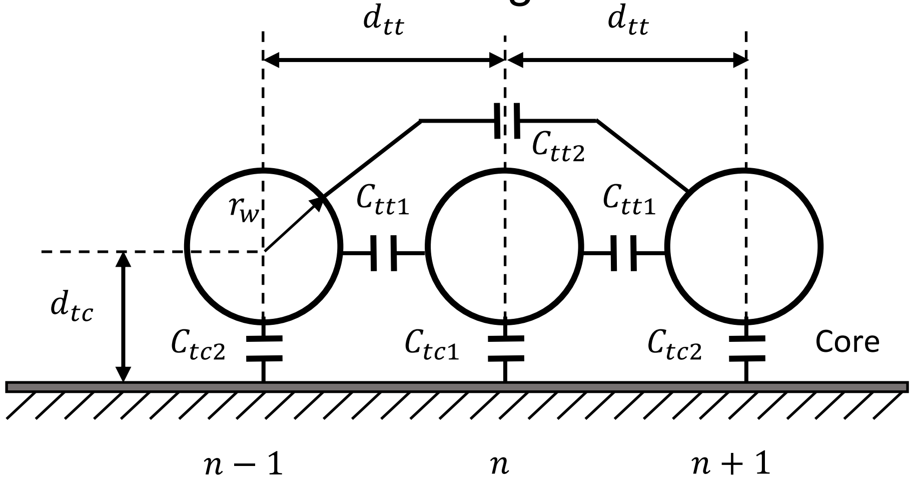

Electric field distribution

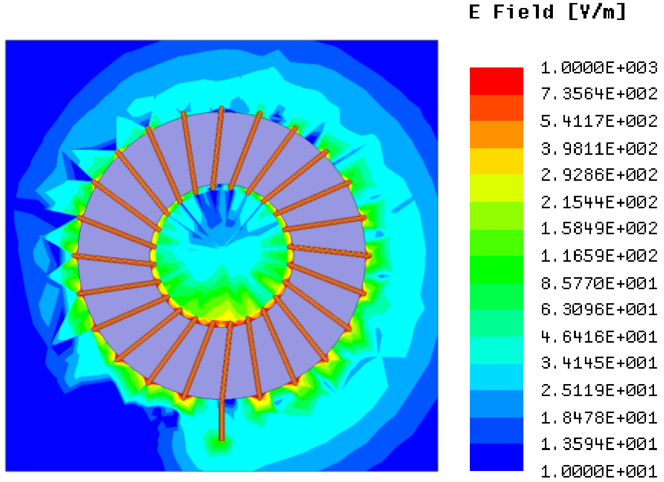

Electric field distribution inside the core

Time varying magnetic field induces time varying electric field inside the core

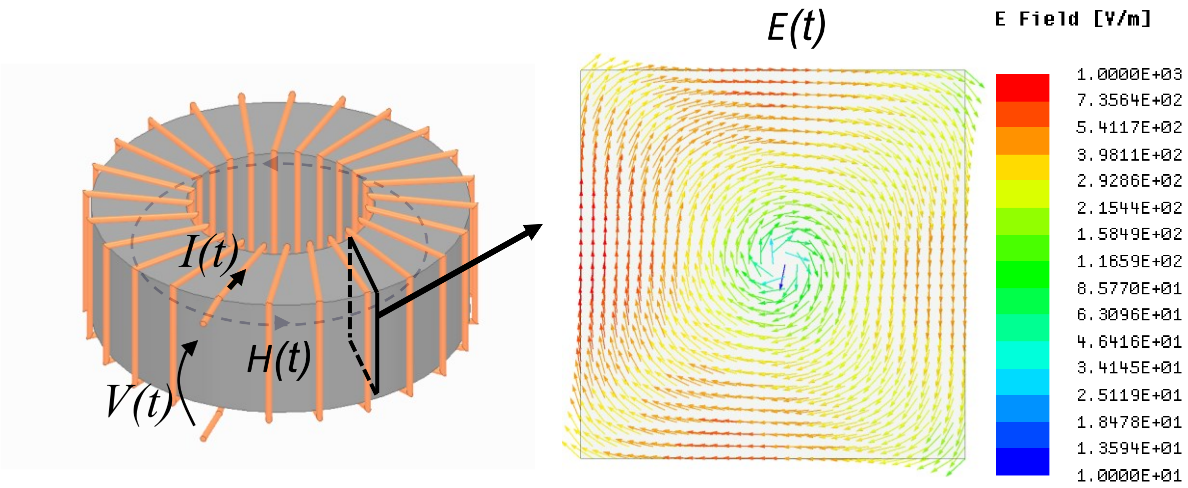

Total electric field energy E_E and EPC:

$$E_E = \frac{EPC}{4}|V_L|^2 = \int_{V_{Space}} \frac{\varepsilon_0}{4}|E|^2 dv + \int_{V_{Core}} \frac{\varepsilon'}{4}|E|^2 dv$$

$$EPC = \frac{4E_E}{V_L^2}$$

Reference: Y. Li and S. Wang, "Modeling and Increasing the High-Frequency Impedance of Single-Layer Mn-Zn Ferrite Toroidal Inductors With Electromagnetic Analysis," in *IEEE Transactions on Power Electronics*, vol. 36, no. 6, pp. 6943-6953, June 2021, doi: 10.1109/TPEL.2020.3039809.

Role of Electric Field in Power Loss and Equivalent Resistance EPR

Power loss of cores:

1. Eddy current power loss P_E
2. Hysteresis power loss P_H
3. Dielectric power loss P_D

Core parameters:

1. Conductivity: σ
2. Permeability: $\mu = \mu' - j\mu''$
3. Permittivity: $\varepsilon = \varepsilon' - j\varepsilon''$

$$P = \frac{|V_L|^2}{2EPR} = P_E + P_H + P_D$$

$$= \int_{V_{Core}} \frac{1}{2}\sigma|E|^2 dv + \int_{V_{Core}} \frac{1}{2}\omega\mu''|H|^2 dv + \int_{V_{Core}} \frac{1}{2}\omega\varepsilon''|E|^2 dv$$

$$EPR = \frac{|V_L|^2}{2P}$$

1. **Electric field impacts both eddy current power loss and dielectric power loss, therefore EPR**
2. **Electric field also impacts winding capacitance EPC**
3. **Electric field therefore plays an important role on inductor's performance**

Power Inductor Impedance's Impact on Conductive EMI

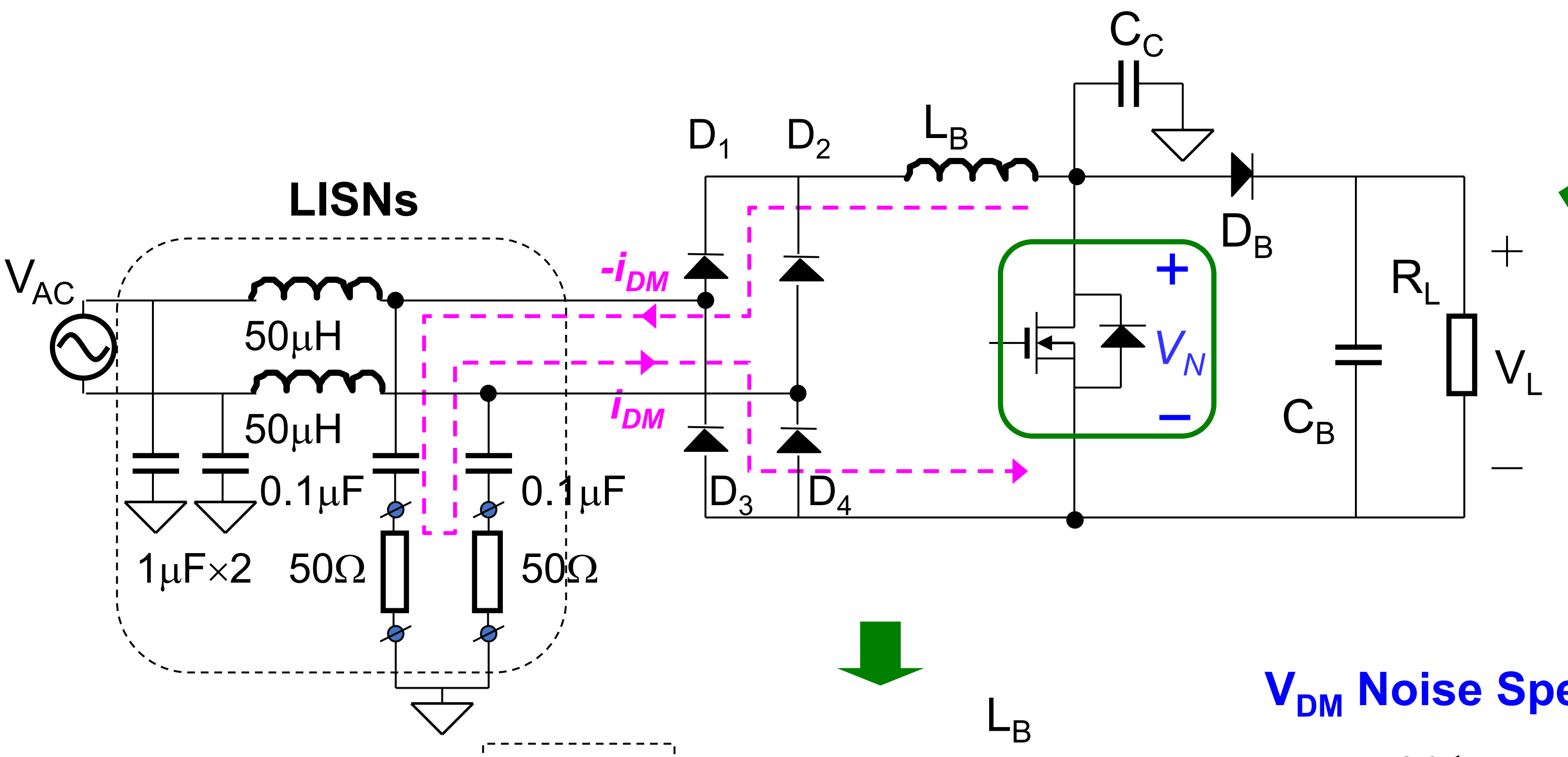

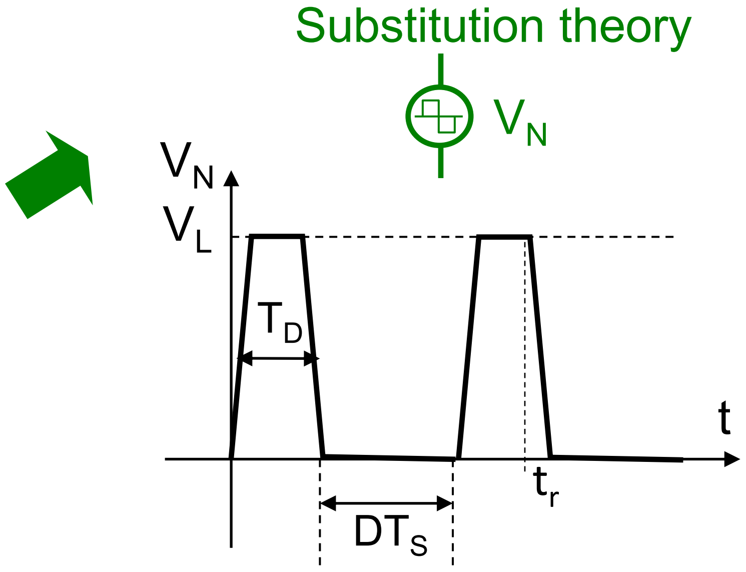

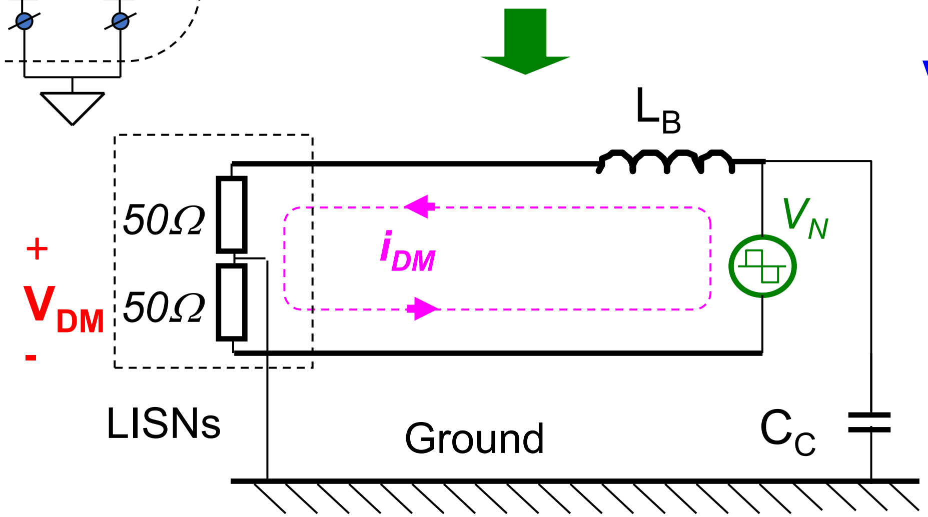

V_{DM} Noise Spectrum:

$$20\log V_{DM} = 20\log\left(\frac{0.5Z_{load}}{Z_{Load}+Z_{LB}+Z_{loop}}\bullet V_N\right)$$

$$= 20\log V_N - 20\log(Z_{Load}+Z_{LB}+Z_{loop}) + 14\log Z_{Load}$$

Noise Source **Path Impedance**

Noise Source and Impedance Determine DM EMI Spectrum

V_{DM} Noise Spectrum:

$$20\log V_{DM} = 20\log\left(\frac{0.5Z_{load}}{Z_{Load}+Z_{LB}+Z_{loop}}\bullet V_N\right)$$

$$= 20\log V_N - 20\log(Z_{Load}+Z_{LB}+Z_{loop}) + 14\log Z_{Load}$$

Noise Source **Path Impedance**

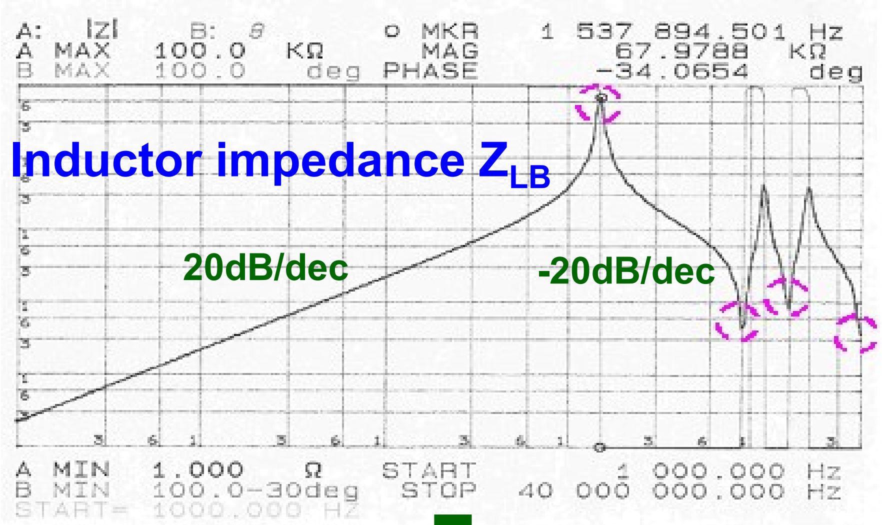

Noise Source Waveform

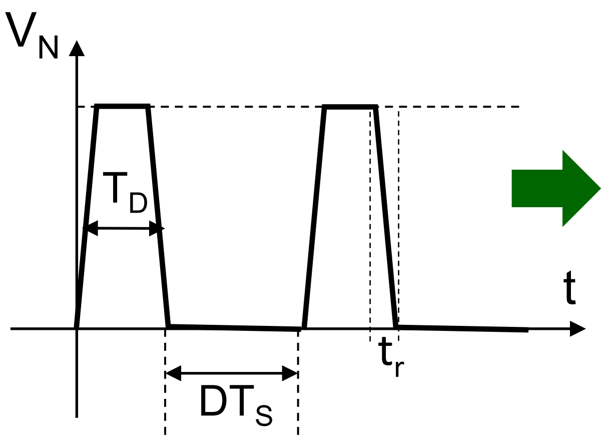

Noise Source Spectrum

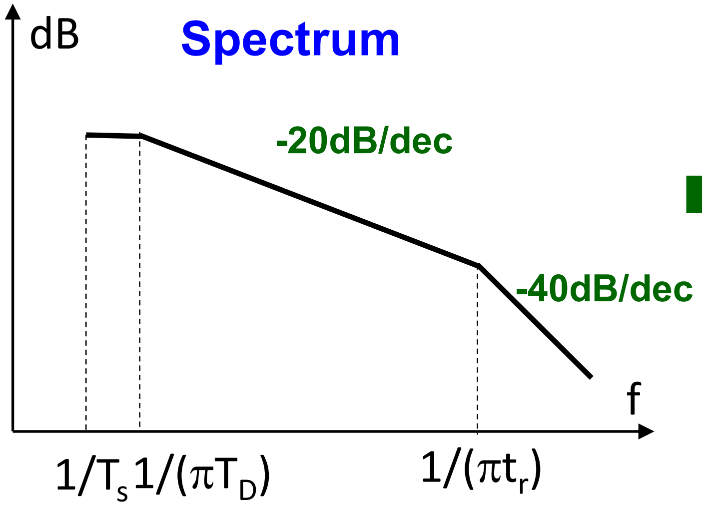

DM Noise Spectrum

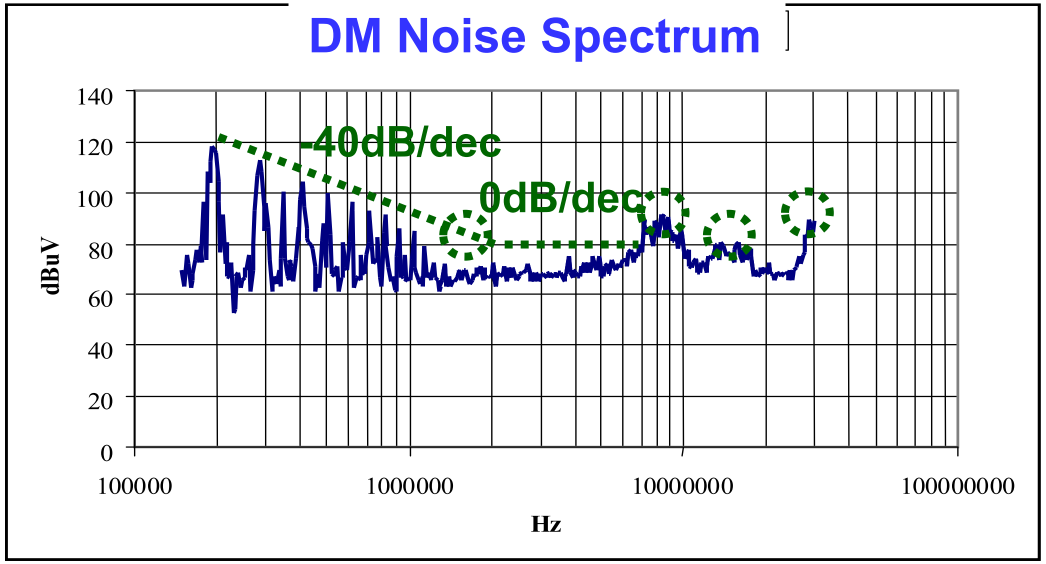

DM EMI Reduction with Optimal Inductor Design

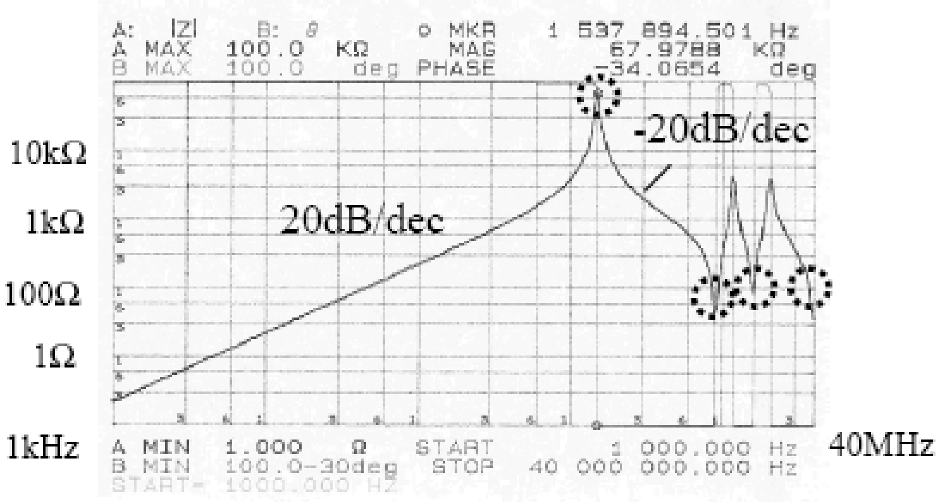

Original (Cool Mu core)

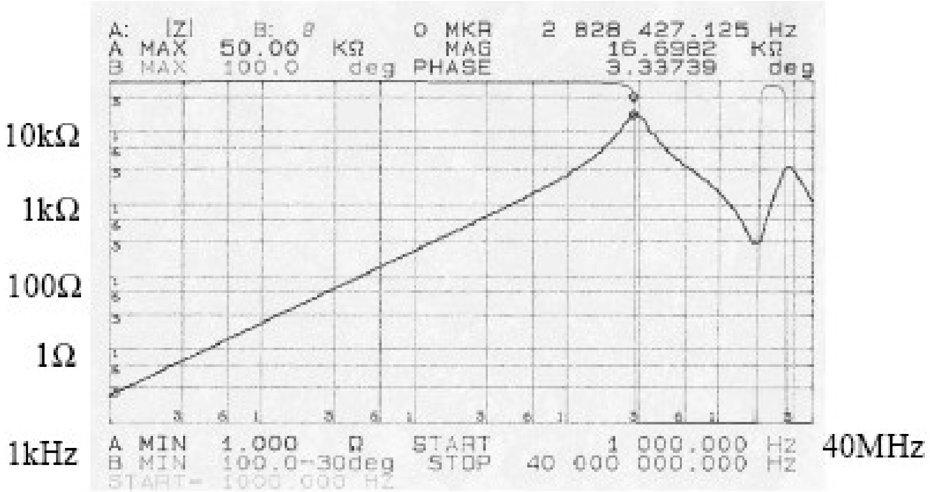

Redesigned (Iron Powder core)

Core materials:

Original: Cool Mu; ur=60

Redesigned: Iron Powder; ur=100

(1) Higher HF core loss(0.46W higher);
----Higher damping at resonant frequencies

(2) Higher permeability therefore fewer number of turns and smaller parasitic capacitances
----Higher first peak frequency. Extending self-attenuation to higher frequency.

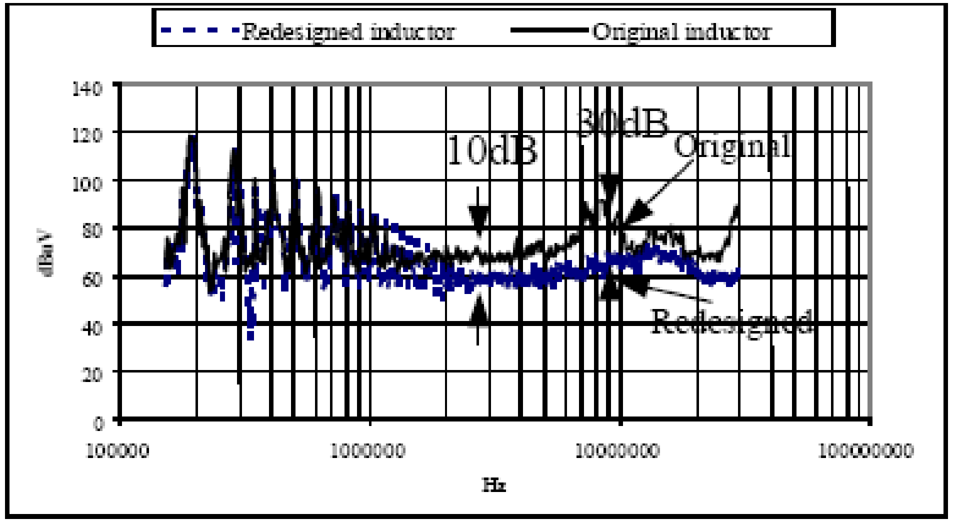

- **HF lossy inductor is good for HF EMI reduction**
- **Always sweep inductor impedance**

Reference: Shuo Wang, F. C. Lee and W. G. Odendaal, "Single layer iron powder core inductor model and its effect on boost PFC EMI noise," *IEEE 34th Annual Conference on Power Electronics Specialist, 2003. PESC '03.*, 2003, pp. 847-852 vol.2, doi: 10.1109/PESC.2003.1218167.

3.1 Near Field Emission in Power Electronics Systems

Dr. Shuo Wang, University of Florida, shuowang@ieee.org

Near Field and Far Field

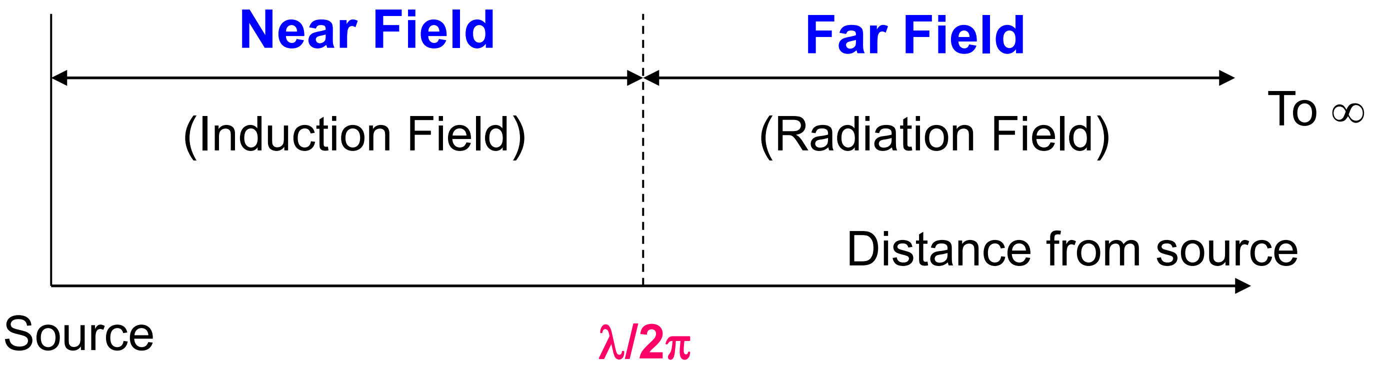

For 1MHz, $\frac{\lambda}{2\pi} \approx 150\,ft = 45m$

For 1GHz, $\frac{\lambda}{2\pi} \approx 0.15\,ft = 4.5cm$

Wave Impedance:

$$Z = \frac{E}{H} = \sqrt{\frac{j\omega\mu}{\sigma + j\omega\varepsilon}}$$

$$Z_{Air} = \sqrt{\frac{\mu_0}{\varepsilon_0}} = 377\Omega$$

High voltage & low current source

High current & low voltage source

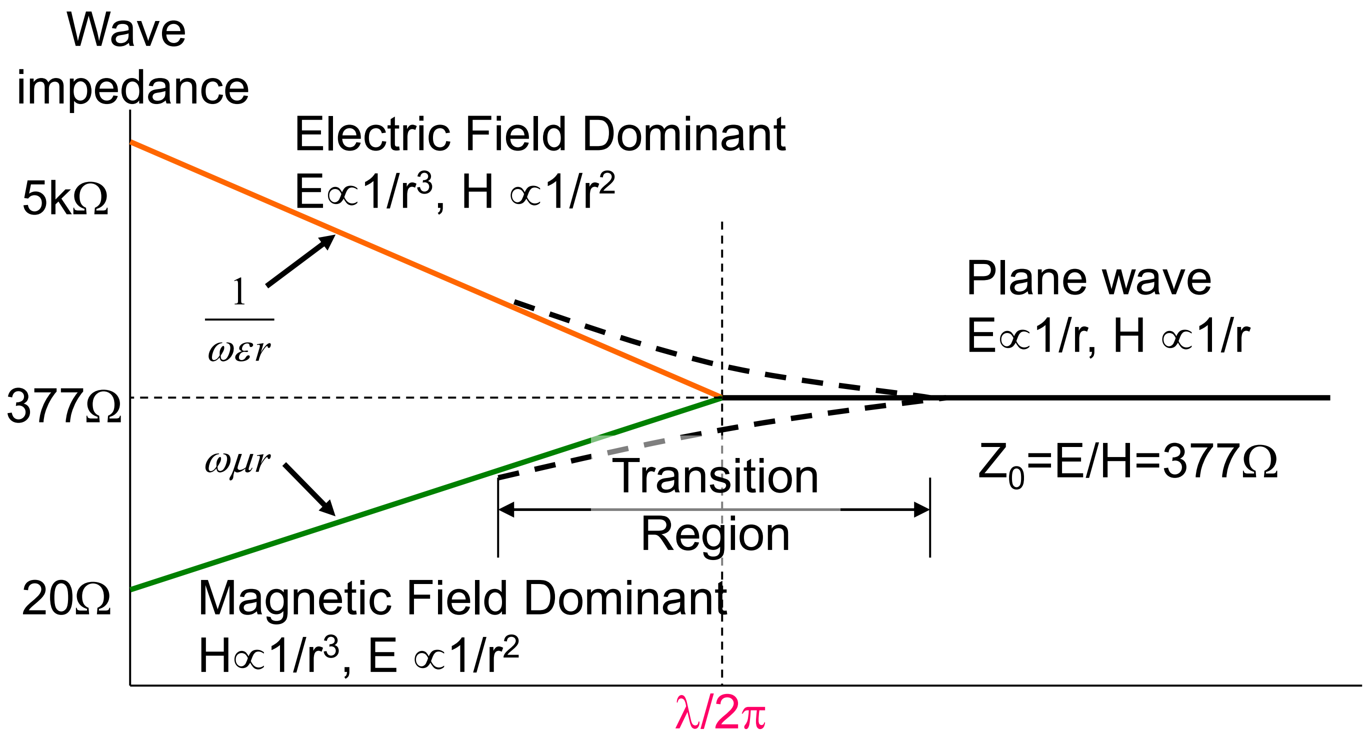

Near Inductive/Magnetic Couplings Modeling

Physical representation

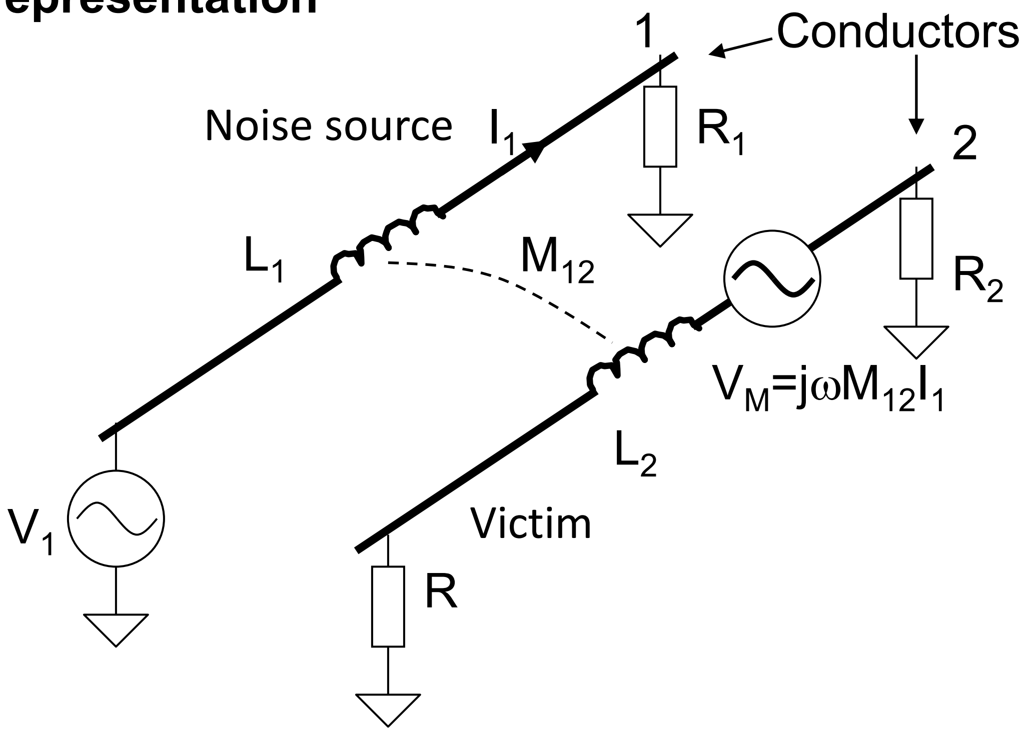

Equivalent circuit

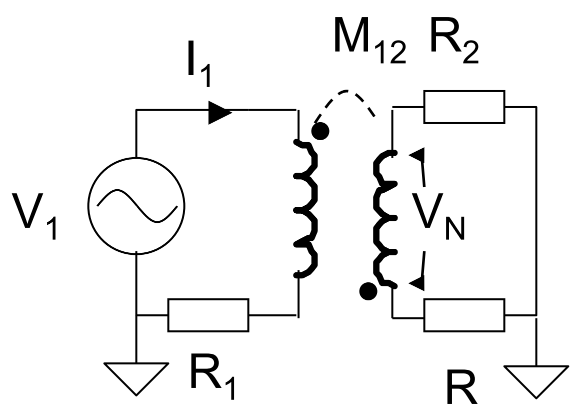

V_N is the noise voltage on two resistors

$$V_N \approx \frac{j\omega M_{12} I_1}{1 + \frac{j\omega L_2}{R + R_2}}$$

At low frequencies:

$$V_N = V_M = j\omega M_{12} I_1$$

Not a function of load: voltage source

At high frequencies:

$$V_N = \frac{M_{12}}{L_2} I_1 (R + R_2)$$

Proportional to load: current source

Near Inductive/Magnetic Field

Near magnetic field sources:

Inductors, transformers, high *di/dt* current loops, HF noise current loops, etc.

CM Inductor w/ DM current excitation

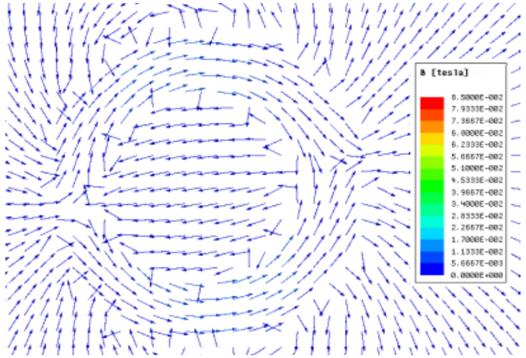

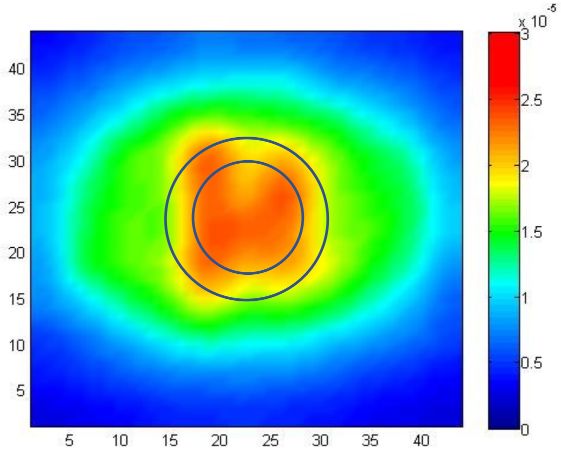

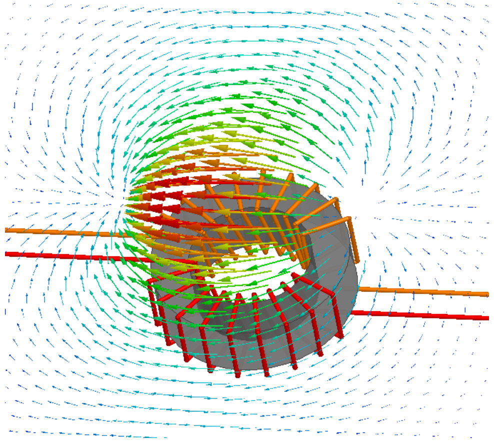

Transformers

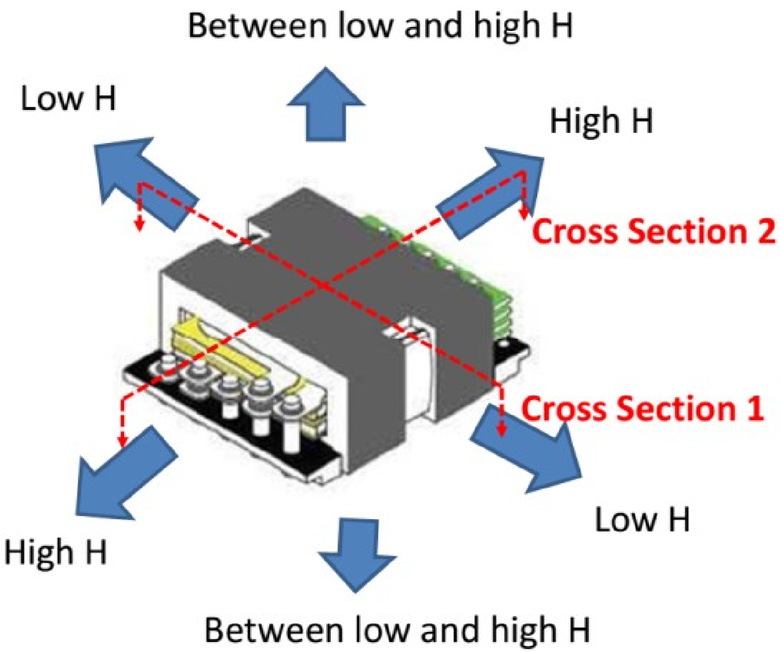

Near Capacitive/Electric Field Coupling Modeling

Physical representation

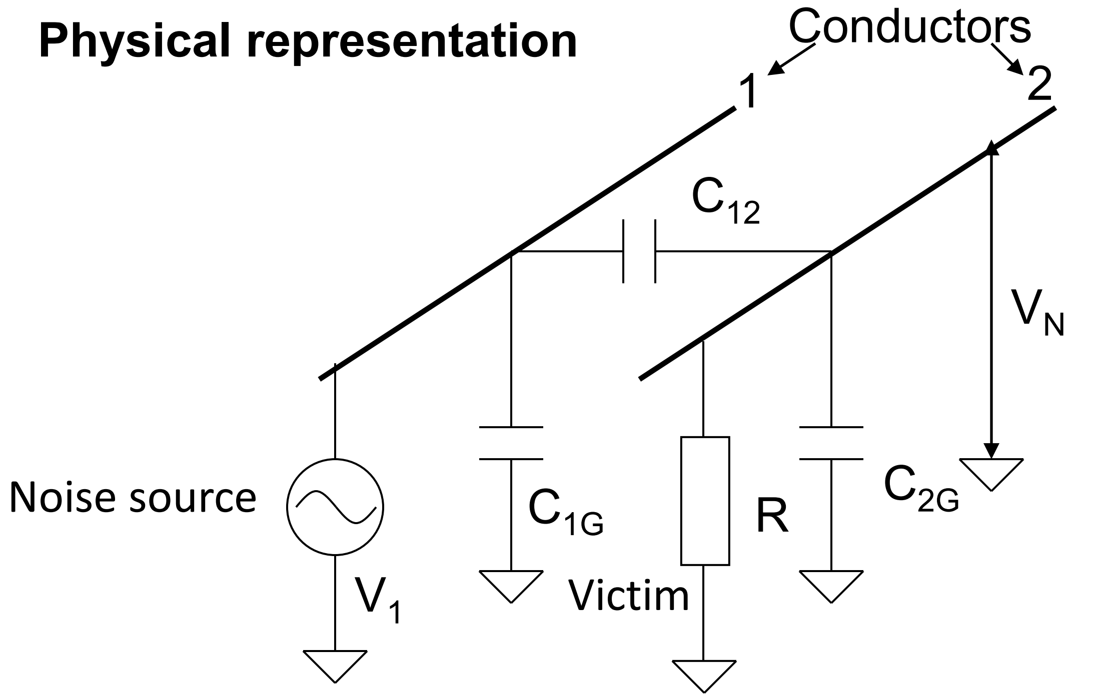

Equivalent circuit

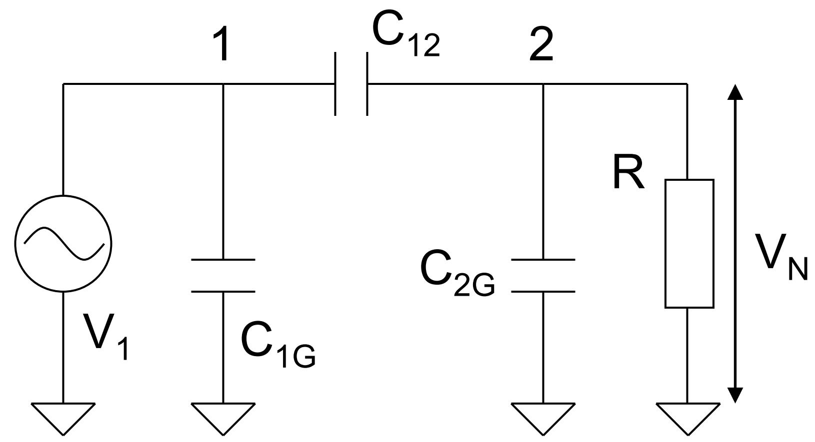

$$V_N = \frac{j\omega[C_{12}/(C_{12}+C_{2G})]}{j\omega + 1/R(C_{12}+C_{2G})} V_1$$

At low frequencies:

If, $R << \dfrac{1}{\omega(C_{12}+C_{2G})}$,

$$V_N = j\omega R C_{12} V_1$$

Proportional to load: current source

At high frequencies:

If $R >> \dfrac{1}{\omega(C_{12}+C_{2G})}$,

$$V_N = \left(\frac{C_{12}}{C_{12}+C_{2G}}\right) V_1$$

Not a function of load: voltage source

Near Capacitive/Electric Field

Near electric field sources:

High *dv/dt* nodes, HF noise voltage nodes, inductors, transformers, etc.

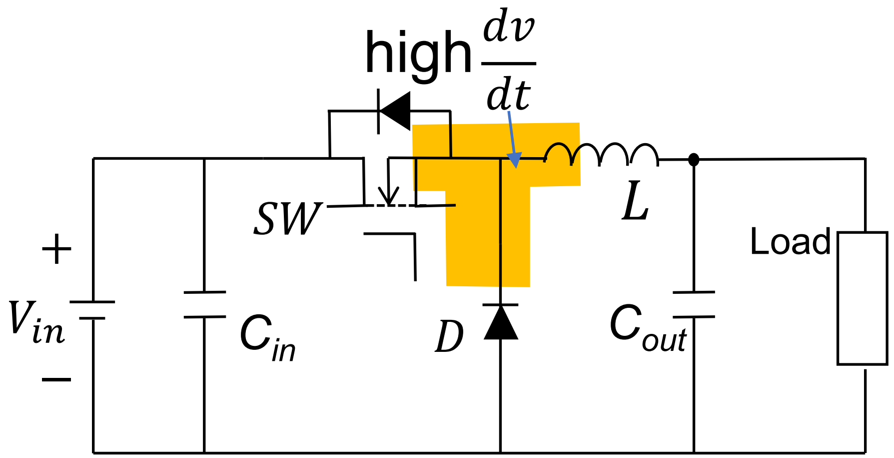

Buck converter

High dv/dt area: PCB node of the inductor, MOSFET and diode

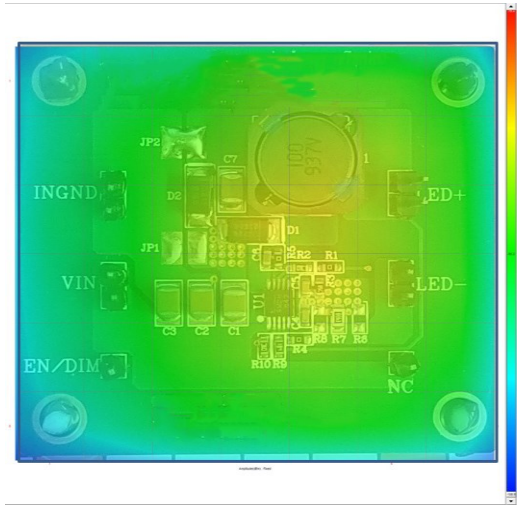

Measured E field at switching f

With shielding

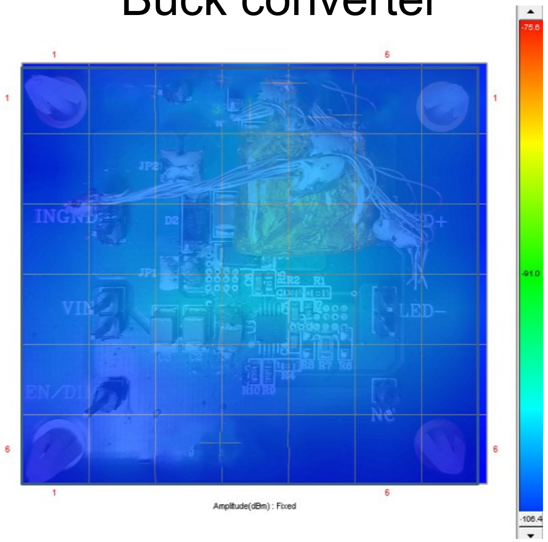

3.2 Power Inductor’s Near Field Emissions

Near Magnetic Field Emission of Power Inductors

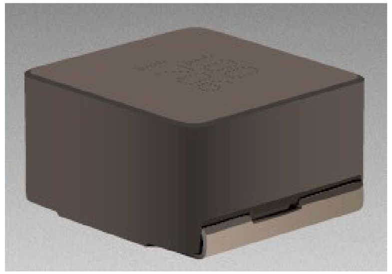

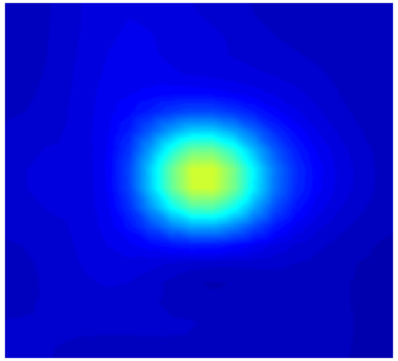

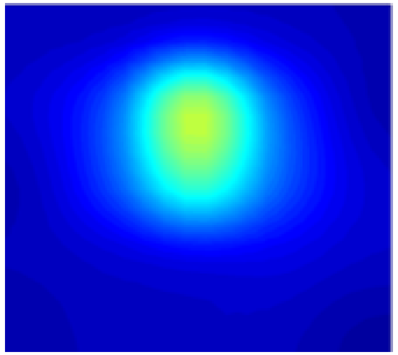

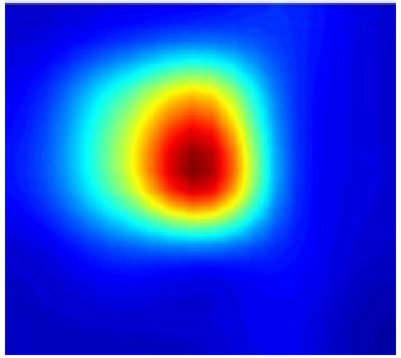

The measured near magnetic field 2cm above the inductors

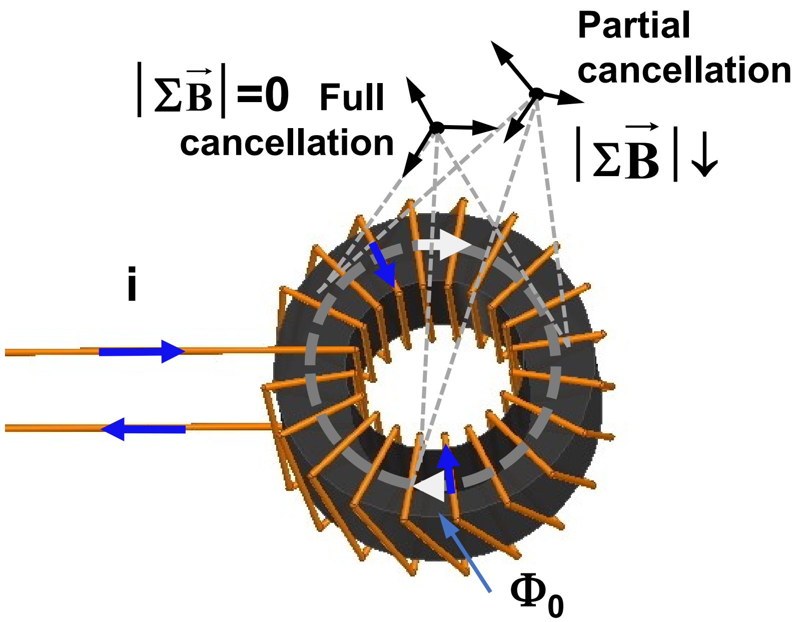

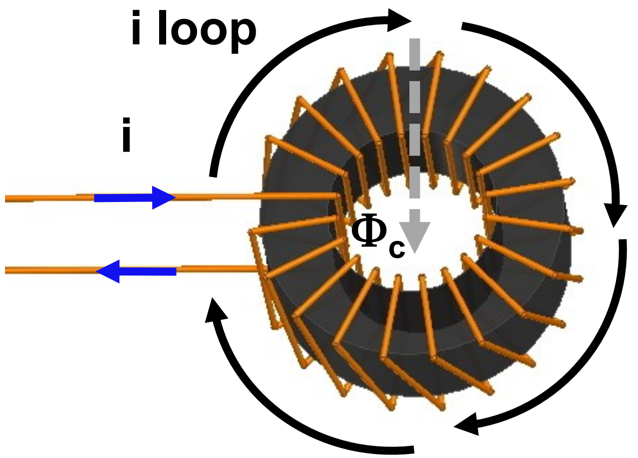

Near Magnetic Field Emission of Power Inductors

The near magnetic field generated from 360° winding turns is small due to partial cancellation

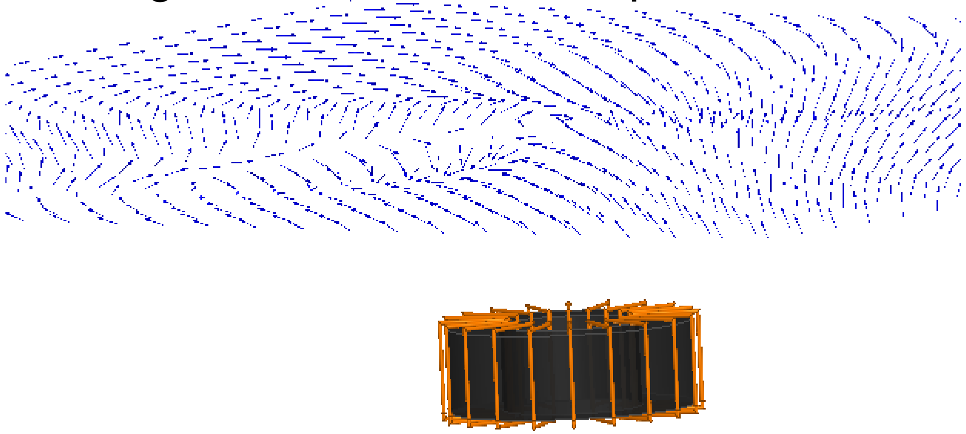

The near magnetic field generated from the equivalent current circle is high

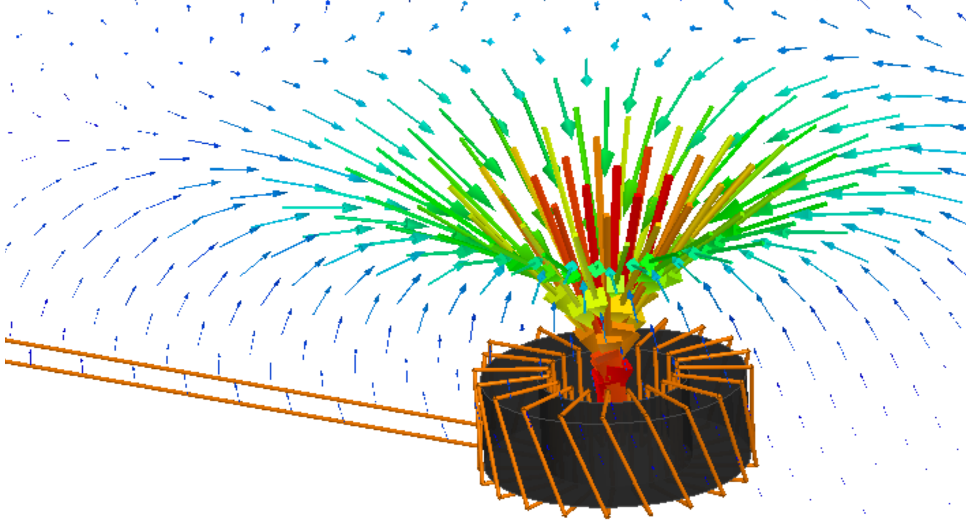

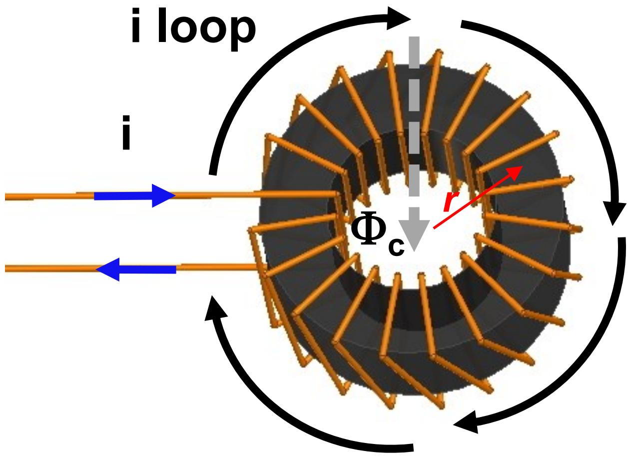

$$\Phi_C = i(\mu_0 r[\ln\left(\frac{1.05r}{a}\right)]$$

r is average radius of the core and
a is wire conductor's radius

Larger *r*, higher magnetic field emission

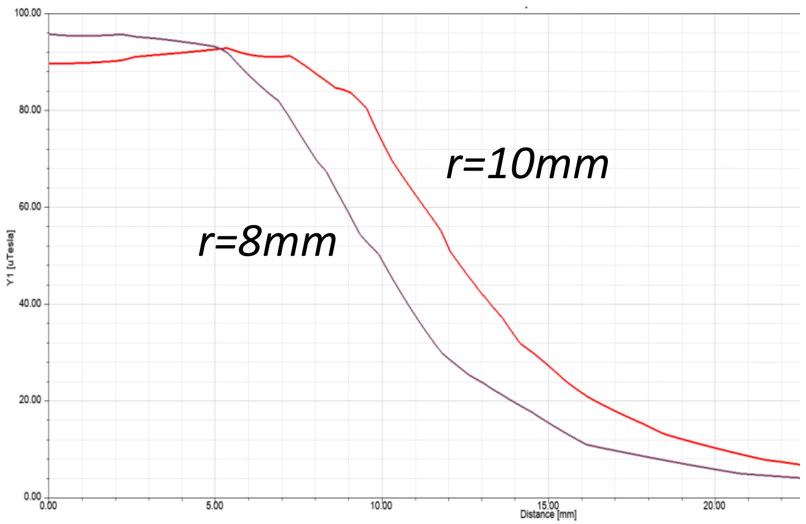

Reference: B. Zhang and S. Wang, "Analysis and Reduction of the Near Magnetic Field Emission From Toroidal Inductors," in *IEEE Transactions on Power Electronics*, vol. 35, no. 6, pp. 6251-6268, June 2020, doi: 10.1109/TPEL.2019.2953748.

Near Magnetic Field Reduction with Twisted Windings

Conventional

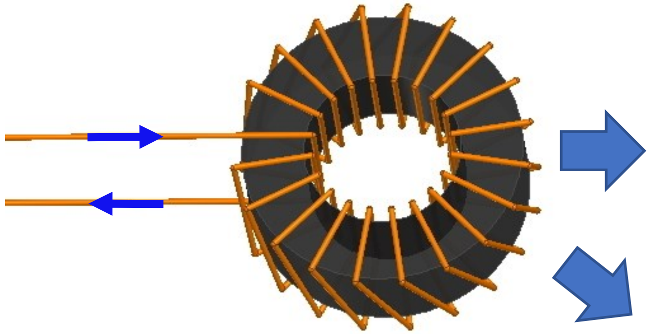

Simulated

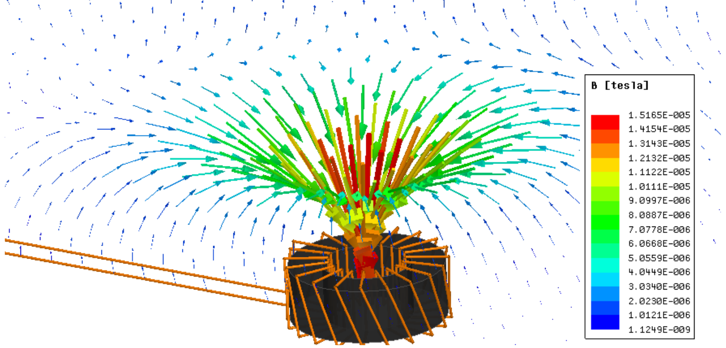

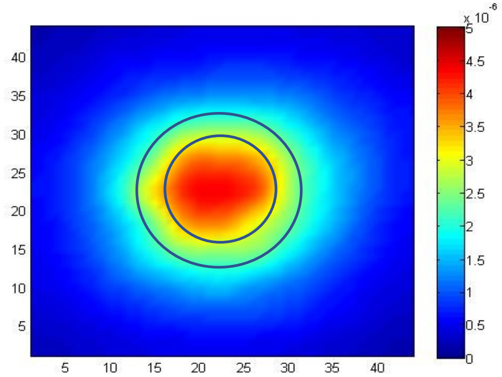

Measured

Twisted Winding

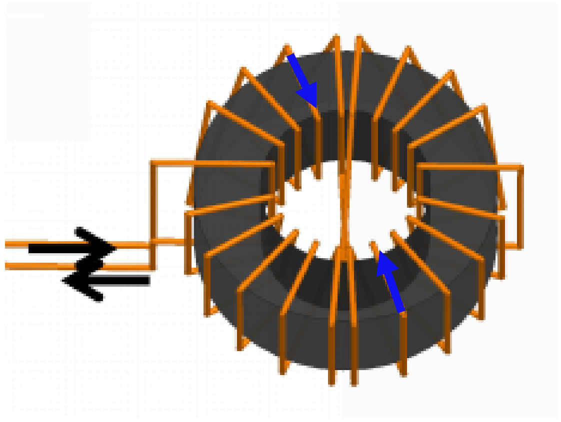

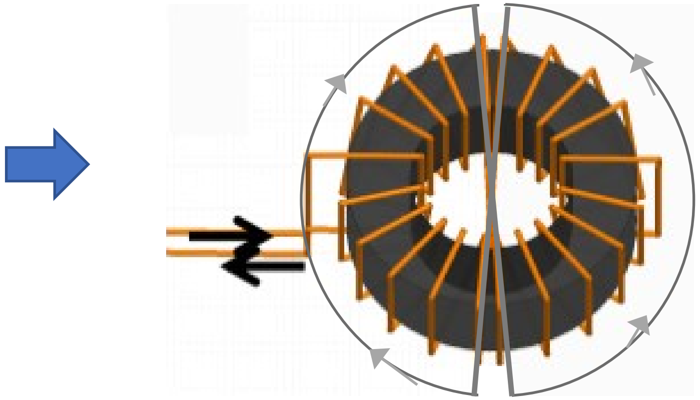

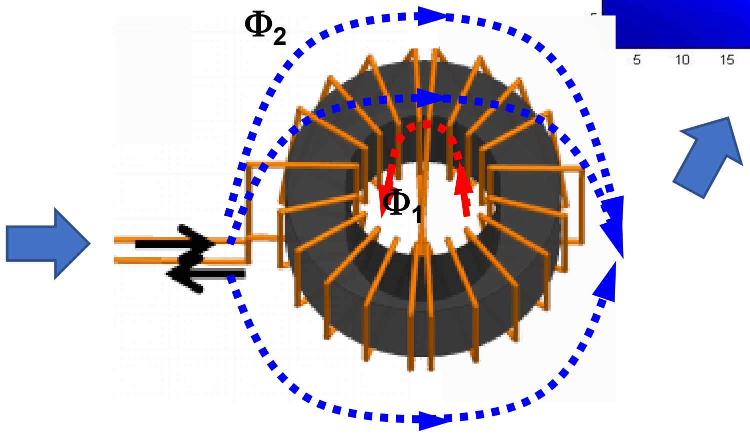

Magnetic field is partially canceled

Measured

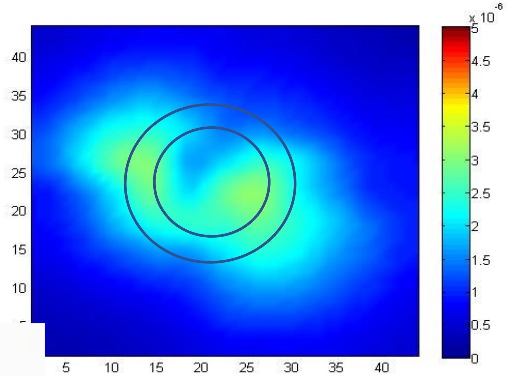

Simulated

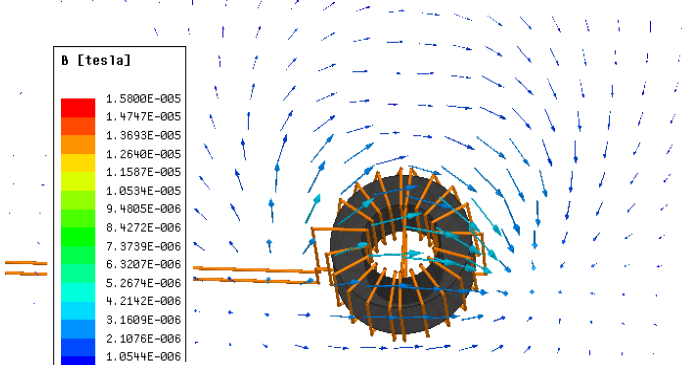

Inductor Near Magnetic Field Emission Modeling with Magnetic Moments

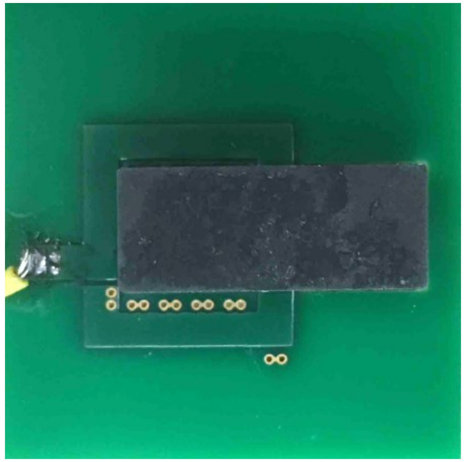

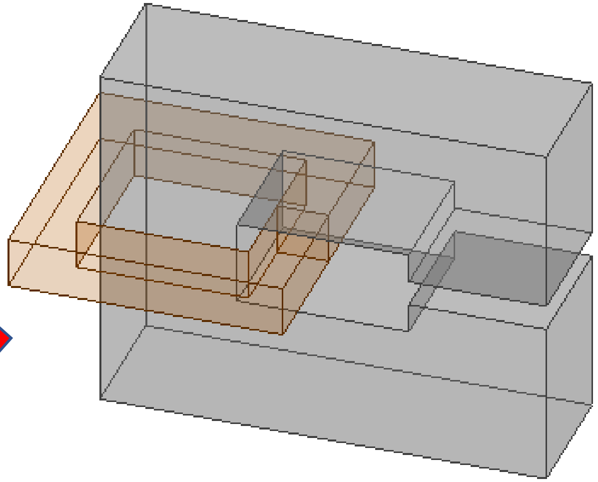

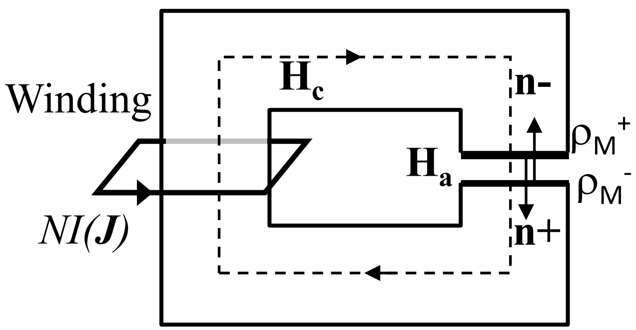

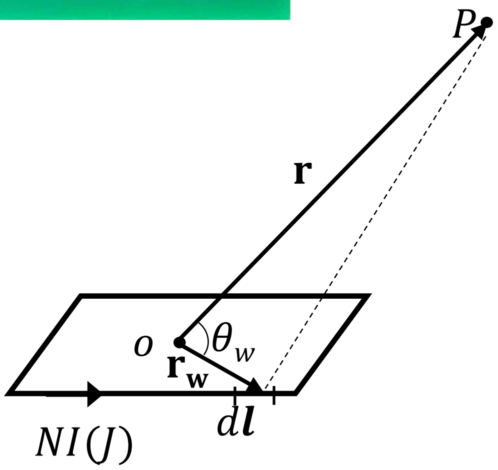

$\mathbf{A}_{Jdip}(\mathbf{r})$

$$\mathbf{m}_J = NI\int d\mathbf{a} = NIA_W\hat{\mathbf{a}}$$

Magnetic vector potential

$$\mathbf{A}_{Jdip}(\mathbf{r}) = \frac{\mu_0 NI}{4\pi r^2}\oint r_w\cos\theta_w d\mathbf{l} = \frac{\mu_0}{4\pi}\frac{\mathbf{m}_J\times\hat{\mathbf{r}}}{r^2}$$

$$\nabla\times\mathbf{A}_J = \mu_0\mathbf{H}$$

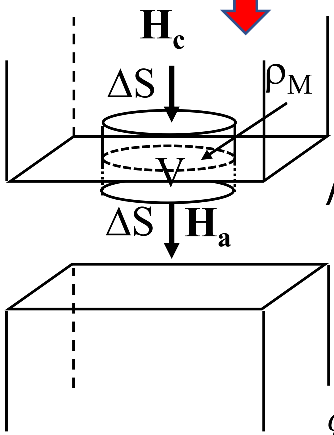

$$\rho_M = \mathbf{n}\cdot(\mathbf{H}_a - \mathbf{H}_c)$$

(Gauss law)

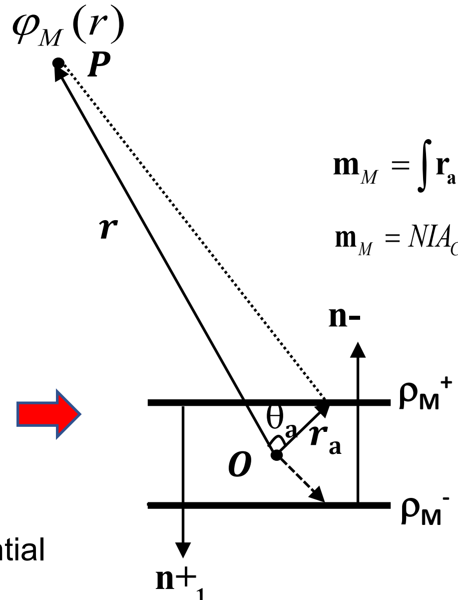

$$\mathbf{m}_M = \int \mathbf{r}_a\rho_M(\mathbf{r}_a)da_c$$

$$\mathbf{m}_M = NIA_C\hat{\mathbf{d}}$$

Scalar voltage potential

$$\varphi_{Mdip}(\mathbf{r}) = \frac{1}{4\pi r^2}\int r_a\cos\theta_a\rho_M(\mathbf{r}_a)da_c = \frac{1}{4\pi r^2}\hat{\mathbf{r}}\cdot\mathbf{m}_M \quad \Rightarrow \quad \nabla^2\varphi_M = \nabla\bullet\mathbf{H}$$

Reference: H. Zhang and S. Wang, "Near Magnetic Field Assessment and Reduction for Magnetic Inductors With Magnetic Moment Analysis," in *IEEE Transactions on Power Electronics*, vol. 37, no. 2, pp. 1641-1652, Feb. 2022, doi: 10.1109/TPEL.2021.3105643.

Inductor Near Magnetic Field Emission Modeling with Magnetic Moments

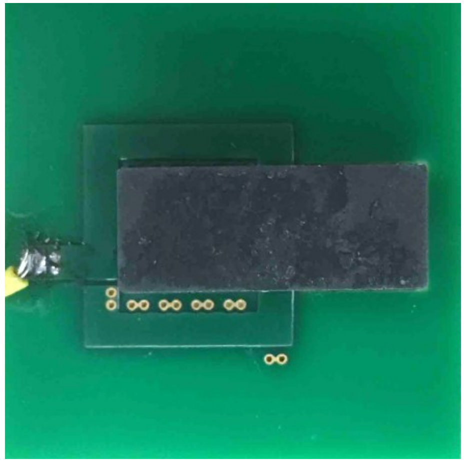

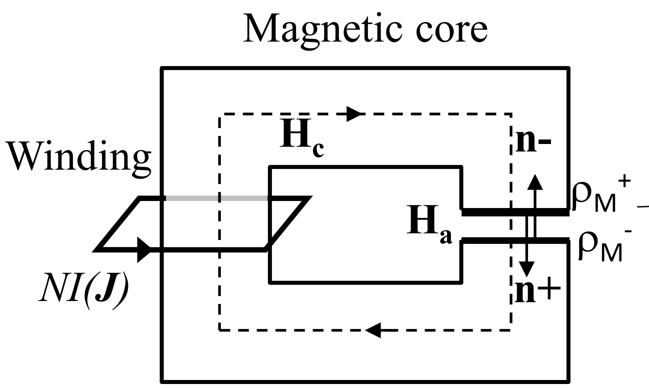

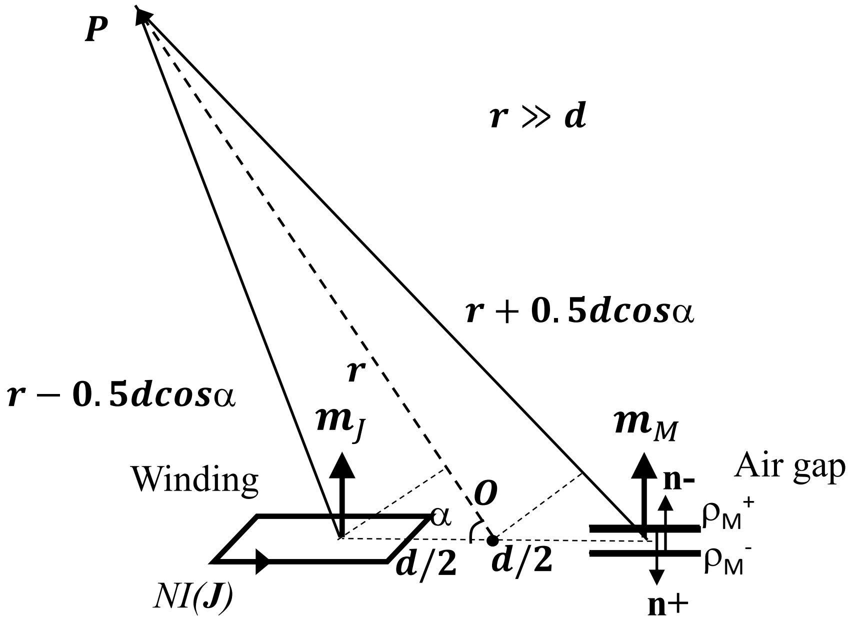

$$\mathbf{H}(r,\theta) = \mathbf{H}_{Jdip}(r,\theta) + \mathbf{H}_{Mdip}(r,\theta) \approx \frac{NI}{4\pi}\left(2\cos\theta\hat{\mathbf{r}} + \sin\theta\hat{\boldsymbol{\theta}}\right)\left(\frac{2A}{r^3}\right)$$

where, $A=0.5(A_W+A_C)$

A better design for near magnetic field reduction

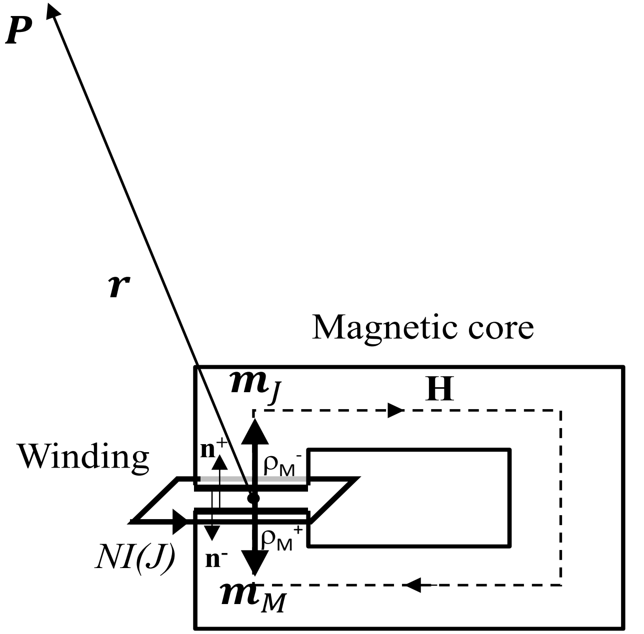

$$\mathbf{H}(r,\theta) = \mathbf{H}_{Jdip}(r,\theta) + \mathbf{H}_{Mdip}(r,\theta) \approx \frac{NI}{4\pi}\left(2\cos\theta\hat{\mathbf{r}} + \sin\theta\hat{\boldsymbol{\theta}}\right)\left[\frac{2\Delta A}{r^3} + \frac{3Ad\cos\alpha}{r^4}\right]$$

where, $\Delta A=0.5(A_W-A_C)$

Near Magnetic Field Emission of Different Inductor Structures

$\mathbf{H} \propto 1/r^4$

No.	F1	F2	F3	F4
Inductors and dipole moments	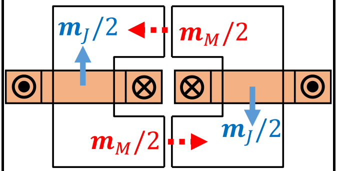	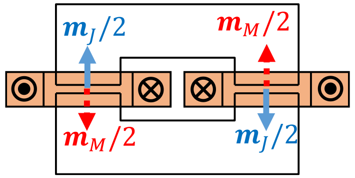	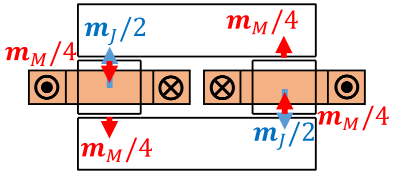	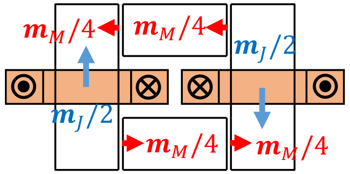
Parameters	$N_{1,2} = 3$ $\mu_r = 3300$ $l_{g1,2} = 0.25mm$ $L = 7.4\ \mu H$	$N_{1,2} = 3$ $\mu_r = 3300$ $l_{g1,2} = 0.25mm$ $L = 6.5\ \mu H$	$N_{1,2} = 3$ $\mu_r = 3300$ $l_{g1,2,3,4} = 0.125mm$ $L = 6.4\ \mu H$	$N_{1,2} = 3$ $\mu_r = 3300$ $l_{g1,2,3,4} = 0.125mm$ $L = 8.5\ \mu H$

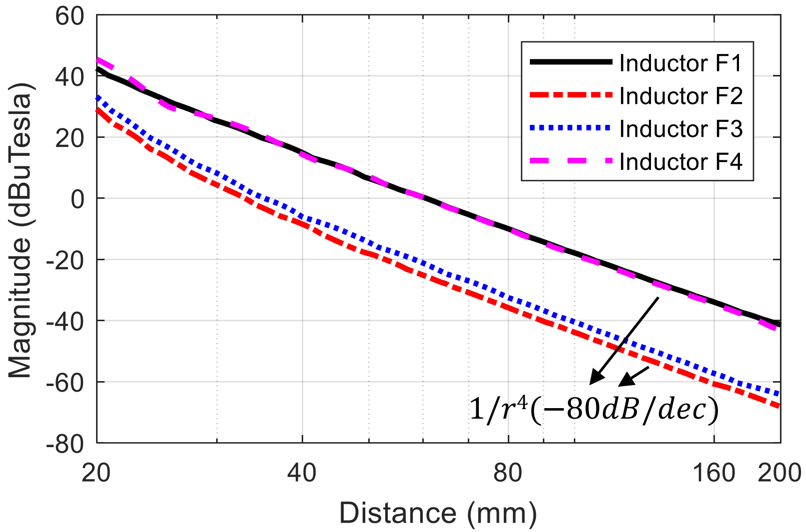

$\mathbf{H} \propto 1/r^3$

No.	No cancellation	P1	P2	P3	P4
Inductors and dipole moments	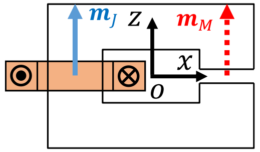	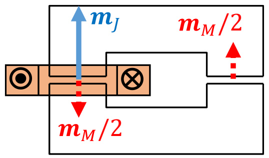	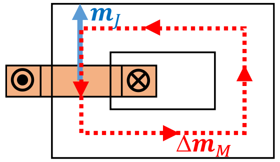	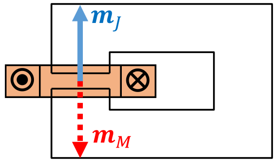	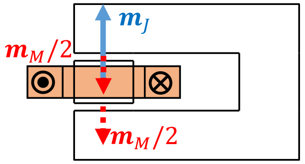
Parameters	$N = 6$ $\mu_r = 3300$ $l_g = 0.5mm$ $L = 7.1\mu H$	$N = 6$ $\mu_r = 3300$ $l_{g1,2} = 0.25mm$ $L = 7.3\mu H$	$N = 6$ $\mu_r = 95$ *distributed airgaps* $L = 7.0\mu H$	$N = 6$ $\mu_r = 3300$ $l_g = 0.5mm$ $L = 7.1\mu H$	$N = 6$ $\mu_r = 3300$ $l_{g1,2} = 0.25mm$ $L = 6.9\mu H$

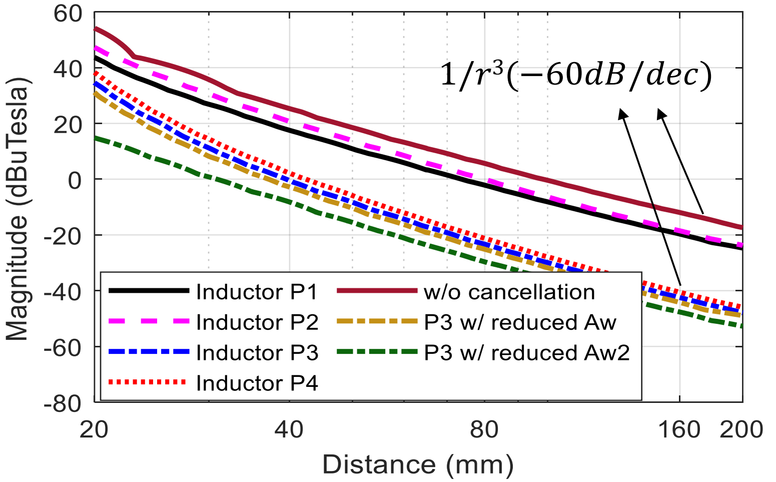

Agree with the predicted based on magnetic moment theory

Validation with Simulations and Experiments

Prototypes

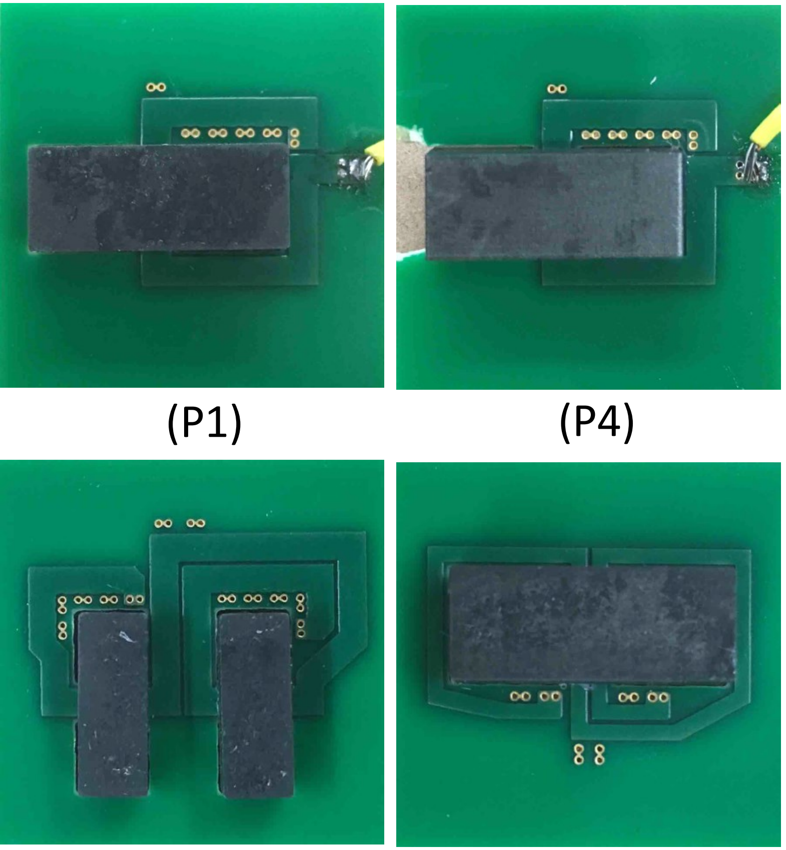

(P1) (P4)

(F5) (F2)

Simulations

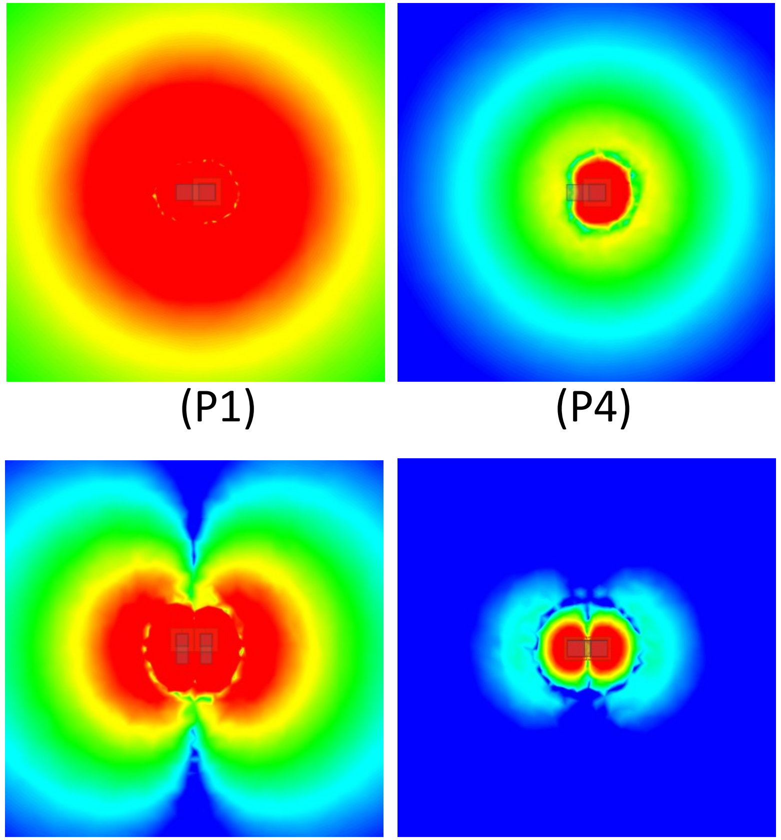

(P1) (P4)

(F5) (F2)

Measurements

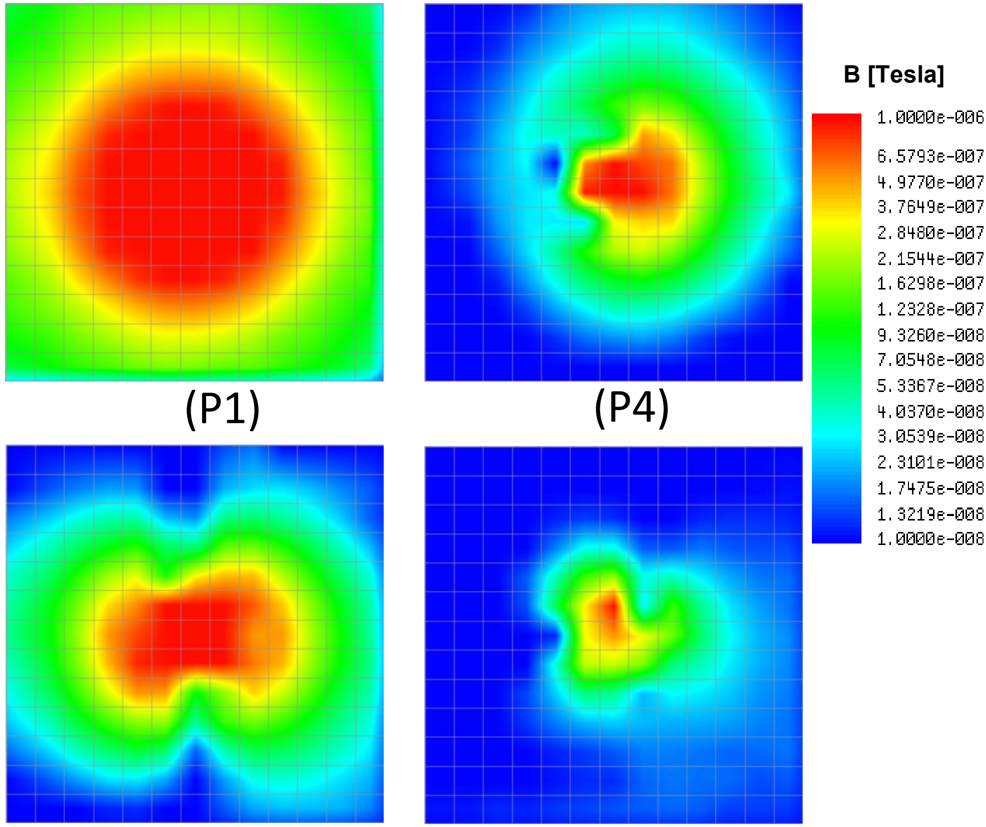

(P1) (P4)

(F5) (F2)

Near Magnetic Field Emission due to Unevenly Distributed Winding Turns

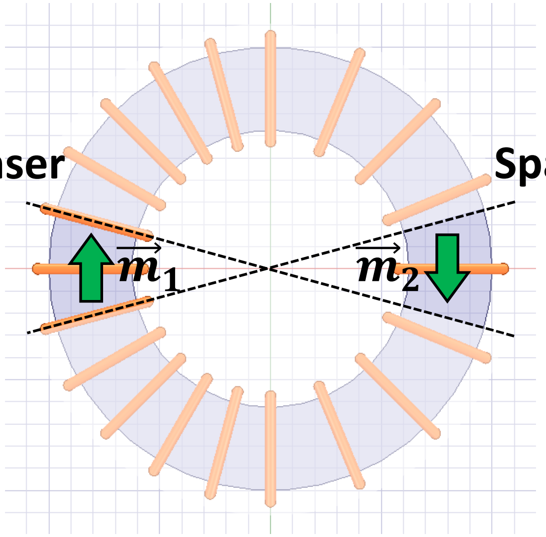

=

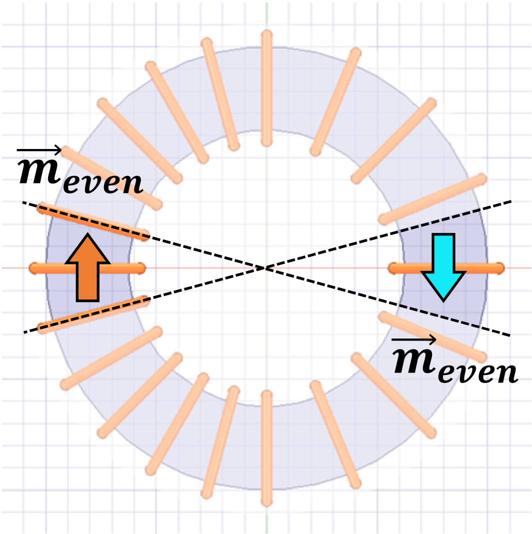

+

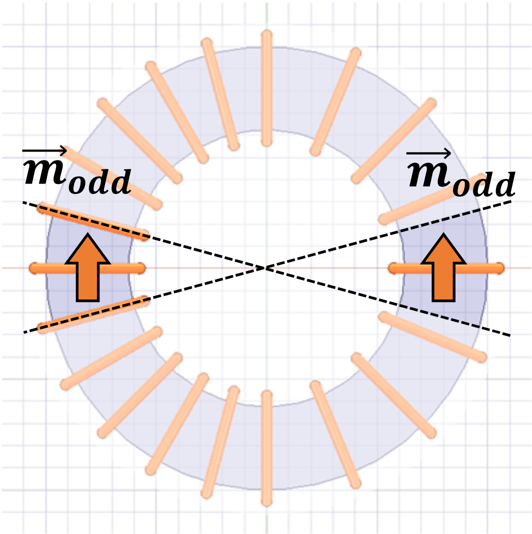

When turns are uneven,
$|\vec{m}_1| \neq |\vec{m}_2|$

Denser side has larger $\vec{m}$.

$$|\vec{m}_{even}| = \frac{|\vec{m}_1| + |\vec{m}_2|}{2}$$

Opposite polarity but same magnitude.

$$|\vec{m}_{odd}| = \frac{|\vec{m}_1| - |\vec{m}_2|}{2}$$

Same polarity and magnitude.

The uneven distribution of turns contribute to near magnetic field emission.

Reference: Y. Yang and S. Wang, "Analysis and Modeling of the Near Magnetic Field Distribution of Toroidal Inductors," in Proc. *IEEE International Symposium of Electromagnetic Compatibility, Signal Integration and Power Integration, 2023*.

Impact of Unevenly Distributed Windings

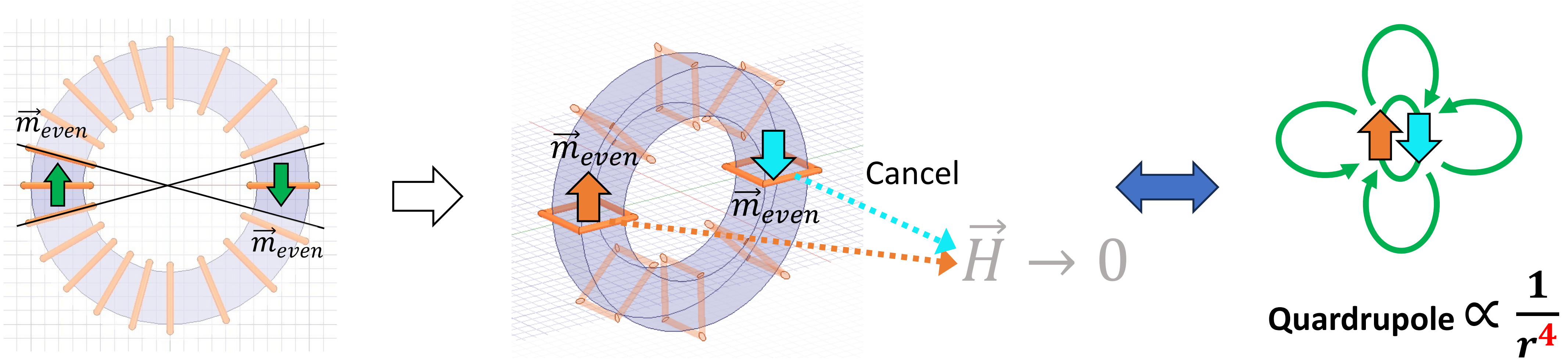

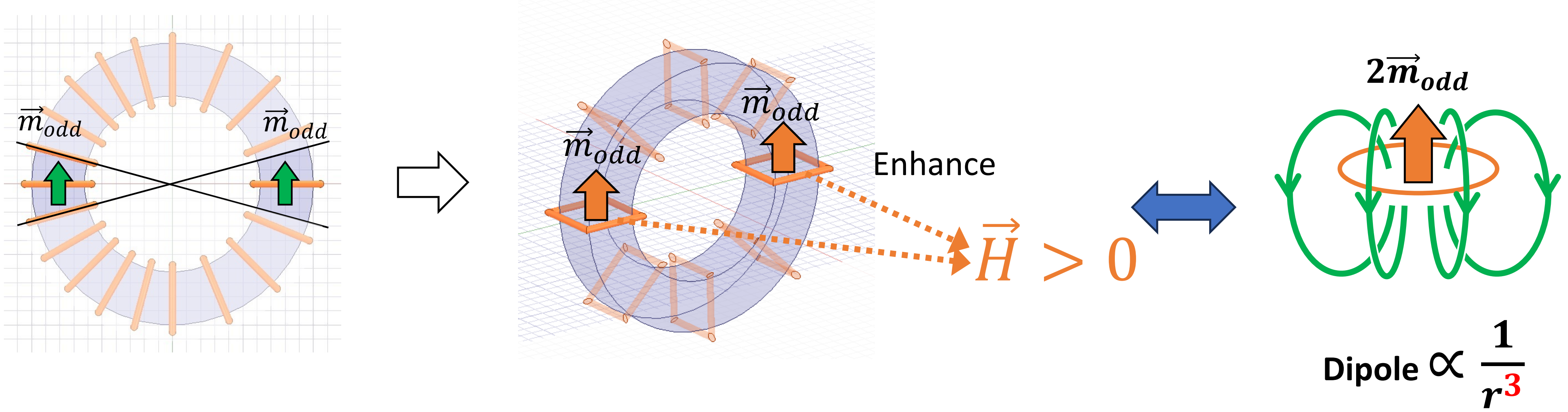

Experimental Verification

Before adjustment

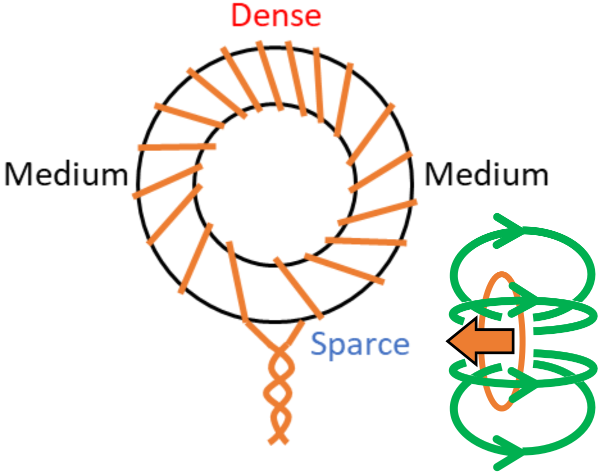

Adjust winding density 1

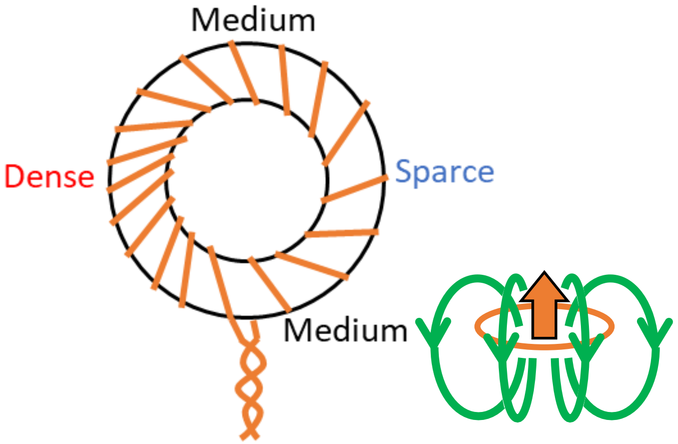

Adjust winding density 2

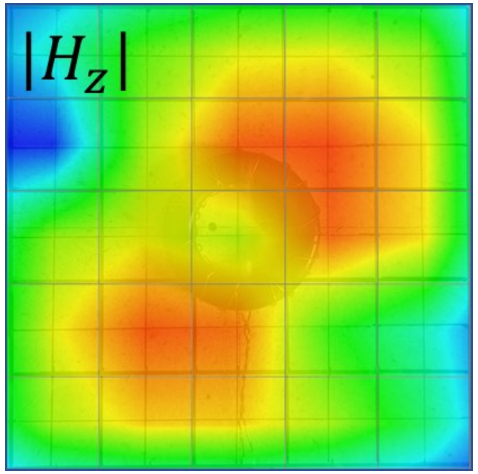

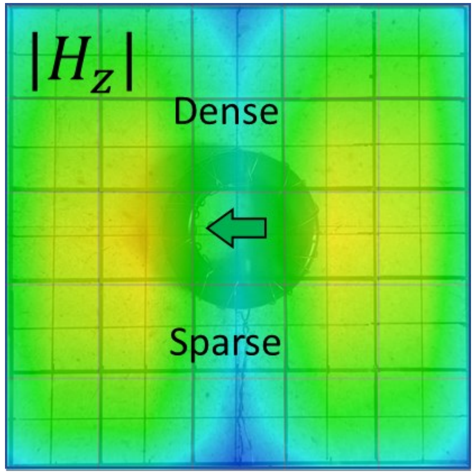

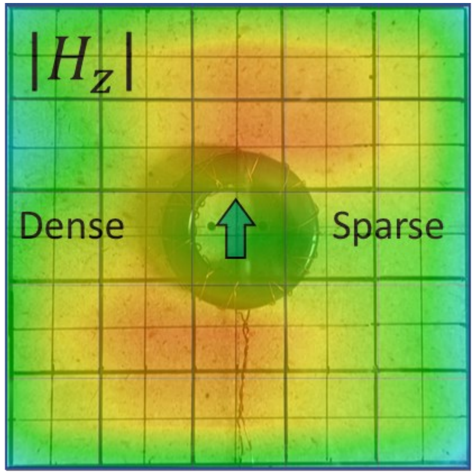

Measurement of Near Field

Measurement setup using a scanner board

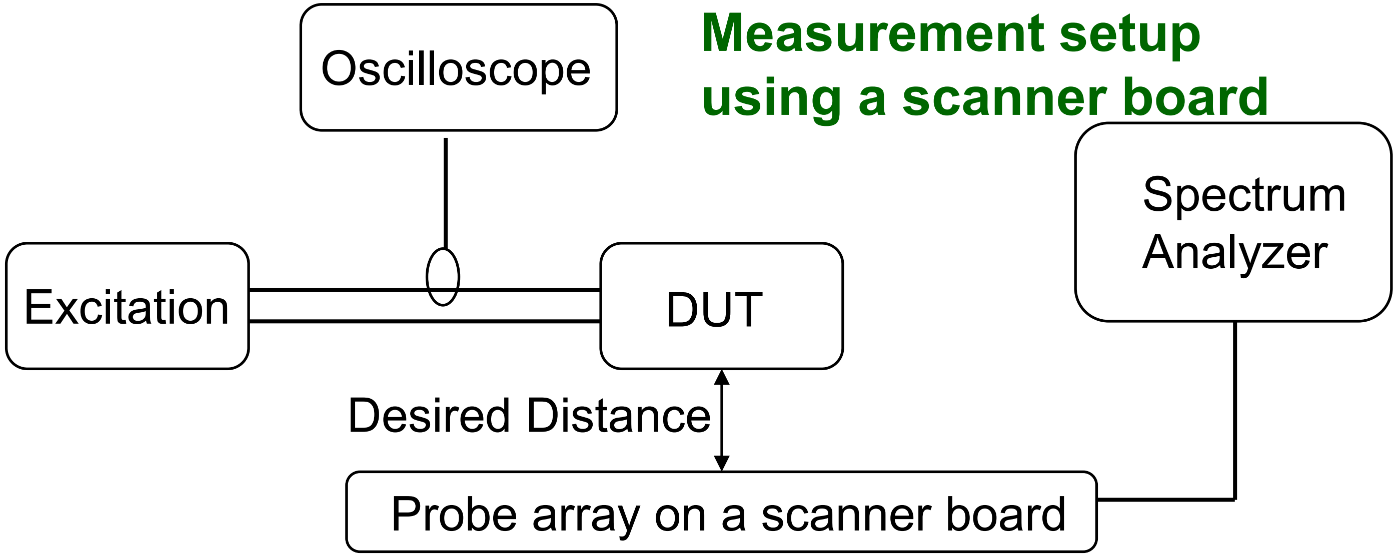

Measurement setup using magnetic probe

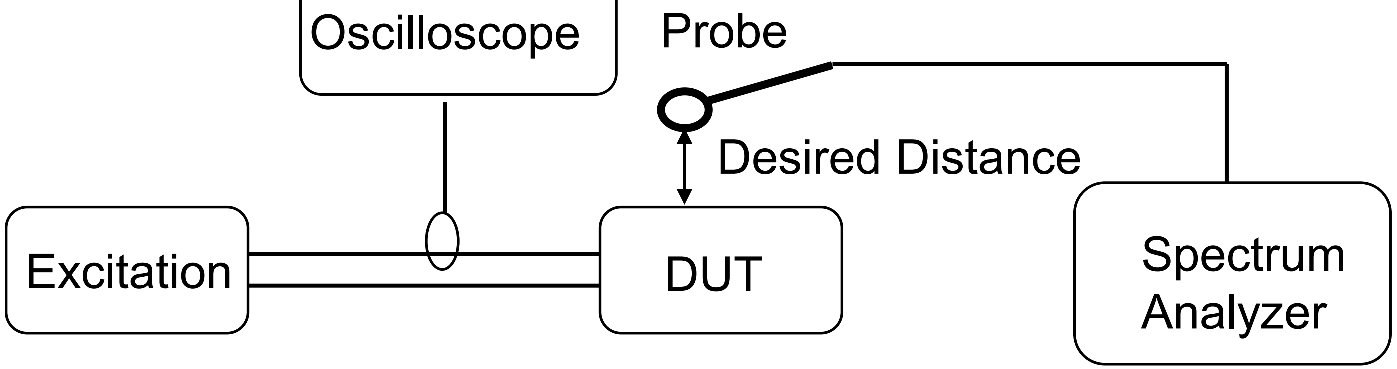

DUT: Device, circuit or components under test
Excitation: Power supply, voltage or current source to provide excitations to DUT
Oscilloscope: Monitor the excitations
Desired distance: The desired distance where the near field is measured
Probes: The near magnetic or electric field probes.
Scanner board: Magnetic field scanner board for magnetic field measurement
Spectrum analyzer: Where the measured near field from the probe or board will be processed and displayed
Sensitivities of probes: The probes have limited sensitivities, so low field cannot be measured. Network analyzers can be used to extract small near field couplings.

Near Field Probes

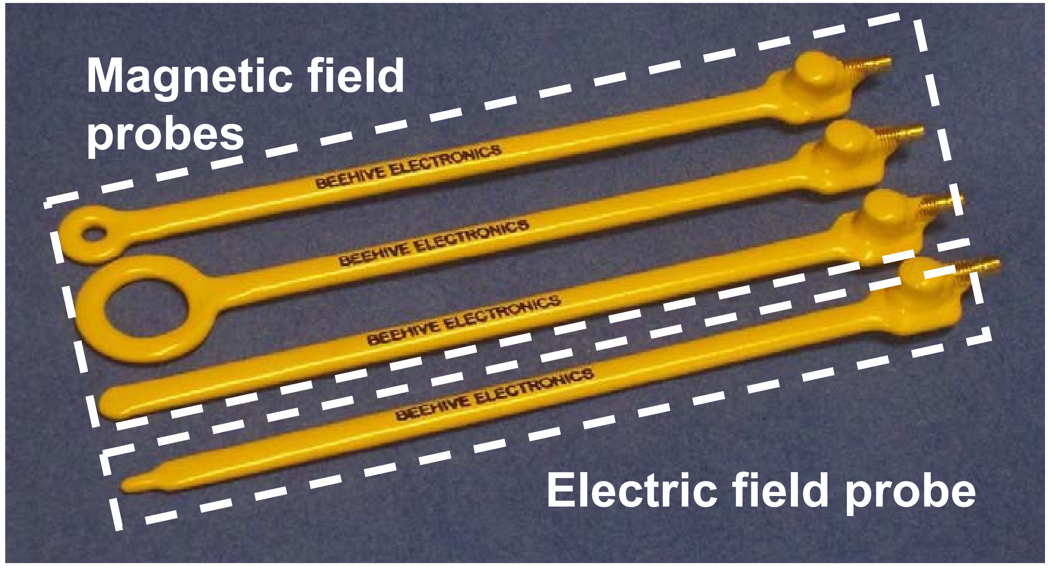

- A probe set has both magnetic and electric field probes
- Different probe loop size provides different spatial resolution
- Bigger probes can measure smaller field but with lower spatial resolution

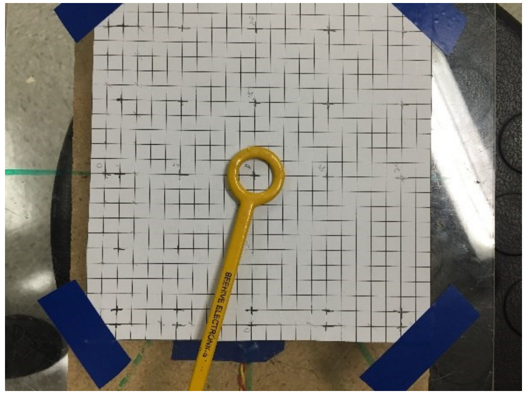

Measuring Z-direction

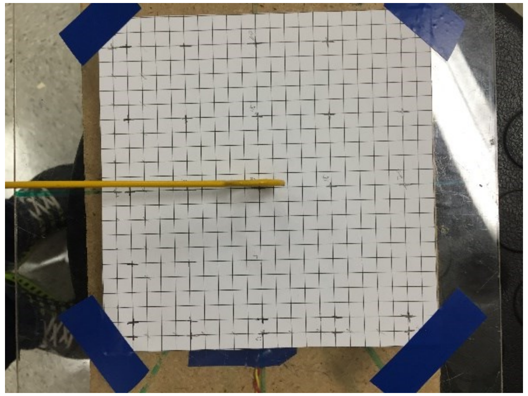

Measuring Y-direction

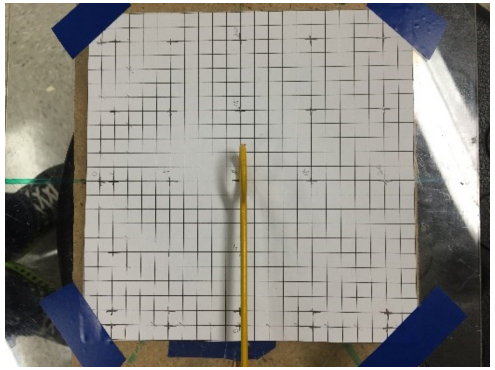

Measuring X-direction

XYZ components of magnetic field should all be measured, then the total magnetic field can be calculated:

$$H = \sqrt{H_x^2 + H_y^2 + H_z^2}$$
$$\vec{H} = H_x\vec{i} + H_y\vec{j} + H_z\vec{k}$$

3.3 Power Inductor’s Near Field Immunity

Near Magnetic Field Immunity of Power Inductors

External Magnetic Field

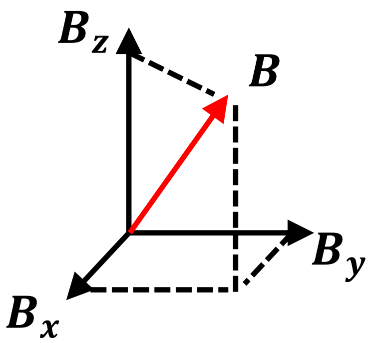

Conventional

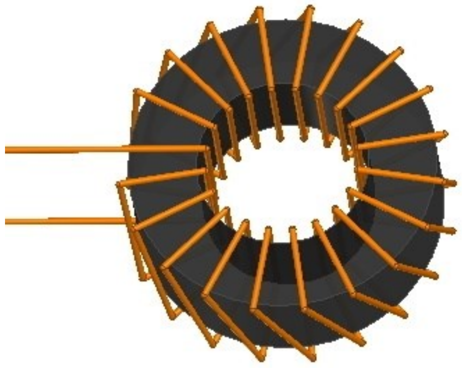

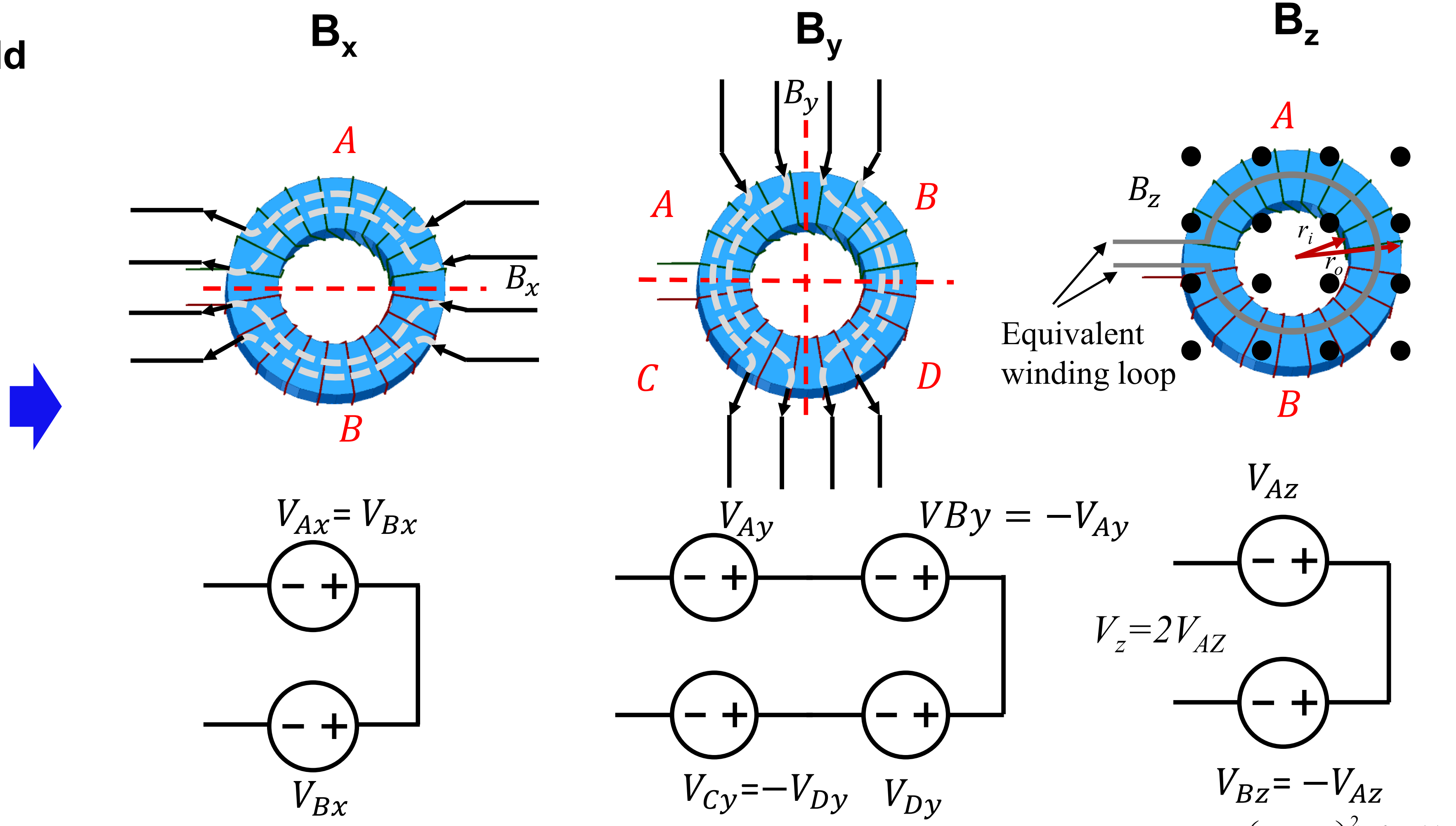

$$V_Z = 2V_{Az} = \pi \left(\frac{r_o + r_i}{2} \right)^2 \frac{dB_z(t)}{dt}$$

Reference: Y. Lai, S. Wang and B. Zhang, "Investigation of Magnetic Field Immunity and Near Magnetic Field Reduction for the Inductors in High Power Density Design," in *IEEE Transactions on Power Electronics*, vol. 34, no. 6, pp. 5340-5351, June 2019, doi: 10.1109/TPEL.2018.2868646.

Improve the Immunity of Inductors with Twisted Windings

External Magnetic Field

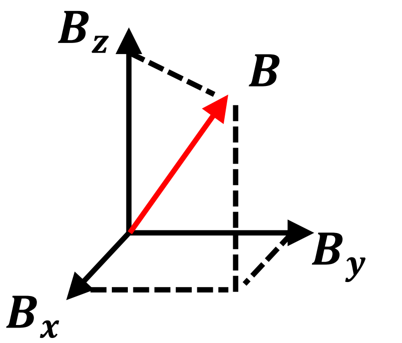

Twisted Winding

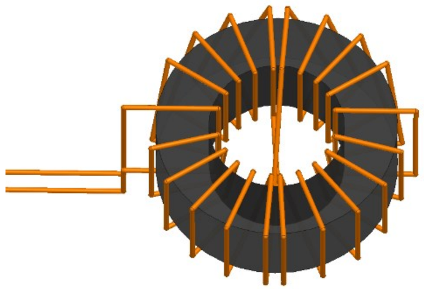

B_x

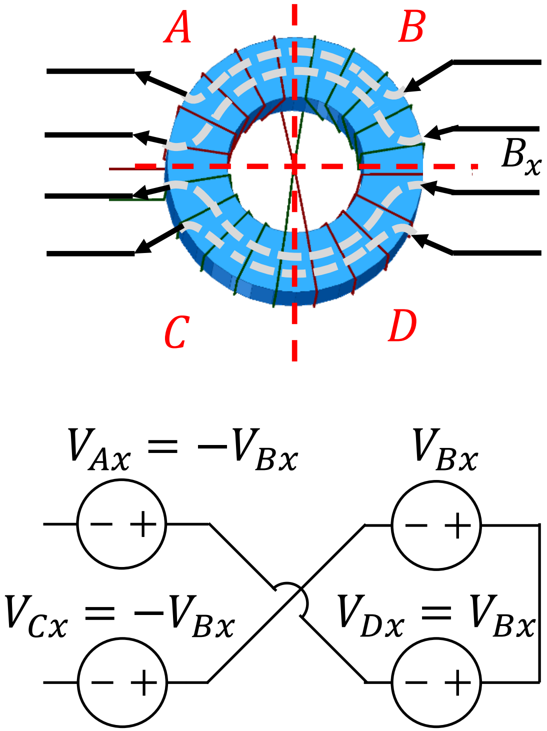

$V_x = 0$

B_y

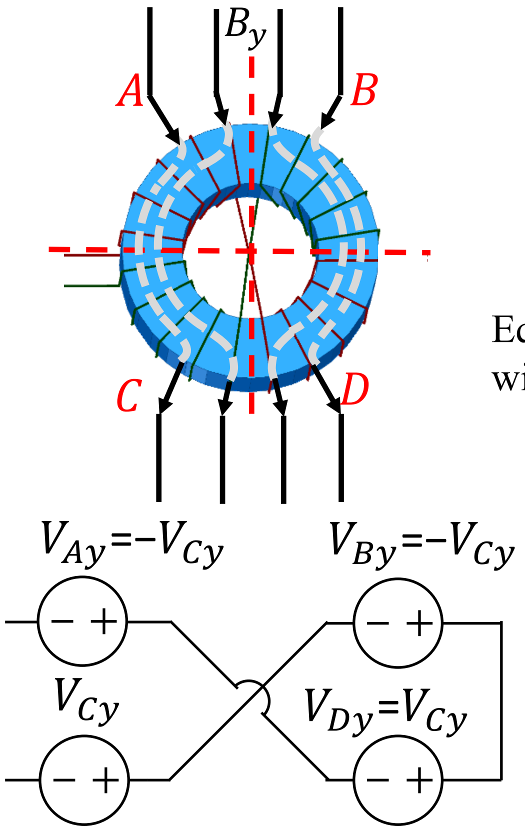

$V_y = 0$

B_z

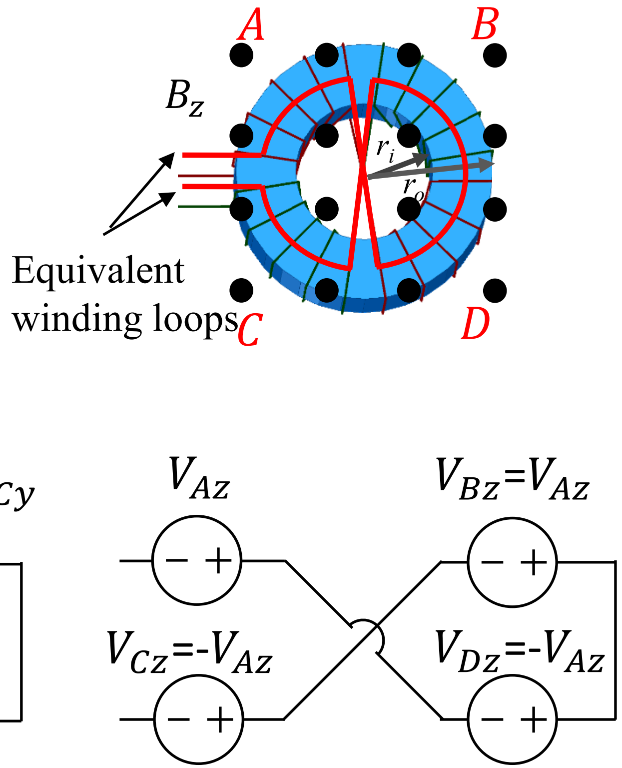

$V_z = 0$

Uneven magnetic field, so only partial cancellation is possible

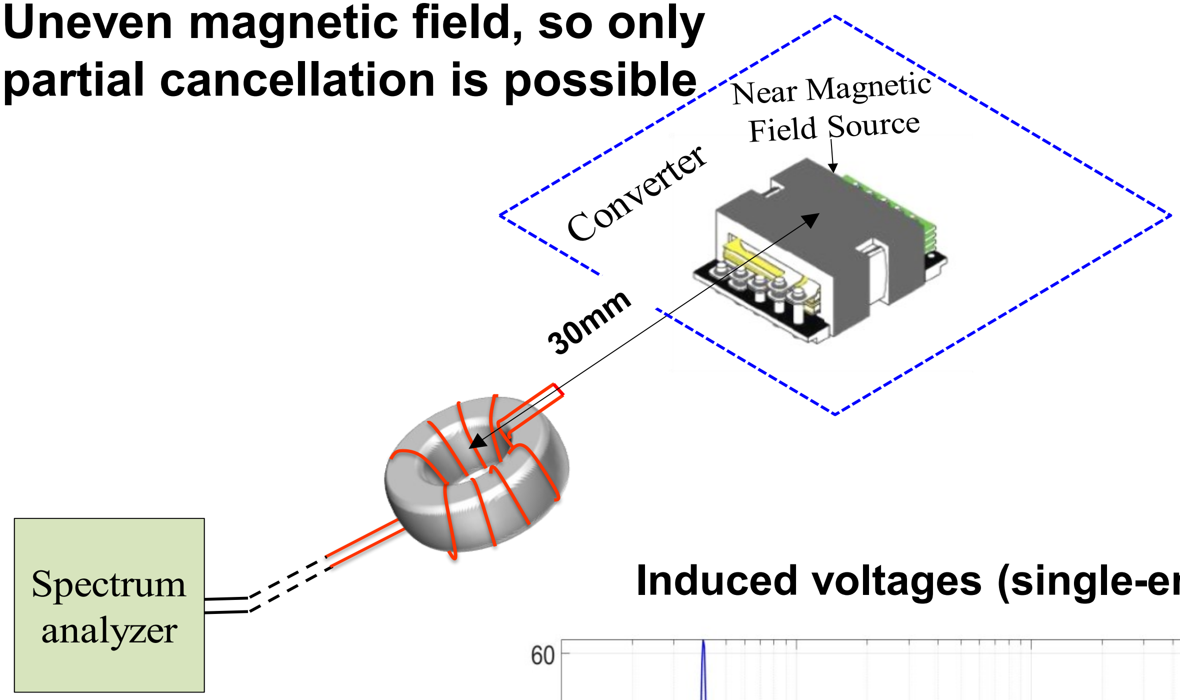

Induced CM voltages (CM L)

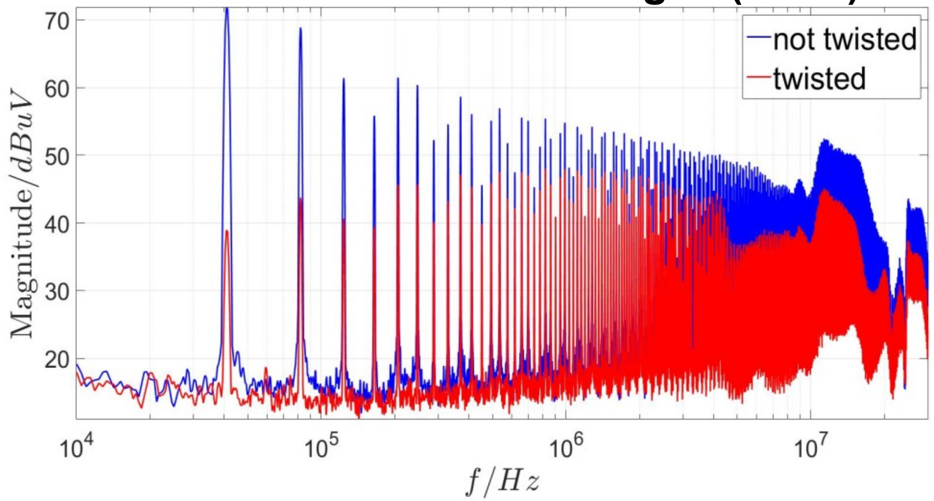

Induced voltages (single-ended L)

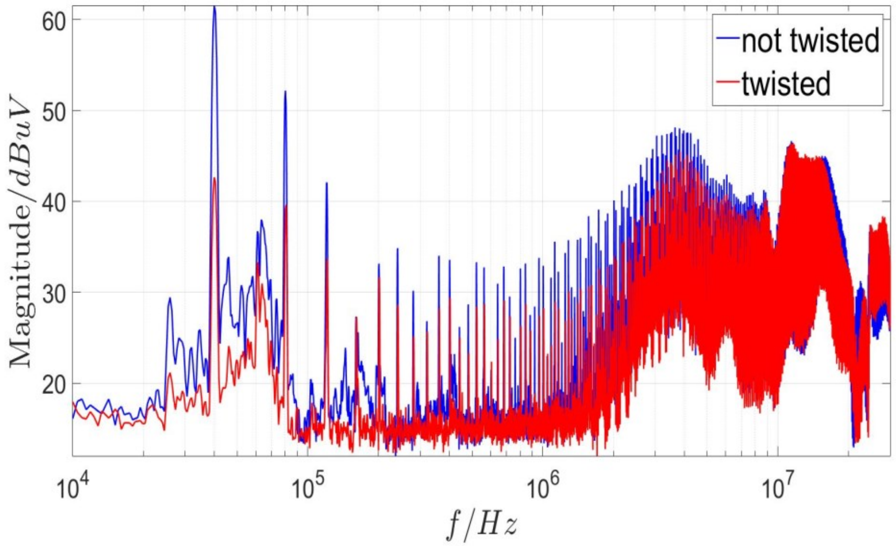

Induced DM voltages (CM L)

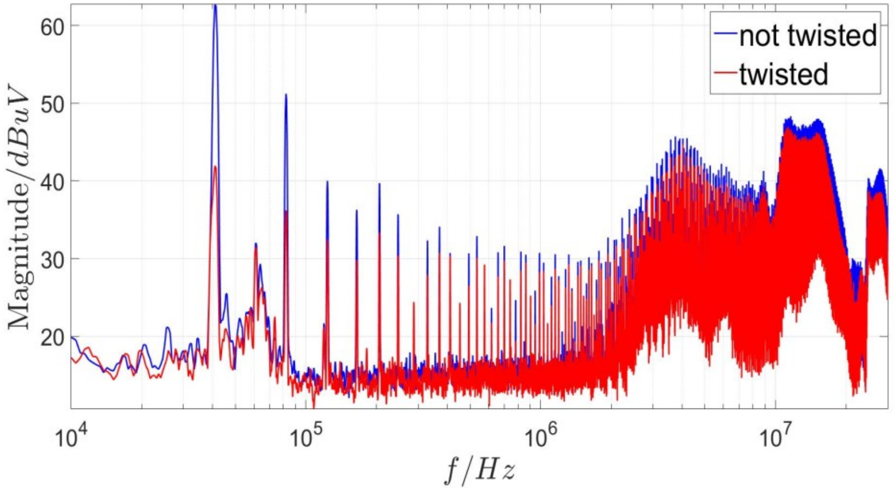

4. Power Inductor’s Low-frequency (LF) Radiative Emissions

Radiated EMI Measurement in Automotive Applications (CISPR25)

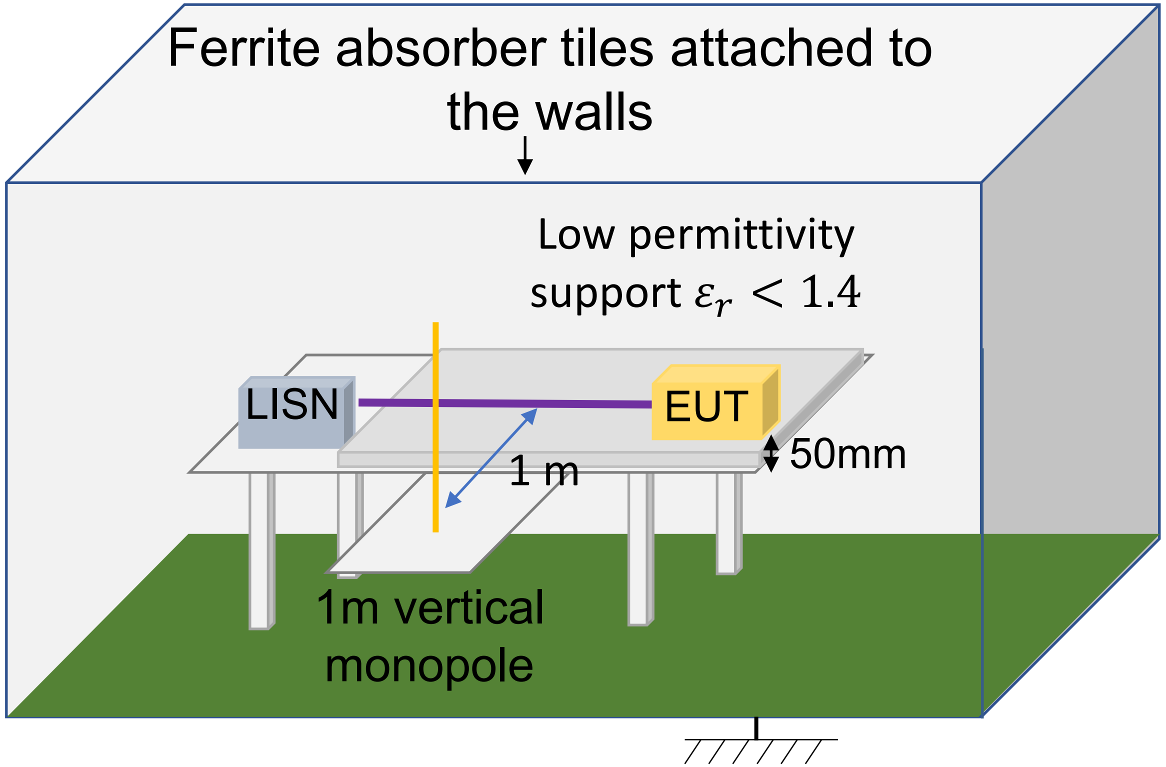

Radiated EMI testing setup (150kHz, 30MHz)

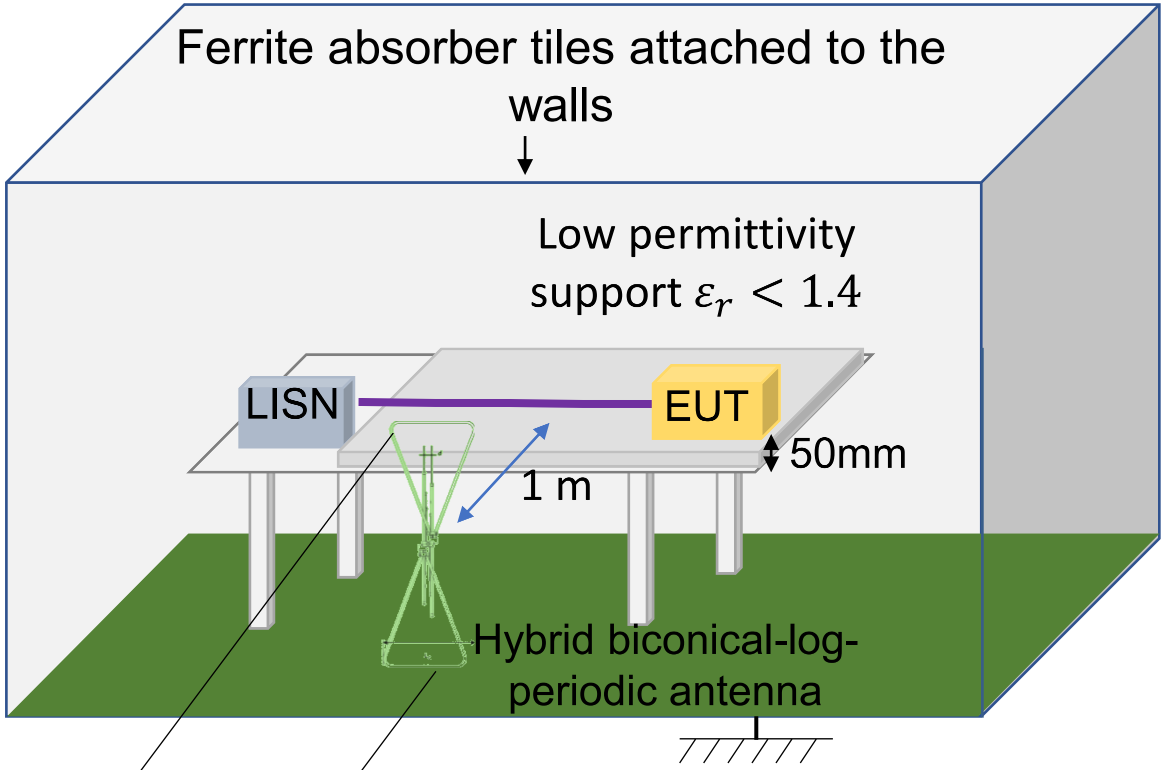

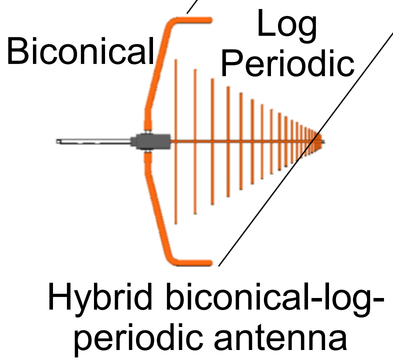

Radiated EMI testing setup (30MHz, 1GHz)

Power Inductors as A Source of LF Radiative EMI

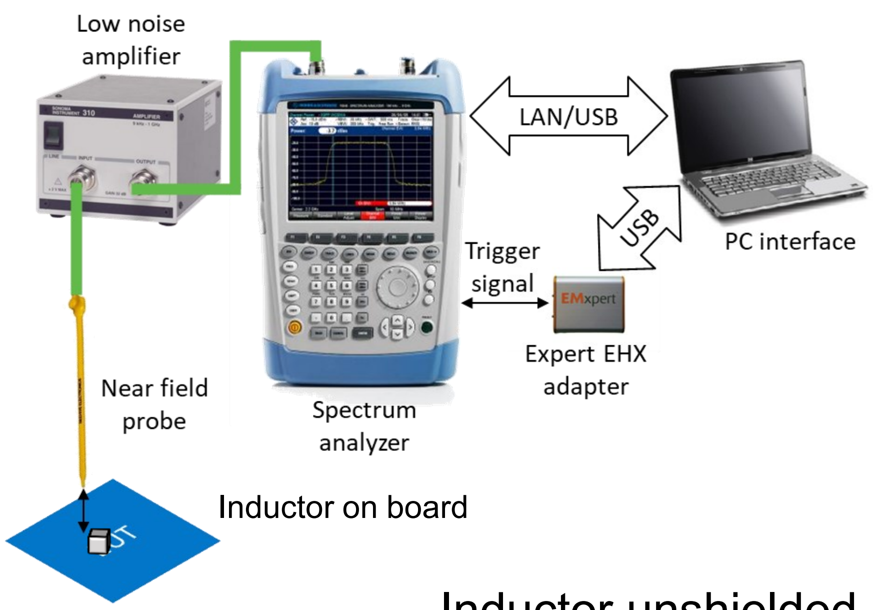

Inductor is a major radiative EMI source below 30MHz

Measured 1-meter radiative emission with a monopole antenna)

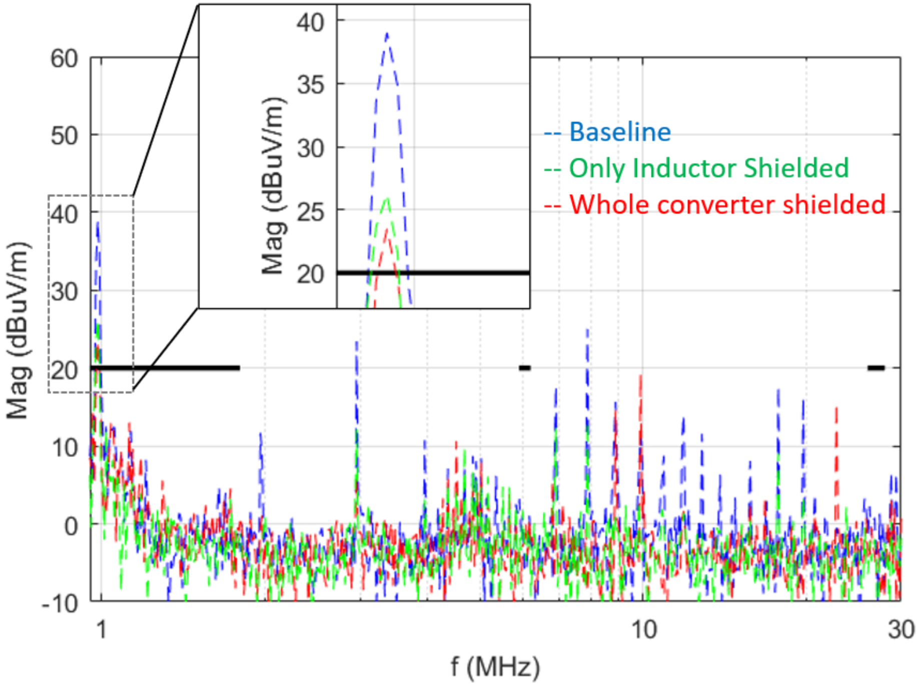

Inductor unshielded

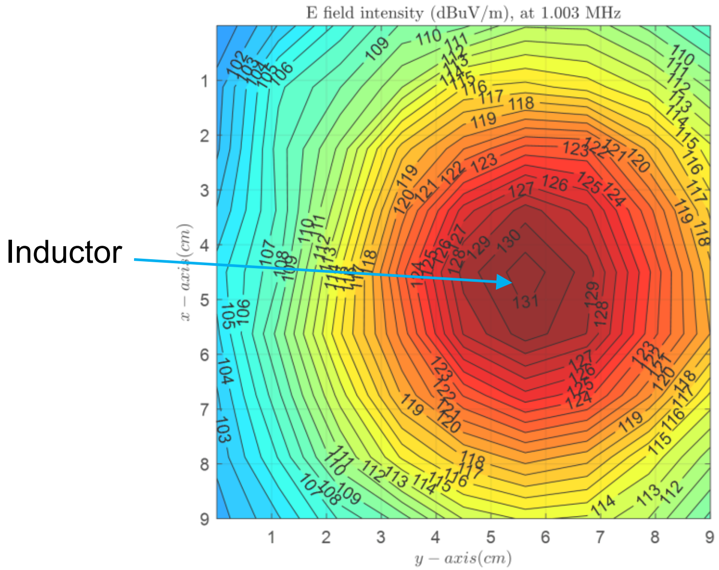

Inductor shielded

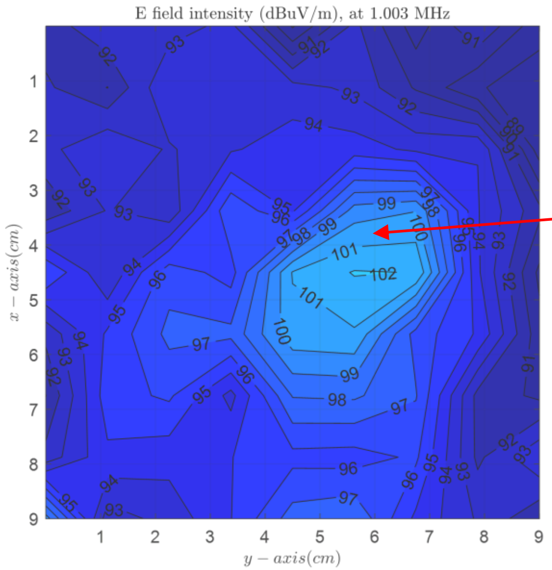

Inductor

Measured <u>Near Electric Field</u> Above the Board @ switching frequency

Decompose Voltage Excitations to CM and DM Voltages

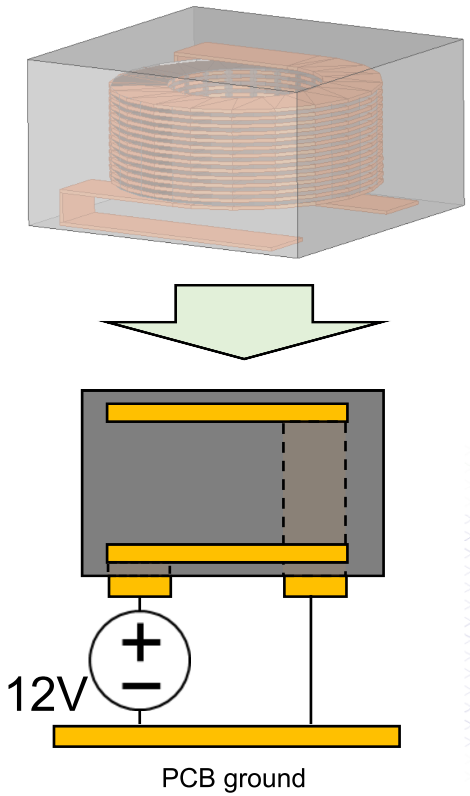

Diagram: An inductor on a PCB

Charge distribution

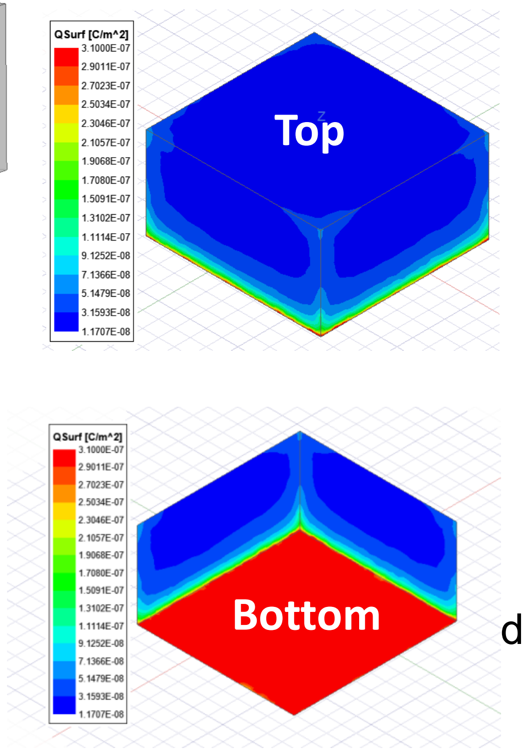

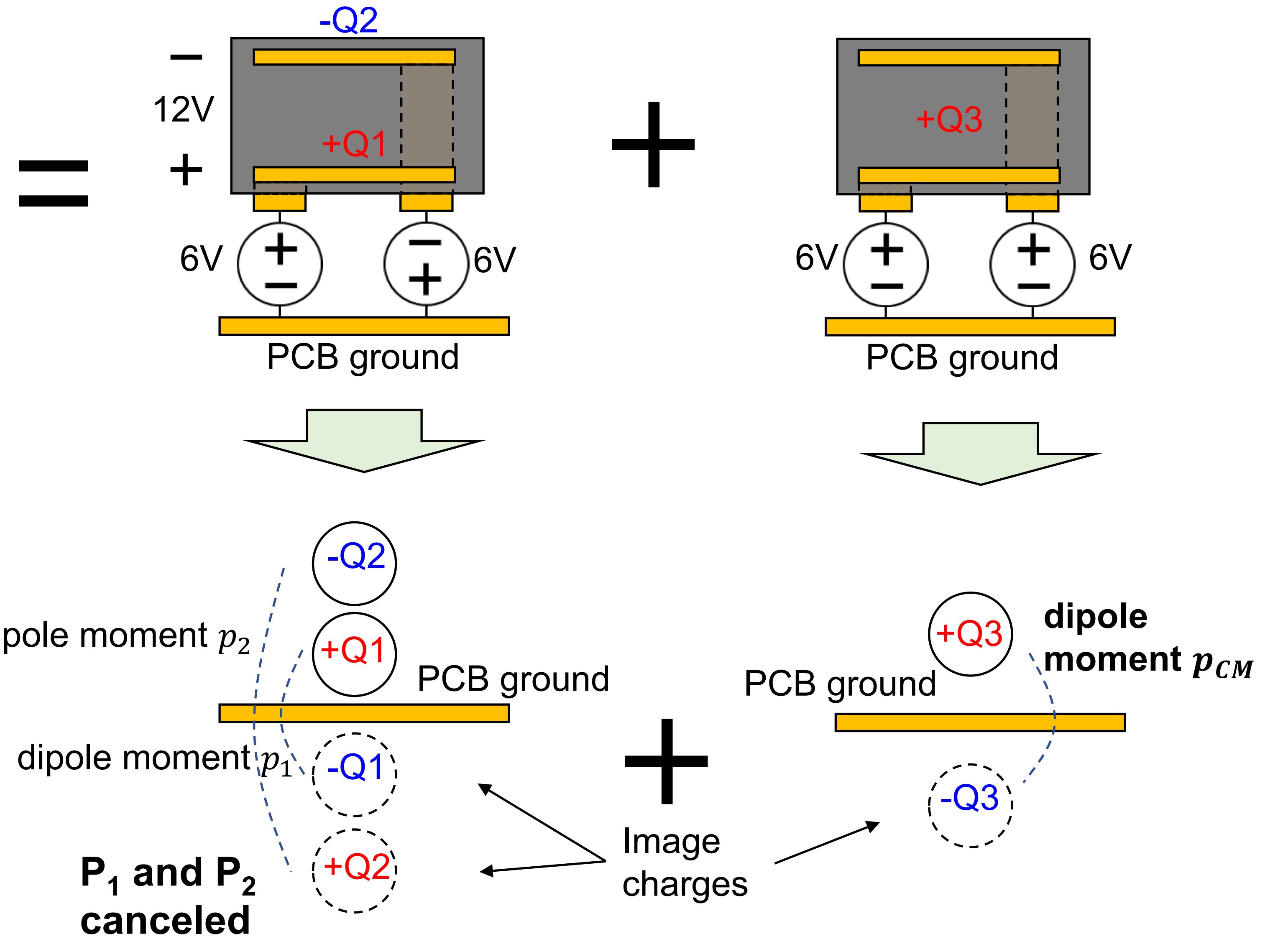

Due to DM voltage

Due to CM voltage

Magnetic Moments due to DM Voltage are Canceled

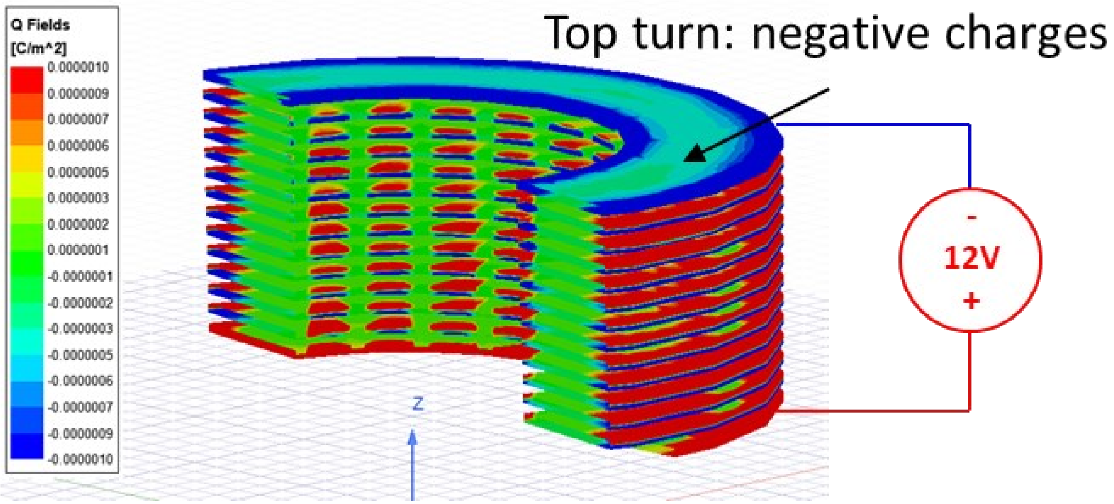

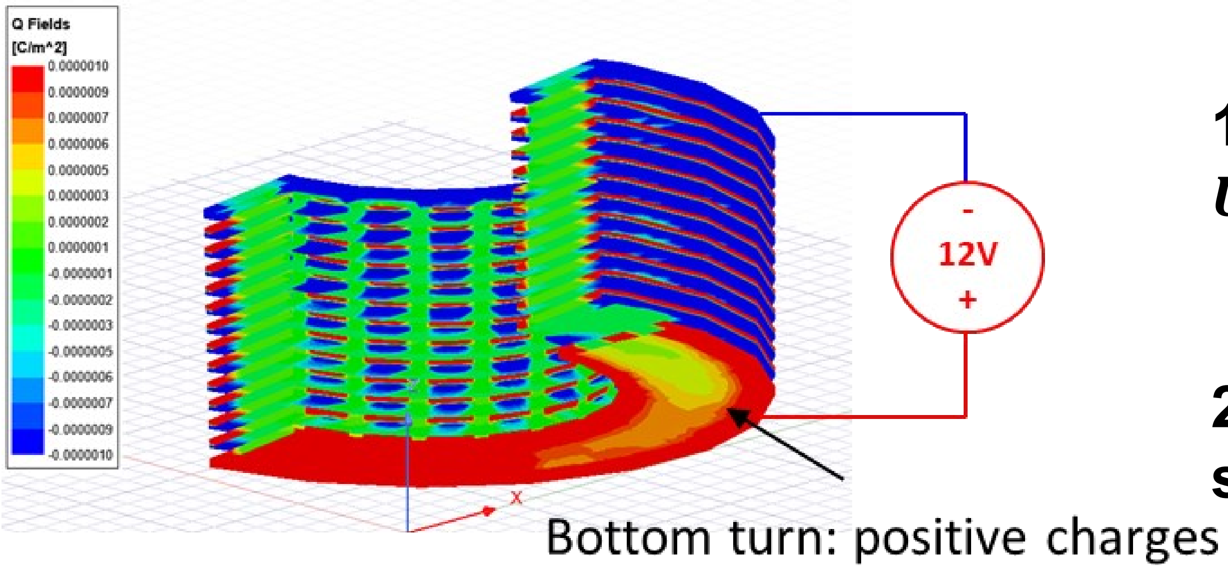

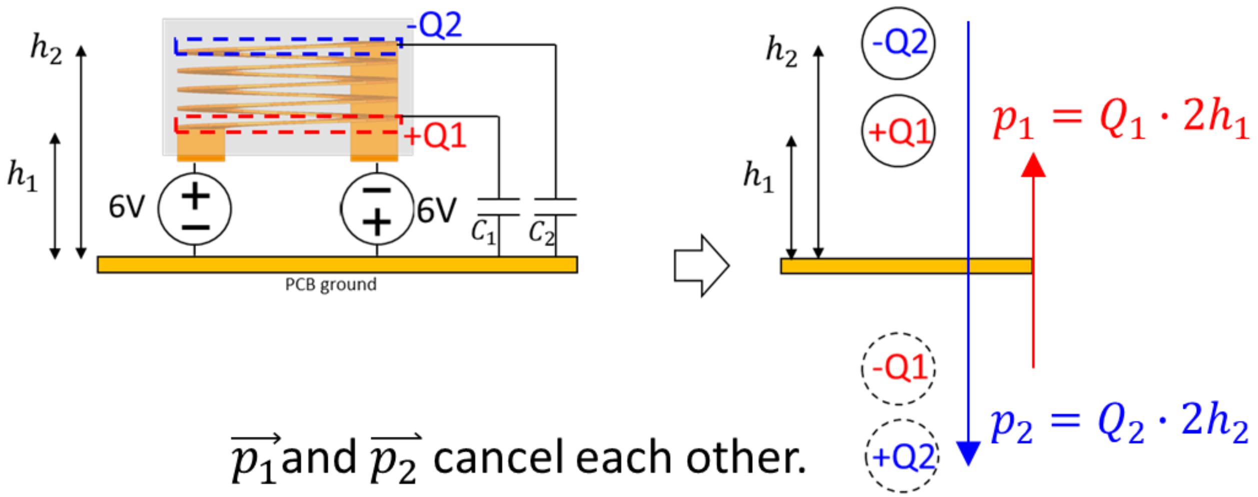

1) The electric moment: $p = Q \times d = C \cdot U \cdot 2h$. The analysis shows that

$$C_1 h_1 \approx C_2 h_2$$

$$\Rightarrow \overrightarrow{p_1} \text{ and } \overrightarrow{p_2} \text{ can cancel each other.}$$

2) Other symmetric pairs have the same story.

Equate All CM Charges to the Bottom Surface w/o Change Original Dipole Moments

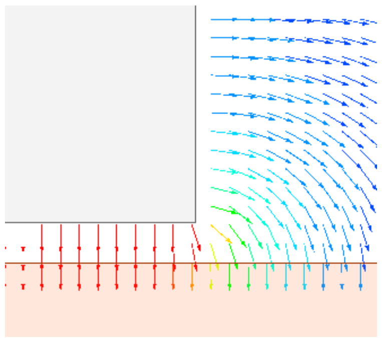

Simulation: electric field distribution

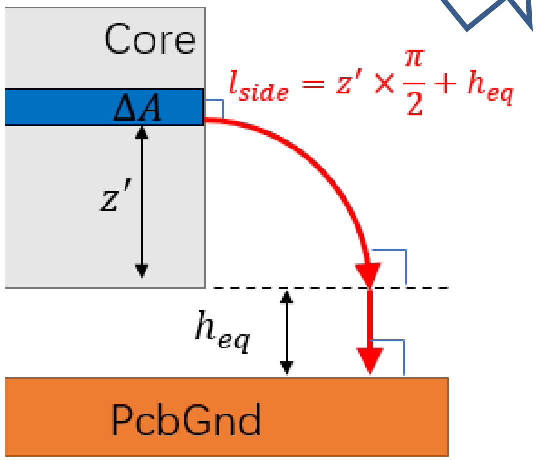

Side surface elements and its capacitance

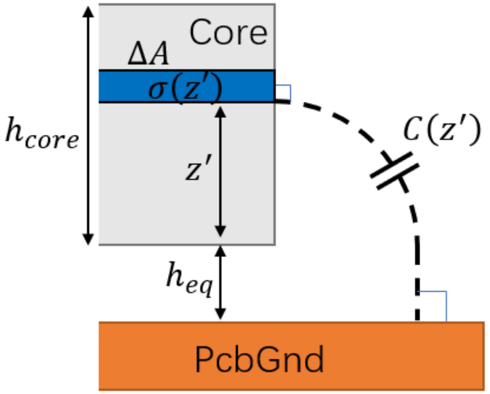

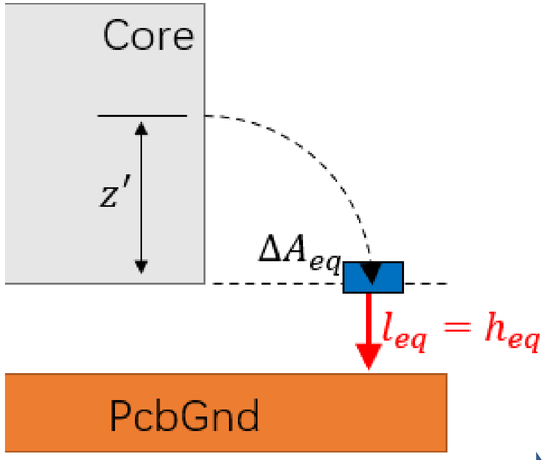

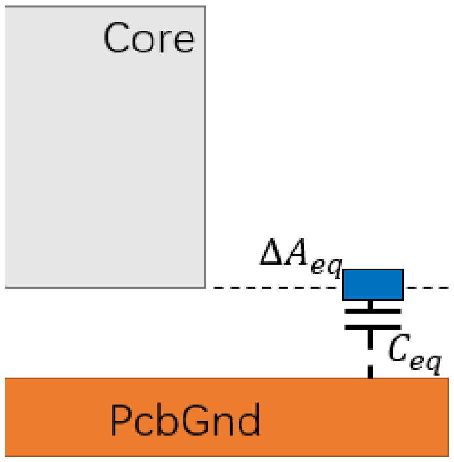

Equivalent capacitance

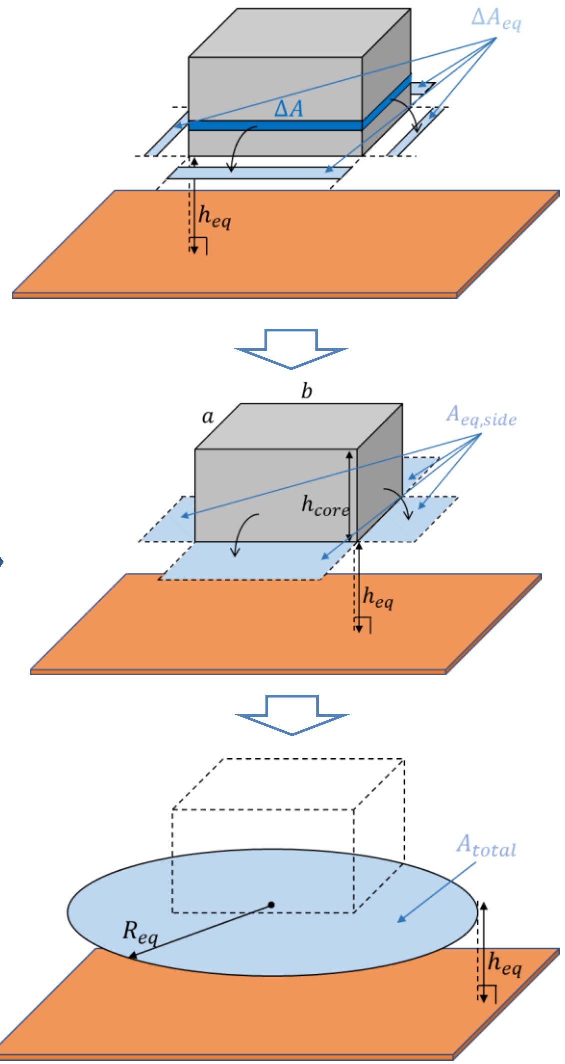

Area conversion of core side surfaces

Prediction of the Radiative Electric Field from Inductors due to CM Voltage Excitation (Electric Dipole Moments)

The electric field due to the dipole moment P_{CM} in the space under spherical coordinate :

$$E_r = \frac{p_{CM}\cos\theta}{2\pi\varepsilon_0 r^3}$$

$$E_\theta = \frac{p_{CM}\sin\theta}{4\pi\varepsilon_0 r^3}$$

$$E_\varphi = 0$$

Coordinate transformation

Cylindrical coordinate for *z* direction E-field prediction

$$E_z = E_r\cos\theta - E_\theta\sin\theta = \frac{p_{CM}}{2\pi\varepsilon_0 r^3}\left(\cos^2\theta - \frac{1}{2}\sin^2\theta\right)$$

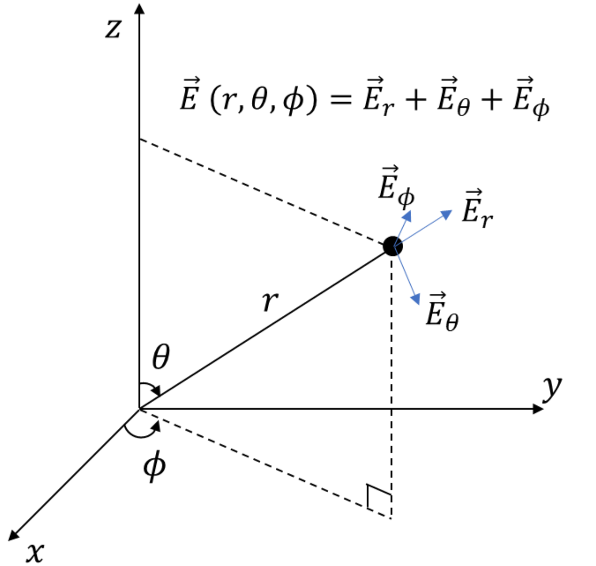

Spherical Coordinate System

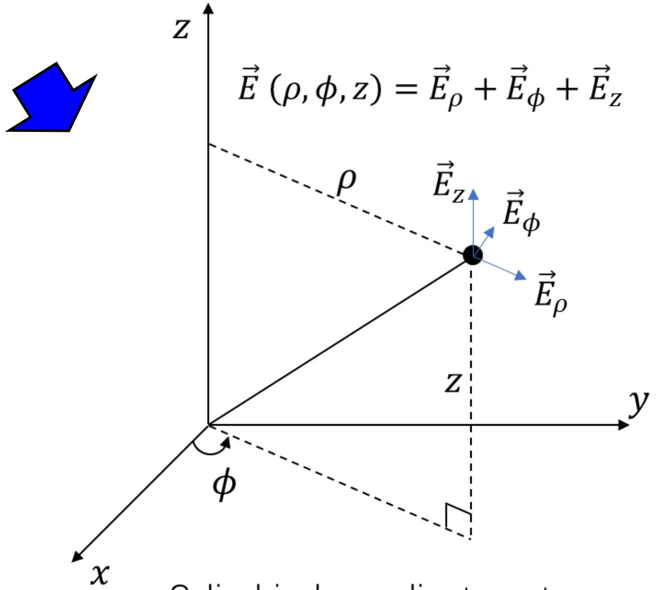

Cylindrical coordinate system

Reference: Y. Lai, Y. Yang, S. Wang and Z. Luo, "A Novel Low-Frequency Radiated Emissions Prediction Technique for the Inductor of a Non-Isolated Power Converter," *2022 IEEE Energy Conversion Congress and Exposition (ECCE)*, Detroit, MI, USA, 2022, pp. 1-8

Experimental Verification of Proposed Prediction Techniques (1-meter Semi-anechoic Chamber)

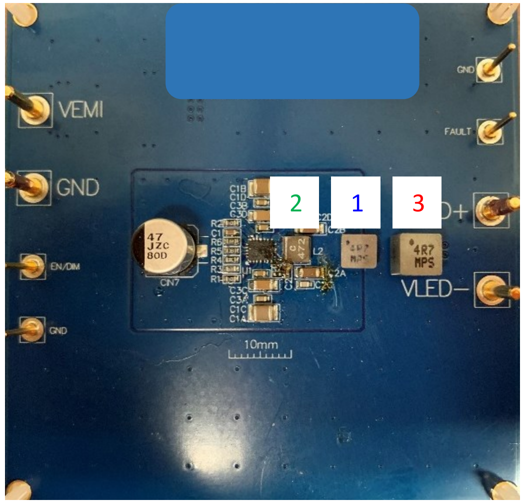

3 inductors are investigated in experiment:

1. $5\times5\times2.9\ \mathrm{mm}^3$ (Baseline)
2. $4\times4\times2.9\ \mathrm{mm}^3$
3. $6\times6\times4.5\ \mathrm{mm}^3$

(Impacts of the chamber setup has been considered in the prediction).

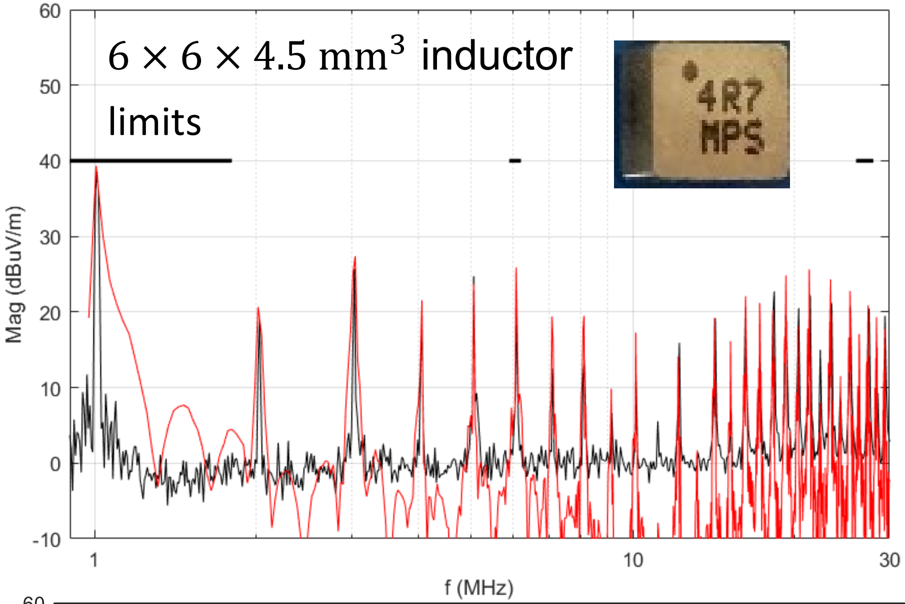

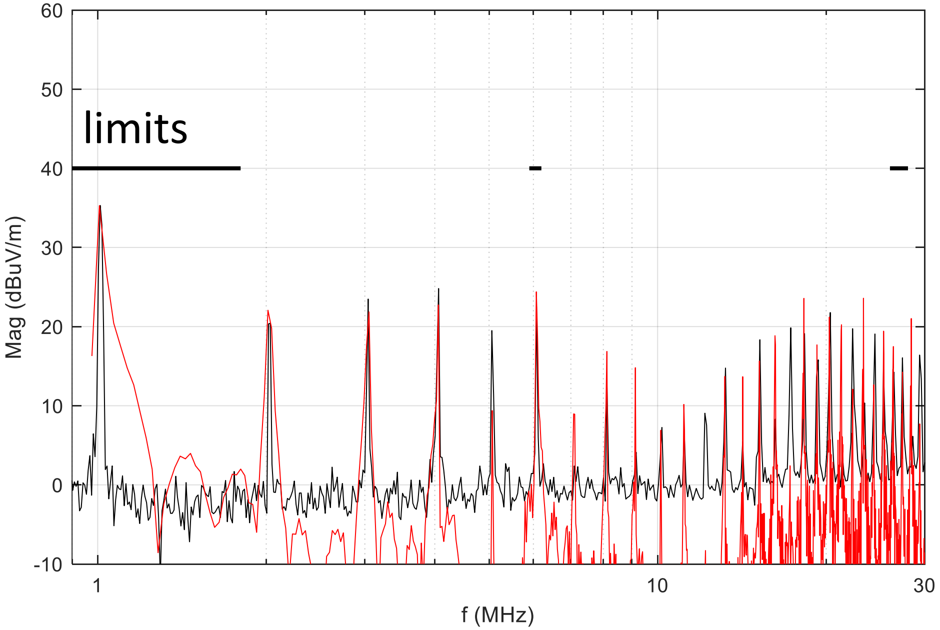

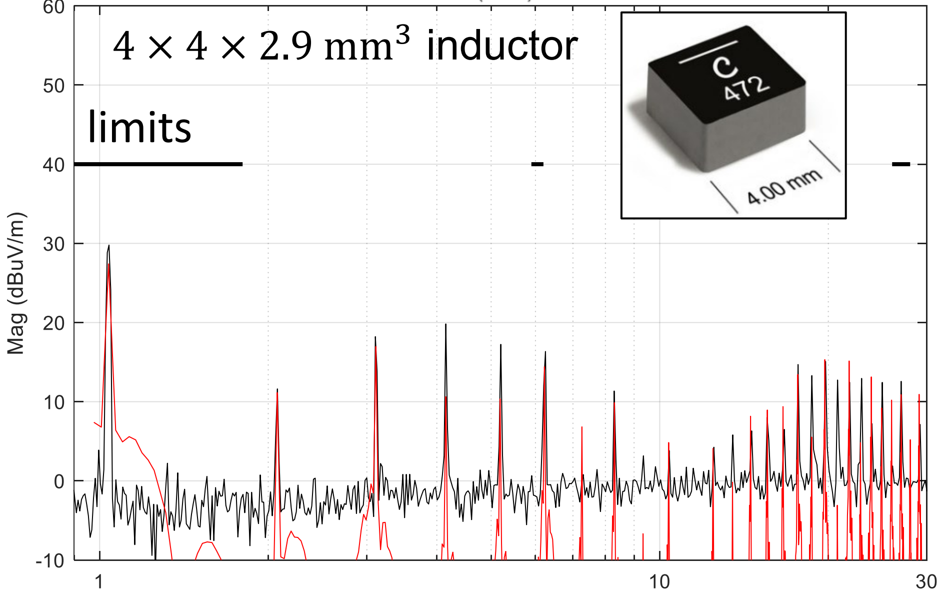

Reduction of Radiative EMI due to Inductors

1. Reduce electric dipole P_{CM} can reduce the radiative EMI
2. Smaller inductors have smaller P_{CM}
3. Shorter inductors have smaller P_{CM}
4. Smaller distance between the PCB ground and the inductor leads to smaller P_{CM}
5. Smaller voltages across inductors have smaller P_{CM}

Questions & Answers